Multidimensional Basin and Petroleum Systems Modeling in the Molasse Basin, Austria

Doctoral Thesis

Dipl.-Ing. Jürgen Gusterhuber

Department Applied Geosciences and Geophysics
Chair of Petroleum Geology
Montanuniversität Leoben

Leoben, November 2013

Danksagung

Reinhard Sachsenhofer gebührt aufrichtiger Dank für die Betreuung dieser Arbeit, angefangen bei der Unterstützung für den UZAG-Antrag, um Förderung für dieses Projekt zu erhalten, bis hin zur kritischen Durchsicht der Publikationen. Besonders positiv hervorheben möchte ich, daß seine Tür jederzeit für eine kurze wissenschaftliche Diskussion, oder zumindest eine wertvolle Anmerkung, offen war.

Ralph Hinsch hat mit seinem Engagement und seiner Geduld hinsichtlich der strukturgeologischen Modellierung beträchtlich zum guten Gelingen der Arbeit beigetragen. Dafür möchte ich ihm herzlich danken.

Das verwendete Softwarepaket PetroMod wurde vom Schlumberger Aachen Technology Center im Zuge einer großzügigen akademischen Lizenz zur Verfügung gestellt. Vielen Dank in dieser Hinsicht an Wolf Rottke, der jederzeit ein offenes Ohr hatte und auf so gut wie jede Frage, die Algorithmen der Software betreffend, eine Antwort wußte.

Der Rohöl-Aufsuchungs AG Wien sei für die Zurverfügungstellung der Daten gedankt, insbesondere Hans-Gert Linzer, der als Ansprechpartner stets ein wichtiges Bindeglied zur Firma war.

Ich danke Frau Ursula Schmid für die sehr persönliche Betreuung und für die so wichtigen administrativen Arbeiten im Hintergrund, ohne die sehr viele wichtige Dinge schlicht nicht funktionieren würden. Reinhard Gratzer und Achim Bechtel danke ich für die vielen positiven Anregungen im Bereich der Geochemie. Dankeschön auch an Sabine Feuchter für die stete Bereitschaft, gemeinsam immer wieder Neues in der Schliffpräparation auszuprobieren.

Doris Groß bin ich in mehrerlei Hinsicht zu grossem Dank verpflichtet. Als unmittelbare Bürokollegin war sie eine großartige Unterstützung in der Bewältigung sämtlicher büroalltäglicher und computernetzwerktechnischer Probleme. Die Kaffeepausen mit Dir und Susanne Strobl haben für unzählige lustige Momente gesorgt und mir geholfen, manchmal Abstand vom Schreibtisch zu bekommen. Darüberhinaus seid ihr beide in den letzten Jahren zu echten Freunden geworden. Das ist zugleich ein Stichwort welches auf Lorenz

Scheucher mehr als zutrifft. Ich danke Dir für ein Jahrzehnt als toller Kollege in Leoben und für das erste Jahrzehnt einer langen Freundschaft.

Meine Mutter Christine war über die Jahre des Studiums unerschöpflich geduldig und jederzeit bedingungslos bereit, meine Ideen zu unterstützen. Lieben Dank dafür.
Damit komme ich zu Barbara, dem wichtigsten Menschen in meinem Leben. Nicht zuletzt deine Fähigkeit, mich wieder aufrichten zu können, wenn es mal nicht nach Wunsch läuft, hat enorm dazu beigetragen, daβ ich jetzt fast am Ende der Doktorarbeit stehen, und diese Zeilen verfassen, darf.

Abstract

This present study deals with basin and petroleum systems modeling in the Molasse Basin of Austria. The Molasse Basin represents the northern foreland basin of the Alps. Hydrocarbon exploration in this basin has been successful for decades. Although most petroleum reservoirs were found yet in the actual foreland region, the oil kitchen is limited to the area beneath the Alpine thrust system at the southern edge of the basin. However, knowledge of geological evolution as well as hydrocarbon potential and timing of generation and migration of this tectonically folded and imbricated part of the basin was still incoherent. This thesis uses two-dimensional basin models from different parts of the basin focusing on the impact of the fold and thrust belt on the petroleum system.

In a first step, a multi-technique approach which combines geological, geophysical and geochemical data was applied to assess amount and timing of uplift and erosion events in the basin. Changes in basin geometry caused by these factors may have significant effects on the petroleum system. Consequently, three different events can be distinguished using this approach: (1) Seismic stratigraphy and isopach maps indicate that the basin tilted to the west in the Early Miocene; (2) Moisture content of coal and thermochronogical data provide evidence for extensive regional uplift during the Late Miocene with an estimated extent of erosion between 500 and 900 m; (3) Shale compaction data indicate that this regional uplift event has been much stronger in the eastern part of the study area where up to 1000 m of sediments were additionally eroded. These new data were considered in the basin models.

In the second part of the thesis, a petroleum systems model was established based on a structural forward model in the western part of the study area (west Upper Austria, Salzburg) with the main goal to investigate the impact of the fold and thrust belt on the petroleum system in and around the Molasse imbricates. Different heat flow scenarios were applied to determine the thermal history along the modeled section. The calculated heat flows are moderate to low and range between 28 and 60 mW/m² in a consistently southward decreasing trend. However, formation temperature data indicate elevated present-day heat flows compared to paleo-heat flows. This sub-recent (approx. 2.5 million years before present) increase in heat flow during the Pliocene and Pleistocene is yet not fully explainable but is supported by different sensitivity analysis. A combination of paleo and present-day heat flows was considered the most likely scenario and applied to the petroleum systems model. The model shows that minor

hydrocarbon generation (transformation ratio <20 %) occurred only in deeper parts of the Molasse imbricates and was caused by the sub-recent heat flow increase. The low transformation ratio represents a charge risk but petroleum generation in the deeper parts of the Perwang imbricates is proven by oil stains and supported by the models. Oil migration outside the imbricates into autochthonous reservoirs was probably limited. Internal migration from deeper into shallower parts of the imbricates remains uncertain.

The third part of the thesis concentrates on the eastern part of the study area near the river Enns. The purpose of these models was to study hydrocarbon generation under the Alpine thrust-belt and to investigate the migration into the tectonically mainly undeformed foreland region. To reach this aim, a 2D basin model was performed based on a structural forward model and a 'Pseudo 3D' model was created based on structure maps. 2D thermal modeling results show that calculated heat flows are moderate to low and range between 26 and 52 mW/m². A southward decrease in heat flow together with an apparent sub-recent (approx. 4 million years before present) heat flow increase show characteristics akin to the model in the west. Hydrocarbon generation under the Alpine nappes commenced in the Early Miocene (about 19 million years before present) and was terminated in the Late Miocene (about 8 million years before present) due to cooling caused by erosion and uplift of the area. Migration of hydrocarbons commenced simultaneously to generation but continued until present-day. This migration model reflects several fundamental observations made in previous independent studies. For instance, model results indicate fault-bounded migration of gas into the Sierning imbricates and diffuse vertical migration of gas in the foreland region up into stratigraphically shallower sequences of the Puchkirchen and Hall Formations.

The structural map-based flow path method of the 'Pseudo 3D' model produced ambiguous results. Some important existing fields were successfully predicted but prediction failed for other fields. Furthermore, the model shows accumulations in the western part of the study area where no hydrocarbons were encountered yet. A model can be useful even if it makes a misfit with prevailing facts. In this case, the mismatch is obviously partly related to low model resolution outside the 3D seismic survey. Apart from that, the mismatch reflects that the absence of fields in the western section of the basin is rather a result of missing charge due to absence of source rocks than of missing structures. Furthermore, the model reflects the importance of deep faults for hydrocarbon migration.

The two-dimensional model across the Sierning imbricates was further used to investigate the influence of heating of potential reservoir rocks during maximum burial on biodegradation of hydrocarbons (paleo-pasteurization). It shows that

deep burial of the northern basin margin about 9 million years before present limited the occurrence of biodegradation to an interval above 800 – 1000 m sub-sea.

Kurzfassung

Die vorliegende Studie befasst sich mit Becken- und Kohlenwasserstoffmodellierung in der österreichischen Molassezone. Die Molassezone repräsentiert das alpine Vorland. Kohlenwasserstoffexploration wurde in diesem Gebiet über Jahrzehnte erfolgreich betrieben. Obwohl sich der Grossteil der Kohlenwasserstofffunde auf das tatsächliche Vorland beschränkt, weiss man, dass sich der Bereich der reifen Kohlenwasserstoffmuttergesteine (‚Ölküche') unter den alpinen Decken am Südrand des Beckens befindet. Trotzdem wusste man bis heute nur wenig über das Kohlenwasserstoffpotential und es fehlte ebenso ein zusammenhängendes Bild darüber, wie Zeitpunkt der Kohlenwasserstoffbildung und Migration mit der geologischen Entwicklung dieses tektonisch komplexen Teils des Beckens zusammenhängen. In dieser Arbeit werden zweidimensionale Beckenmodelle präsentiert, die zeigen, welchen Einfluss der alpine Überschiebungsgürtel auf das Kohlenwasserstoffsystem hat.

Änderungen an der Geometrie des Beckens während dessen Bildungszeit, hervorgerufen durch Erosionsereignisse oder Hebung des Beckens, können grossen Einfluss auf ein Kohlenwasserstoffsystem nehmen. Deshalb wurde in einem ersten Schritt versucht, unter Verwendung von geologischen, geophysikalischen und geochemischen Daten, derartige Ereignisse zu rekonstruieren und zeitlich, sowie quantitativ zu erfassen. Mit dieser Herangehensweise konnten 3 ‚Events' unterschieden werden: (1) Seismikinterpretation und die Verwendung von Mächtigkeitskarten zeigen eine regionale Kippung des Beckens gegen Westen während des frühen Miozäns an; (2) der Wassergehalt von Kohleproben und Spaltspurendatierung liefert Information über ausgedehnte Hebung des Beckens während des späten Miozäns einhergehend mit Erosion von 500 – 900 m Sedimenten; (3) die Auswertung von Akustikbohrlochmessungen zeigt, dass der östliche Teil des Untersuchungsgebietes zur selben Zeit noch viel stärker herausgehoben wurde. Dabei wurden zusätzlich bis zu 1000 m mächtige Sedimente erodiert. Die Erkenntnisse dieser Teilstudie flossen später in die Beckenmodellierung ein.

Der zweite Teil der Arbeit befasst sich mit dem Einfluss des Überschiebungsgürtels auf das Kohlenwasserstoffsystem innerhalb und in umittelbarer Nähe der tektonischen Schuppen. Für diese Untersuchung wurde ein Profil, welches auf einem geologischen Strukturmodell basiert, aus dem westlichen Teil des Untersuchungsgebietes (westliches Oberösterreich, Salzburg) ausgewählt. Für die Modellierung wurden verschiedene Wärmeflussszenarien kreiiert um die thermische Entwicklung entlang der Sektion zu erfassen. Die

berechneten Wärmeflüsse sind niedrig bis moderat, schwanken zwischen 28 und 60 mW/m² und nehmen von Norden nach Süden kontinuierlich ab. Reifedaten zeigen einen wesentlich niedrigeren Paläowärmefluss an, als dieser heute (basierend auf rezenten Formationstemperaturdaten) ist. Dieser vermutete junge Anstieg des Wärmeflusses während des Pliozäns bis Pleistozäns ist nicht vollständig geklärt, bleibt jedoch auch nach Sensitivitätsanalysen am Modell und Kontrolle der Kalibrationsdaten, vorhanden. Deshalb wurde ein Wärmeflussszenario, welches für Reifedaten und für rezente Temperaturdaten angemessen ist, angewendet. Das Modell zeigt, dass selbst in tieferen Bereichen der Schuppen bis dato maximal 20 % der möglichen Kohlenwasserstoffe generiert wurden. Diese Genese war ein Resultat des jungen Wärmeflussanstiegs. Obwohl dieser niedrige Umsetzungsbetrag von <20 % ein hohes Risiko in Hinblick auf Füllung möglicher Strukturen mit Kohlenwasserstoffen birgt, ist die Existenz von Öl in diesem Bereich durch Ölspuren aus Bohrkernen belegt. Ölmigration aus den Schuppen in benachbarte autochthone Bereiche war vermutlich sehr limitiert. Ölmigration von tieferen in seichtere Bereiche der Schuppen bleibt überhaupt unsicher.

Der dritte Teil der Arbeit geht auf die Kohlenwasserstoffbildung unterhalb des alpinen Überschiebungsgürtels ein und untersucht die Migration von Öl und Gas nach Norden in den Bereich des Vorlandes. Dafür wurde ein 2D Beckenmodell aus dem östlichen Bereich des Untersuchungsgebietes (nahe der Enns) benützt, welches auf einem tektonischen Vorwärtsmodell basiert und es wurde ein „Pseudo 3D“ Modell basierend auf geologischen Strukturkarten konstruiert. Das 2D Temperaturmodell zeigt, dass sich die berechneten Wärmeflüsse mit Werten zwischen 26 und 52 mW/m² auf niedrigem bis moderatem Niveau befinden. Ebenso wie im Modell aus dem westlichen Bereich des Beckens können auch hier der nach Süden hin abnehmende und im Pliozän ansteigende Wärmefluss beobachtet werden. Die Kohlenwasserstoffbildung unterhalb des Überschiebungsgürtels begann während des frühen Miozäns (vor ca 19 Mio. Jahren), war jedoch ungefähr 8 Mio Jahre vor heute zu Ende. Dies ist auf Abkühlung der Sequenz aufgrund von Erosion und Hebung des Gebietes zu dieser Zeit zurückzuführen. Die Migration der Kohlenwasserstoffe begann gleichzeitig mit der Zeit der Bildung und blieb bis heute aktiv. Dieses Modell unterstützt viele Annahmen früherer Studien. Das beinhaltet insbesondere Erkenntnisse über die Migration von thermischem Gas im Becken. Die Modellierergebnisse lassen darauf schliessen, dass Gas entlang von Störungszonen in die Sierninger Schuppenzone eingedrungen ist. Ausserdem zeigt das Modell vertikale Migration von Gas im Bereich des Vorlands in die Puchkirchen und Hall Formationen an.

Die erzielten Ergebnisse des auf geolgischen Untergrundskarten basierenden ‚Pseudo 3D' Modells sind ambivalent. Während die Position einiger wichtiger Ölfelder korrekt vorhergesagt werden konnte, gelang dies bei anderen Feldern nicht. Darüberhinaus wurden im westlichen Untersuchungsgebiet Akkumulationen angezeigt, wo bis heute keine Felder gefunden wurden. Ein Modell kann auch wertvoll sein wenn es Diskrepanzen mit gültigen Fakten aufweist. In diesem Fall resultieren diese Unterschiede zum Teil aus der schlechteren Auflösung der Karte ausserhalb der 3D Seismik. Abgesehen davon spiegelt das Ergebnis jedoch wider, dass die Abwesenheit von Ölfeldern im westlichen Untersuchungsgebiet eher auf fehlendes Muttergestein und nicht auf fehlende Fallenstrukturen zurückzuführen ist. Ausserdem stützt das Modell die These, dass Migration nicht nur entlang der Hauptkohlenwasserstoffträgergesteine sondern vielfach auch über tiefe Störungssysteme verlaufen ist.

Das zweidimensionale Modell aus dem östlichen Bereich des Untersuchungsgebietes wurde weiters dafür verwendet, Aufschluss darüber zu geben, wie sich ein Temperaturanstieg in potentiellen Reservoirgesteinen während der Zeit der maximalen Versenkung auf die Biodegradation von Gas (‚Paläopasteurisierung') auswirkt. Es zeigt, dass tiefe Versenkung des nördlichen Beckenrandes vor ca. 9 Mio. Jahren die Möglichkeit der Biodegradation von Gas auf einen Tiefenbereich oberhalb von 800 – 1000 m unter NN begrenzt hat.

Table of Contents

1 Introduction

1.1 Background, Motivation and Introduction to this Thesis

This thesis deals with basin and thermal modeling applied to the Molasse Basin in its Austrian part. The basin is part of the Alpine-Carpathian Foredeep located in Central Europe (Fig.1). It represents a typical asymmetric foreland basin at the northern rim of an orogenic belt. It developed due to the collision of the Alps with the southern margin of the European shelf during the Middle Paleogene (Roeder and Bachmann, 1996; Sissingh, 1997).The entire basin extends about 120 km in N-S direction and 700 km in E-W direction from Geneva (Switzerland) to Vienna (Austria).

Hydrocarbon exploration has been successful in the Austrian part of the basin for decades. Early drilled wells provided important insights on the stratigraphic and tectonic evolution of the basin (e.g. Janoschek, 1961; Kollmann, 1977; Wagner et. al., 1986) and most discoveries were made in mainly undeformed sedimentary rocks in the northern part of the basin. A first basin modeling approach based on 1-dimensional models (Schmidt and Erdogan, 1993) suggested that reservoirs in the foreland were charged from beneath the Alpine nappes. This means that oil and gas discovered in the foreland region required long-distance lateral migration from underneath the Alpine nappes. While hydrocarbon trap formation in the foreland is rather well constrained due to extensive exploration activity, architecture and evolution of the folded and imbricated southernmost part of the basin (Fig. 1) are still poorly understood and its impact on hydrocarbon timing and generation as well as the hydrocarbon potential are not fully explored.

Even though new large economic discoveries are unlikely, a Yet-to-Find analysis indicates that up to several hundred small fields remain to be discovered in the Molasse basin (Véron, 2005). New wells, additional geochemical results and extended 3D seismic acquisition pushed the understanding of relevant geo-processes in recent times and exploration activity was extended further towards the thrust belt in the south. Evaluation of new data as well as the application of balancing techniques (Hinsch, 2013) allowed now for the first time the application of multi-dimensional basin modeling techniques in this tectonically complex area.

The first part of the thesis focuses on timing and amount of erosion and uplift in the Molasse Basin. Both factors have a reasonable impact on the thermal evolution of the basin as well as on the appearance of potential prospects. The second part deals

mainly with the western study area and concentrates on the effect of the fold and thrust belt on the petroleum system within the imbricated zone and its surroundings at the southern basin margin. The third part highlights the eastern part of the study area and investigates the hydrocarbon generation potential as well as timing of generation in the Alpine sub-thrust region and creates the link to the foreland migration. In addition, this chapter addresses the risk of biodegradation of gas in the basin.

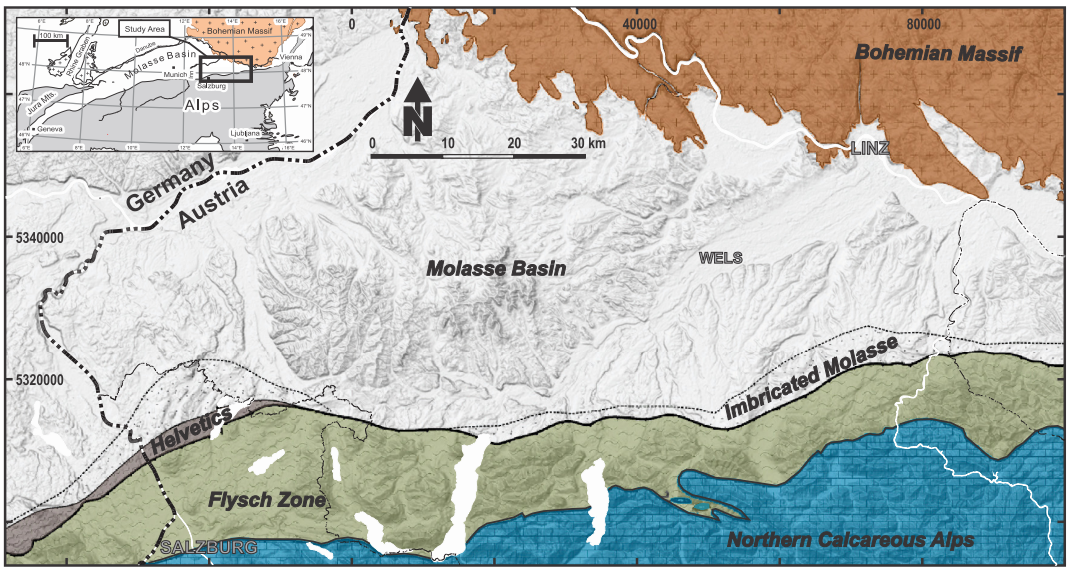

Figure 1: Simplified geological map of the study area superposed on shaded relief digital elevation model created from SRTM data (SRTM, 2004). The inset map (top left) shows the position of the study area in the frame of the Northern Alpine Foreland.

1.2 The Geological Evolution of the Pre-Molasse Basin Area

The following Pre-Molasse evolution of the area is described after Nachtmann and Wagner (1987) and Wagner (1996; 1998). The basement is formed by crystalline rocks of the Bohemian Massif overlain by Jurassic to Cretaceous limestones and siliciclastics. Permo-Carboniferous sediments are only locally preserved in a distinct graben structure at the western margin of the "central swell zone", a subsurface basement high which forms the southeastern extension of the "Landshut-Neuoetting-High" in Bavaria. The Mesozoic succession started with the deposition of Middle Jurassic shallow-marine to fluvial sandstones with intercalated coaly layers. Late Jurassic series formed an extensive carbonate platform on the tropical shelf of the Bohemian landmass. The Late Jurassic facies distribution indicates progressive shallowing from southwest below the thrust-belt towards the Bohemian Massif in the north. During the Early Cretaceous the area experienced an erosion and uplift phase accompanied by tectonic activity along NW-SE striking fault systems to the

southwest of the central swell zone and the Bohemian Massif. Reactivation of pre-existing fault-systems triggered differential uplift of individual fault blocks and deep truncation of Jurassic series. Above a major hiatus Late Cretaceous evolution started with the deposition of transgressive Cenomanian marls and storm-dominated glauconitic sandstones partly underlain by fluvial sandstones. The latter, often coarse-grained so called “Schutzfels Beds” infill the Jurassic karst up to a depth of 100 m below the Jurassic surface. The transgressive Cenomanian clastics are conformably overlain by Turonian clays containing glauconitic storm deposits. Campanian sediments consist of shallow-marine sandstones derived from the Bohemian Massif in the north and shallow-marine mudstones deposited under outer-shelf conditions. The top of the Cretaceous corresponds to a regional unconformity throughout the basin due to major tectonic deformations in the Latest Cretaceous to the Earliest Paleogene. During this time, the area became uplifted and transected by NW-SE and NNW-SSE trending fault systems. At the same time individual fault blocks tilted uniformly to the east with the result that Late Cretaceous sediments are generally preserved in their eastern part. The central swell zone which had come into existence during the Early Cretaceous, became reactivated and uplifted with erosion cutting down through its Cretaceous cover and locally even through the underlying Jurassic layers into the crystalline basement.

1.3 Basin Fill History

The Paratethys Sea transgressed progressively on the evolved peneplain during the Late Eocene. Series of fluvial and shallow marine transgressive sandstones rest unconformably on top of the peneplain representing the onset of Molasse sedimentation. Due to subsequent overthrusting and tectonic shortening the original basin was much wider at this time than the present remnant (Wagner, 1996). Flexural downward bending of the European lithosphere due to the advancing nappe system led to the development of mainly south-dipping E-W trending faults but also to reactivation of NNW-SSE trending normal fault systems and to rapid subsidence of the area to deep water conditions. Extensive tectonic activities changed the Eurasien configuration around the Eocene-Oligocene border and separated the Tethys Sea into the Paratethys in the north and the Mediterranean Sea in the south. As a consequence, cold boreal water entry to the Paratethys was now restricted to corridors towards the Rhine Graben and the North Sea (Roegl, 1999). Deep basins with oxygen deficient bottom conditions and reduced circulation led to the deposition of marine organic matter rich rocks which are the source for thermogenic hydrocarbons in the Molasse Basin (Schulz et al., 2002; Sachsenhofer and Schulz, 2006; Sachsenhofer et al.,

2010). Thereafter, new seaways opened from the Mediterranean and the Indian Ocean to the Paratethys causing normal oxygenated bottom conditions (Roegl, 1999). Changing water currents caused a breakdown of the water column stratification and stopped the deposition of organic-rich rocks during the Oligocene (Schulz et al., 2002). In the Late Oligocene and Earliest Miocene the southern part of the basin became integrated in the advancing thrust system. A longitudinal deep water channel belt (Linzer, 2002; De Ruig and Hubbard, 2006) developed along the evolved E-W trending Puchkirchen trough consisting of multiple debris-flow and turbidity current events (Bernhardt et al., 2012). Along the northern margin of the study area contemporaneous sediments of the deep-water Lower and Upper Puchkirchen Formation are represented by brackish to continental clays and sands (Krenmayer, 1999). Deep-water conditions persisted in the Early Miocene with the deposition of the Lower Hall formation. Slope-delta progradations across the area initiated the infill of the basal Hall trough and are first indications for a gradual transition to shallow-water sedimentation (Hinsch, 2008; Hubbard et al., 2009; Grunert et al., 2013). Marine conditions also continued during the deposition of the overlying Innviertel Group (Ottnangian) (e.g. Grunert et al., 2010). While Early and Middle Ottnangian transgressive and highstand phases are represented by fully-marine, tidal dominated silts and sands, during a Late Ottnangian regressive phase brackish to fluvial sediments (Oncophora Beds) were deposited (Roegl, 1998; Grunert et al., 2012). Because of the brackish character, affiliation of the Oncophora Beds to the Innviertel Group is still in discussion (Rupp et al., 2008). Deep-water conditions prevail in the study area (east of Munich) until Early Miocene times (Wagner, 1996). In contrast, Molasse sediments west of Munich are mainly characterized by shelf conditions with transgression and regression cycles (Bachmann and Mueller, 1992; Kuhlemann and Kempf, 2002). Following on a major hiatus during Karpatian times, a thick succession of coal-bearing sediments and fluvial gravels was deposited (Upper Freshwater Molasse). Deposition commenced in the Early Badenian in the western part of the study area and became gradually younger towards the east where Pannonian coals directly overlie Ottnangian deposits (Czurda, 1978). This indicates that sedimentation proceeded eastwards on a slightly southwest dipping peneplain (Pohl, 1968; Groiss, 1989). Most of the Upper Freshwater Molasse sediments have been eroded due to post-depositional uplift since 8 Mio. years before present (Gusterhuber et al., 2012). Quaternary deposits partly cover the Molasse sequence.

1.4 Petroleum Systems of the Molasse Basin

Two petroleum systems can be distinguished in the Molasse basin east of Munich: (1) a Lower Oligocene to Mesozoic thermally generated oil system and (2) an Oligocene-Miocene biogenic gas system (Wagner, 1996, 1998).

1.4.1 Thermogenic Hydrocarbons

Reservoir rocks: The most important reservoirs for oil and minor thermal gas are Upper Eocene basal sandstones and carbonates. The up to 30 m thick sequence comprises shallow marine sands onlapping northwards onto coastal to fluvial deposits. The succession is characterized by highly variable facies associations but shows generally good reservoir quality. Coastal sands show the best reservoir quality within the Eocene succession having average porosities of 15 to 25 % as well as permeabilities ranging from several mD up to 2000 mD respectively (Wagner, 1980). The overlying "Lithothamnium Limestone" contains less oil-producing sandstone layers in its lower part (Malzer et al., 1993). While pore space of the latter is sometimes cemented by calcite, the porosity of Upper Eocene sandstones may be reduced by solid bitumen in the eastern part of the study area (Sachsenhofer et al., 2006). Additional reservoirs occur in Mesozoic horizons. Herefrom up to 60 m thick marine Cenomanian sandstones are most important. These glauconitic beds can reach porosity values of up to 17 % and permeability values between 10 and 400 mD (Malzer et al., 1993).

Source rocks: Lower Oligocene fine-grained marine sediments occur from the western boarder of the Alpine Foreland (France) to the Mangyshlak region (Caspian Sea region) in the east (Báldi, 1984; Vetö, 1987). Organic carbon rich intervals within these sediments are considered source rocks in several basins within the Paratethyan realm (Wehner and Kuckelkorn, 1995; Ziegler and Roure, 1999). Within the Molasse Basin of Austria and Bavaria, these deep-water deposits include from the base to the top:

- The Schoeneck Formation (formerly "Lattdorf Fischschiefer"), a typically 10-20 m thick succession consisting of organic rich marls (lower part) and shales (upper part). The lower part of the Schoeneck Formation is characterized by an average TOC (total organic carbon) of 2.3 % and HI (Hydrogen Index) values around 500 mg HC (Hydrocarbon)/g TOC. TOC values above 5 % and slightly higher HI values (around 600 mg HC/g TOC) occur in the upper black shale unit. Deposition of the Schoeneck Formation occurred in a stagnant basin under oxygen-depleted water conditions (Schulz et al., 2002). Dohmann (1991) proposed a deepening of

the basin during deposition of the Schoeneck Formation reaching a maximum water depth of 800 m.

- The Dynow Formation (formerly "Heller Mergelkalk"), about 5-15 m thick, is mainly composed of light-coloured marlstones and partly built up by coccolithophorides (Schulz et al., 2004).
- The Eggerding Formation (formerly "Bändermergel – Banded marl") typically ranges between 35 and 50 m in thickness. The boundary between Dynow and Eggerding Formations is characterized by a gradual decrease in carbonate contents. In its lower part the formation consists of dark grey laminated pelites deposited in an oxygen-deficient environment. TOC contents are around 5 % corresponding to a HI of up to 600 mg HC/g TOC (Sachsenhofer et al., 2010).
- The Zupfing Formation (formerly "Rupel Tonmergel – Rupelian Marl") follows above a sharp boundary marked by an increase in carbonate contents. It consists of up to 450 m thick clay marl. Oxygen depleted conditions persisted during the deposition of the Zupfing Formation but only the lowest part of the sequence is organic matter rich with a TOC of 1.5 % (Sachsenhofer et al., 2010).

Slides and pebbles of Eocene Lithothamnium limestone within the Schoeneck Formation in some western wells show that erosion on the upper basin slope and re-deposition at the lower basin slope had commenced already during the earliest Oligocene and reached its maximum during deposition of the late stages of the Eggerding Formation (Sachsenhofer and Schulz, 2006). As all relevant formations were deposited under marine conditions (Dohmann, 1991), all erosional events are considered as submarine processes probably triggered by Paleogene earthquakes. However the source rock potential of the re-deposited "Oberhofen facies" is considerably lower (average TOC 1.3 %; HI up to 400 mg HC/g TOC) compared to the normal source rock facies (Sachsenhofer and Schulz, 2006).

1.4.2 Biogenic Gas

Isotopically light gas in Upper Oligocene and Miocene horizons was probably generated by bacterial activity (Malzer et al., 1993; Schulz and van Berk, 2009). Source rocks and reservoir rocks are closely connected. Claystone layers with potential source rock characteristics intercalate and seal the reservoir sediments (Schulz et al., 2009). Based on isotope data and gas wetness, Reischenbacher and Sachsenhofer (2011) described mixing of thermogenic and biogenic hydrocarbons including condensate.

Reservoir rocks: The bacterial gas is associated with thermally immature potential source rocks which contain more than 0.5 % TOC. Different subfacies of the

Puchkirchen and Hall channel and delta systems may serve as gas reservoirs (De Ruig and Hubbard, 2006; Hubbard et al., 2009): the main channel fill, tributary channels, ponded slope fans occurring directly in front of the Alpine thrust front or in piggyback basins on the thrust sheet, and minor overbank lobes. Overbank wedges represent important top seals for many of the gas fields in the Puchkirchen channel system (De Ruig and Hubbard, 2006).

2 Methods

2.1 Basin and Petroleum Systems Modeling

'Basin Modeling' considers geological, geophysical and geochemical parameters to simulate the burial history of a sedimentary basin in a forward modeling approach through time. This includes factors like sediment compaction, subsequent porosity decrease, but also temperature, heat flow history as well as related parameters like maturation of organic material (Hantschel and Kauerauf, 2009). General principles of basin modeling are described in Welte and Yukler (1981), Welte et al. (1997) and numerous references herein.

The term 'Petroleum Systems Modeling' is used if fluids (liquid and vapor) in a basin are also considered in the simulation process. This means that pore fluid movement is simulated beside hydrocarbon generation, migration and accumulation over the time (Yuekler et al., 1978; Tissot and Welte, 1984; Welte and Yalcin, 1987; Poelchau et al., 1997; Hantschel and Kauerauf, 2009). Both 'Basin Modeling' and 'Petroleum Systems Modeling' can be combined to a 'Basin and Petroleum Systems Model' (BPSM; Peters et al., 2009). In the present study the Software tool PetroMod 11 SP4 was used which was developed by the Schlumberger Technology Center Aachen, Germany.

The prerequisite for a BPSM is a conceptual model where the evolution of the basin is separated into several discrete events. Each event represents a time span during which deposition, erosion or hiatus occurs. Each layer is deposited during one single event but different geological processes can occur in different parts of the basin at the same time (Wygrala, 1988). This model, which is based on geometrical data, is then divided into different cells ("gridding" process). Geological, physical and chemical processes are determined for each cell even including mutual effects of neighboring cells (Wygrala, 1989).

Each determined BPSM needs to be compared with preferably unbiased measured calibration data from rocks, fluids or borehole measurements.

Heat flow history over geological times is one of the most important constraints for modeling hydrocarbon generation (Tissot and Welte, 1984). Interpretation of the tectonic basin setting allows a first rough assessment of paleo heat flows (Allen and Allen, 1990). Calibration of heat flow history is mainly based on temperature sensitive parameters like vitrinite reflectance (Teichmueller, 1982; Stach et al., 1982;

Sachsenhofer and Littke, 1993; Taylor et al., 1998) and present-day temperatures (Yalcin et al., 1997). The reaction kinetic algorithm EASY % Ro from Sweeney and Burnham (1990) was used in the study to calculate the vitrinite reflectance in the models with depth and time.

Thermal conductivity of rocks depends on different properties like porosity as well as habitus and arrangement of grains (Brigaud et al., 1990). Particularly porosity affects thermal conductivity to a high degree, because pore fluids have lower thermal conductivities than the rock matrix.

This fact makes porosity to an important factor controlling the thermal properties of sediments and sedimentary rocks. Also the geometrical design of the more or less homogenous layers is related to rock porosity changes. Usually a decompaction routine is integrated in the software to allow the reconstruction of initial sediment thicknesses of each layer calculated from present day data. However, the TecLink concept of PetroMod which was applied to integrate the structural forward modeled sections uses predefined paleo-sections to determine porosity change. Therefore, compaction of autochthonous sediments was first computed in a preliminary model, where thrusting was simulated by increasing thicknesses of thrust sheets through time (using PetroMods ´salt movement tool´). The achieved compaction data were later integrated in the thermal basin model built with the TecLink tool.

The capability of fluids flowing through sediments or sedimentary rocks is expressed by permeability. Anisotropy effects where the ratio of horizontal to vertical permeability is high, is particularly important in shale layers and has an impact on flow direction. The 2D migration modeling package of PetroMod includes different migration modeling techniques. These methods include Flow path, Darcy flow, and Hybrid (Hantschel and Kauerauf, 2009).

Flow path migration is a solely buoyancy driven migration method which allows fast, high-resolution modeling. The method requires an arbitrary definition of seal/carrier and therefore represents an incomplete physical method. Darcy flow integrates all relevant physical parameters such as PVT (Pressure, Volume, Temperature) and requires long computer processing times (Baur, 2010).

The Hybrid migration method was applied in this study. It combines Darcy and flow path migration methods (Hantschel et al., 2000) and was introduced to allow proper accumulation tracking through time including timing and retention issues. This technique applies the flow path method to all lithologies which have more than 100 millidarcy permeability and a higher porosity than 30 % during the evolution of the actual layer. Beyond that it applies full Darcy calculations (i.e. hydrocarbon

retention) to all layers having less permeable lithologies. Also, it is the preferred method to use for layered structures in conjunction with a low number of open faults.
As variations, caused by the actual surface temperature, penetrate deeply into the earth crust (Barker, 2000), a surface water interface temperature (SWI) was set for the models to represent the upper boundary condition for heat transport in the basin. Paleo mean surface temperature values are based on global paleo-temperature distribution maps which were corrected in terms of ocean water depths and implemented into PetroMod (Wygrala, 1989).
The conversion of kerogen to hydrocarbons can be described by time and temperature dependent reaction kinetic processes (e.g. Tissot and Welte, 1984). PetroMod uses the continuous temperature record over the time to calculate a particular hydrocarbon yield from the source rock. Each generation of oil and gas is described by activation energy and a designated initial petroleum generation potential. The initial potential of generated hydrocarbons is expressed by the Hydrogen Index HI (Espitalié et al., 1977).

3 Calibration Data

Source rocks are rocks which already generated or have the capability to generate petroleum (Tissot and Welte, 1984). The quality of a source rock is defined by the type and the amount of kerogen and bitumen as well as on the stage of maturity. Kerogen is a fraction which is insoluble by chemical solvents and consists mainly of algae, spores, pollen, higher plant material and some animal matter. There are several environmental and depositional/diagenetic characteristics that privilege preservation of sufficient organic matter for an actual source rock. However it requires organic matter preserved in sediment to be heated and subjected to pressure to generate thermogenic hydrocarbons which are volumetrically most significant.

Source rocks can be described by the total organic carbon (TOC) content. As conversion of organic matter to hydrocarbon depends on factors like convertibility of organic matter, not the whole amount of TOC is available for hydrocarbon generation. This means that the TOC content provides just an order of magnitude assessment of the quantity of petroleum formed (Dow, 1977). A minimum TOC content for potential source rocks to generate sufficient petroleum to expulse is difficult to assess. However a threshold value exists since a critical concentration of hydrocarbon in the source rock has to be reached to allow expulsion from rocks (Dow, 1977). An estimated minimum TOC value for shales is 0.5 % TOC. A good source rock has more than 2 % TOC.

The kerogen type depends on environmental conditions during deposition/diagenesis and on the composition of the original organic matter. General depositional environments for source rocks comprise continental (lakes, freshwater swamps), shorelines (deltas and paralic shorelines) and marine (restricted basins, open shelf, continental slopes) environments. Generally, lacustrine and marine organic matter (kerogen types I and II) have higher petroleum generation potential than terrestrial organic matter (type III) (Tissot and Welte, 1984). Type IV kerogen is mainly composed of reworked terrigenous organic matter having the lowest petroleum potential.

Macerals are components of coals and kerogen (Stach et al, 1982; Taylor et al., 1998). According to reflectivity, macerals can be divided into three different groups: vitrinite, liptinite and intertinite. The reflectance of vitrinite is considered the most important calibration parameter for determining the maturity of sedimentary rocks

(Teichmueller, 1982; Durand et al., 1986; Teichmueller, 1987). The optical properties of vitrinite appear to alter more consistent and are also more resistant compared to other macerals (Dow, 1977). Therefore, vitrinite is generally used for rank determination. Reflectance measurements can be determined over the entire range of maturity from lignite to anthracite. The best results are obtained from coaly material as it contains the highest amount of vitrinite compared to detrital material which contains high amounts of mineral matter which may bias the photosensitive measurements due to irradiation.

3.1 Vitrinite Reflectance

Vitrinite reflectance is measured on rocks containing remnants of landplants. Only reliable data (mainly from coals) have been used for calibration in the present study. The analyzed samples were embedded in synthetic resin, ground and finally polished. The polished resin blocks were used for the analyses. For the present study reflectance measurements were conducted under standard conditions (Leica DMRX reflected-light microscope; wave length of monochromatic light at 546 nm). The procedure follows Taylor et al. (1998) using an isotropic Yttrium-Aluminium-Garnet glass standard with 0.899 % of reflectance under oil immersion. 50 measurements per sample were determined. Following ISO 7404, 100 measurements per sample would be required to get a reliable result but none of the samples contained enough particles to get this number of measurements. To minimize the error caused for instance by variations in light intensity of the lamp, several samples were remeasured.

3.2 Other Organic Calibration Parameters

For the present study a standard Rock-Eval Pyrolyzer (Vinci Technolgies) was used. For the pyrolysis procedure, about 100 mg of pulverized rock are heated in an inert atmosphere based on a specific heating rate. First, the amount of hydrocarbon thermally extracted at 300 °C (already in the subsurface generated hydrocarbons and hydrocarbons from living organisms) is counted as S1 peak. Further during the heating-up, thermal breakdown of the kerogen produces additional hydrocarbons (S2 peak). Carbon dioxide released from the kerogen is then recorded as S3 peak. The Tmax is the temperature value during the heating-up process at which hydrocarbon generation reaches its maximum. It can be used as kerogen maturation parameter but its application is limited since the Tmax is a kerogen type dependent maturity parameter (Espitalié et al., 1985; Peters and Moldowan, 1993). In this study the Tmax was used to support vitrinite reflectance data.

With the formula *Ro (calculated) = 0.0180 * Tmax – 7.16* it is possible to convert Tmax to reflectance (Peters et al., 2005). The equation was derived from a collection of shales and can be applied for low sulphur type II and type III kerogen (Jarvie et al., 2001). Another related equation which can be used to calculate vitrinite reflectance is derived from the methylphenanthrene index (MPI-1): *Rc = 0.60 * MPI-1 + 0.40*. The methylphenanthrene index is a maturity parameter based on the relative abundances of phenanthrene and methylphenanthrenes which are part of the three-ring aromatic hydrocarbons (Peters et al., 2005). Calibrations between methylphenanthrene indices and vitrinite reflectance were published by Radke and Welte (1983). Hopane and sterane isomerization can also be applied as maturation calibration parameter (Mackenzie and McKenzie, 1983; Rullkoetter and Marzi, 1989). The biomarker ratios for steranes (20S / (20S + 20 R)) and hopanes (22S / (22S + 22R)) can be directly used in the simulation eliminating the need for recalculation to vitrinite reflectance (Welte et al., 1997). Hopane isomerization is a biomarker maturity ratio which describes the conversion of the biological 22R to the geological 22S configuration of homohopane molecules. Sterane isomerization also describes conversions between biological and geological configurations at several asymmetric centers of the molecules (Peters et al., 2005).

4 Aim of this Study

Basin modeling represents a numerical simulations approach which is used to show and quantify burial and temperature histories of sedimentary basins over the time. Beyond that, petroleum systems modeling is largely used in industry to assess hydrocarbon generation, migration and accumulation.

Until recent past, geo-scientific research including application of basin modeling was either based on the description of individual geological processes or was limited to one dimension (i.e. wellbore). However, modern-day multidimensional basin and petroleum systems modeling considers all geo-processes, their relationships to each other, the vertical and lateral variability over the time, and are even able to treat the occurrence of different processes at the same time. The importance of numerical simulation for handling complex models where properties like pressure, volume and temperature are causally and chronologically linked was firstly described by Welte and Yalcin (1988).

The main goal of this study is to provide for the first time a regional-scale model of the Alpine Foreland Basin of Austria in terms of thermal basin evolution, hydrocarbon generation and migration based on cross-sections and structure maps. Data availability to calibrate the two-dimensional models is satisfying in the actual foreland region due to hundreds of exploration wells drilled, geochemical studies and extensive seismic data acquisition. In a first step, these data were used to reconstruct the evolution of the basin and to establish a better understanding of the heat flow history through time.

However, data is sparse in the vicinity of the hydrocarbon source kitchen under the Northern Alpine fold and thrust belt to the south. Hence, the necessity to link the source kitchen with potential reservoirs faced two important issues: First, it was essential to consider the impact of the tectonically complex fold and thrust belt. On the other hand less calibration data was available to test the models. The integration of (tectonic) structural forward models into the basin and petroleum systems modeling processes turned out to be the only option to tackle this issue. And in fact, this approach was highly valuable. During the last decade, basin and petroleum systems modeling developed quite fast and gained results appear more and more accurate. Nevertheless, consideration of tectonically complex areas in modeling petroleum systems represents a rather new scientific field and publications presenting

systematic approaches are rare (e.g. Baur et al., 2009; Burberry et al., 2010; Parra et al., 2011).

In order to confine uncertainty caused by lack of calibration data, numerous different model runs were performed using different heat flow scenarios. Furthermore, extreme values for heat flows and erosion/uplift rates were applied in sensitivity analysis to define boundary conditions.

Results gained in this study will lead to a better understanding of the Austrian Molasse Basin petroleum systems. Also, it represents an important guideline for future studies on hydrocarbon exploration and development in this basin.

5 Summary of Publications and Contribution to the Field

Publication I

Preliminary model results in the forefront of the PhD study showed that erosion and uplift may have a considerable impact on timing of generation, charging and also on the preservations of hydrocarbons. This paper presents a multi-technique approach to assess amount and timing of uplift and erosion events in the Austrian Molasse Basin. The approach includes application of shale compaction data, fission track data, isopach maps, moisture content of lignite and seismic stratigraphy. Integration of the different data sets allowed the differentiation of different tectonic events during Neogene times.

Tilted prograding clinoforms on 2D seismic sections within the Hall Formation (Eggenburgian) indicate a regional westward tilting event. Overlying Ottnangian sediments of the Innviertel Group have uniform thickness which suggests that tilting occurred at least after Ottnangian time. In addition, onlapping Lower Badenian and Lower Pannonian sequences onto the top of the Innviertel Group indicate that tilting occurred before the Badenian. Thus, the timing of tilting can be attributed to the Karpatian.

Moisture content of lignite samples taken from the Hausruck coal mining district indicate that the supposed Late Miocene paleo-land surface was located at about 1250 m above sea-level. This assumption implies extensive erosion after deposition of Upper Freshwater Molasse, i.e. in post-Early Pannonian time. This time is supported by thermochronological data which indicate regional exhumation of the area after 10 million years before present. The supposed amounts of erosion range between 450 and 800 m. The amount of cooling of 20 °C derived from thermochronological data is poorly constrained. However, estimated erosion of 500 – 700 m fits well to the range of erosion inferred from the moisture content of coal, if a typical geothermal gradient of 3 °C/100 m for this part of the basin is taken into account.

If hydrostatic pressure predominates in an area, shale compaction trends derived from sonic logs can be used to estimate thickness of eroded rocks. Results of this approach suggest that erosion may have been significantly stronger in the eastern part of the study area. Compared to the central part of the study area, up to 1000 m of sediments

were additionally eroded. This local eastern uplift occurred probably contemporaneous with the regional uplift mentioned above.
Changes of basin geometry have an effect on thermogenic and biogenic hydrocarbon systems. Tilting of the basin alters the spill point of potential reservoirs and may change oil-water contacts. Moreover, it controls the trend of migration pathways. Erosion and uplift in the basin may also cause termination of petroleum generation. Other possible related consequences for petroleum systems include changes in gas-oil ratios due to pressure decrease and preferred biodegradation or biogenic gas generation due to cooling of the system. In contrast, burial and temperature increase may intensify the effect of paleo-pasteurization of gas. Publication II and III will provide answers on most of these issues.

Publication II

Recently drilled exploration and development wells and extension of 3D seismic surveys, together with balancing techniques, improved the general understanding of the structure of the Molasse imbricates at the southern basin margin in the recent past. However, the structural evolution of the imbricated and folded southernmost part of the basin is still poorly understood and the hydrocarbon potential is not fully explored. The aim of the present study was to focus on the impact of the fold and thrust belt on the petroleum system mainly within but also beneath the Molasse imbricates. To reach this goal, a two-dimensional thermal basin model was performed along a north-south cross-section in the Perwang imbricates located in the western part of the Austrian Molasse Basin. The thermal model is based on a structural forward model to take the complex kinematic evolution into account. Recent changes in basin geometry due to erosion and uplift events (see Publication I) were considered in this study.
Results from a cross-section restoration have been used to constrain a structural forward model which mimics the evolution of the Perwang imbricates. Although slight simplifications of the geometry of the imbricated zone have been conducted to validate the model for a larger area, it provides a realistic input for the petroleum systems model. In the structural model it is supposed that total tectonic shortening in the section is at least 35.6 km which corresponds to 56 % of shortening.
Heat flow scenarios were applied to determine the thermal history along the modeled section. Formation temperatures indicate moderate present-day heat flows decreasing southwards from 60 to 41 mW/m². In contrast, maturity data indicate lower paleo-heat flows (44 to 28 mW/m²) in a similar southward decreasing trend. The higher present-day heat flow probably indicates a sub-recent increase in heat flow during the

Pliocene and Pleistocene. The cause for the increase is yet not clearly understood. To assess the uncertainty of the model, three different heat flow scenarios were applied. One scenario has been applied to obtain a fit with corrected bottom hole and recent formation temperature values. A second scenario was chosen to obtain a good fit with maturity data. Finally, a combination of these two different scenarios fitting to both maturity and present-day temperature data was applied to the model. In this scenario which is considered most likely, minor hydrocarbon generation (transformation ratio <20 %) occurs only in the deeper parts of the Molasse imbricates and is caused by the described sub-recent heat flow increase. As the amount of heat flow increase depends on the erosion estimate, extreme values were set for sensitivity analysis and different shapes of the paleo-wedge were tested. Model results show that consideration of different amounts of erosion and different geometries of the paleo-wedge surface have little influence on this result.

The low transformation ratio represents a charge risk. However, hydrocarbon generation in the deeper parts of the Perwang imbricates is proven by oil stains and supported by the models shown. Also, it can be concluded that deeper parts of the imbricates are supposed to have a higher hydrocarbon potential and a lower charge risk compared to the smaller, shallower frontal imbricates.

Oil migration out of the Perwang imbricates into nearby autochthonous units was probably limited. If there was any oil migration from deeper to shallower parts of the imbricates remains uncertain. Hence, the potential for future oil exploration will strongly depend on the existence of fault conduits along thrust planes during charge and on the existence of potential traps which retained their integrity during recent basin uplift.

Publication III

The purpose of this publication was to determine hydrocarbon generation in the Alpine sub-thrust and to investigate hydrocarbon migration into the tectonically mainly undeformed foreland. While the stratigraphic evolution of the foreland is relatively well constrained by long-time exploration activity, the imbricated and folded southernmost part is still poorly understood and the hydrocarbon potential is not fully explored.

Therefore, a two-dimensional basin and petroleum systems modeling study was performed, based on a structural forward model, crossing the Sierning imbricates in the eastern part of the study area. This model provides new insights on the hydrocarbon potential as well as on timing of hydrocarbon generation and migration.

Maturity data indicate rather low paleo-heat flows along the modeled section decreasing from north to south from 32 to 26 mW/m². Formation temperatures indicate elevated present-day basal heat flows decreasing in the same direction from 52 to 37 mW/m². Consequently, a heat flow scenario involving a sub-recent (~4 Ma before present) increase in heat flow was assumed as most likely and therefore applied to the model. Modeling results show that the generation of hydrocarbons commenced during the Early Miocene due to deep burial beneath the Alpine nappes and was terminated in the Late Miocene due to cooling caused by uplift and erosion.

Migration of hydrocarbons commenced contemporaneously with their generation, but in contrast, migration continues until present-day. In addition, the 2D migration model reflects numerous observations made in previous independent studies. These include: (1) long distance (> 50 km) northward lateral migration of oil and gas to the foreland; (2) lateral oil migration along the source rock layer and subsequent vertical migration to stratigraphically deeper reservoir horizons as soon as appropriate fault systems (i.e. having enough offset) are reached; (3) Gas migration along faults into the Sierning imbricates zone; (4) Apparent diffusive vertical migration of gas in the foreland region up into Oligocene and Miocene Puchkirchen and Hall formations.

In a next step, a flow path modeling approach was applied based on structure maps of the two main carrier/reservoir horizons. This ‘Pseudo 3D’ model produced ambiguous results. While some major existing fields were successfully predicted, the approach failed predicting other fields. Beyond that, the model shows accumulations in the western study area where no hydrocarbons were found yet. On the one hand, the mismatch between modeling results and prevailing facts is partly related to low model resolution outside the 3D seismic coverage. On the other hand, the mismatch supports insights from previous independent studies. Sachsenhofer and Schulz (2006) emphasized that source rocks in the western study area have been removed by tectonic erosion and are now integrated in the Molasse imbricates. This suggests, together with the model results, that the absence of fields in this sector of the basin is rather a consequence of missing charge (due to absence of source rocks) than of missing structures. Moreover, the model reflects that migration did not only occur along main carrier beds but also along major fault systems.

Furthermore, this study addresses biodegradation of gas. The 2D modeling results indicate that deep burial of the section at about 9 million years before present increased the temperature in potential reservoir rocks and led to ‘paleopasteurization’ of gas reservoirs in the vicinity of the northern basin margin. The model may also explain that occurrence of biodegradation of gas in the Austrian Molasse Basin is limited to a depth interval above 800 – 1000 m sub-sea.

References

Allen, P.A. and Allen J.R., 1990. Basin Analysis – principles and applications. Blackwell Scientific Publications, 642 pp.

Bachmann, G. H. and Mueller, M., 1992. Sedimentary and structural evolution of the German Molasse Basin. Eclogae Geologicae Helvetiae, 85, 519–530.

Báldi, T., 1984. The terminal Eocene and Early Oligocene events in Hungary and the separation of an anoxic, cold Paratethys. Eclogae Geologicae Helvetiae, 77, 1–27.

Barker, C., 2000. A paleoatitude approach to assessing surface temperature history for use in burial heating models. Coal Geology, 43, 121-135.

Baur, F., Di Benedetto, M., Fuchs, T., Lampe, C. and Sciamanna, S., 2009. Integrating structural geology and petroleum systems modeling – A pilot project from Bolivia's fold and thrust belt. Marine and Petroleum Geology, 26, 573-579.

Baur, F., 2010. Quantification of heat and fluid flow through time by 3D modeling: an example from the Jeanne d'Arc basin, offshore eastern Canada. PhD thesis, RWTH Aaachen, 170 p.

Bernhardt, A., Stright, L. and Lowe, D.R., 2012. Channellized debris-flow deposits and their impact on turbidity currents: the Puchkirchen axial channel belt in the Austrian Molasse Basin. Sedimentology, DOI: 10.1111/j.1365-3091.2012.01334.x.

Brigaud, F., Chapman, D. and Douran, S., 1990. Estimating thermal conductivity in sedimentary basins using lithologic data and geophysical logs. AAPG Bulletin, 74, 9, 1459-1477.

Burberry, C., Greb, M., Laughland, M., Dudley-Murphy, B. and Nash, G., 2010. Integrated Remote Sensing, Structural and Petroleum Systems Modeling of the Iraqi-Kurdish Fold Belt. 2010 AAPG Annual Convention and Exhibition, Abstract.

Czurda, K., 1978. Sedimentologische Analyse und Ablagerungsmodell der miozänen Kohlemulden der oberösterreichischen Molasse. Jb. Geol. B.-A., 121, 123-154.

De Ruig, M.J. and Hubbard, S.M., 2006. Seismic facies and reservoir characteristics of a deep marine channel belt in the Molasse foreland basin. AAPG Bulletin, 90, 735-752.

Dohmann, L., 1991. Die unteroligozaenen Fischschiefer im Molassebecken. Ph.D. thesis, Ludwig Maximilian Universitaet, Munich, 365 pp.

Dow, W., 1977. Kerogen studies and geological interpretations. Journal of Geochemical Exploration, 7, 79-99.

Durand, B., Alpern, B., Pittion, J. and Pradier, B., 1986. Reflectance of vitrinite as a control of thermal history of sediments. 1st IFP Exploration Research Conferences, 441-474.

Espitalié, J., LaPorte, J.L., Madec, M., Marquis, F., Leplat, P., Poulet, J. and Boutefeu, A., 1977. Méthode rapide de charactériasation des roches mères de leur potential pétrolier et de leur degré d´evolution. Revue de l´Institut Francais du Pétrole, 32, 23-42.

Espitalié, J., Deroo, G. and Marquis, F., 1985. Rock Eval Pyrolysis and its applications. IFP, France.

Groiss, R., 1989. Geologie und Kohlebergbau im Hausruck (Oberösterreichische Molasse). Arch. f. Lagerst. Forsch. Geol. B.-A. Wien, 11, 167-178.

Grunert, P., Soliman, A., Harzhauser, M., Müllegger,S., Piller, W. E, Roetzel, R. and Rögl, F., 2010. Upwelling conditions in the Early Miocene Central Paratethys sea. Geologica Carpathica, 61, 129–145.

Grunert, P., Soliman, A., Coric A., S. Roetzel, R. Harzhauser, M. and Piller, W.E., 2012. Facies development along the tide-influenced shelf of the Burdigalian Seaway: An example from the Ottnangian stratotype (Early Miocene, middle Burdigalian). Marine Micropaleontology, 84-85, 14-36.

Grunert, P., Hinsch, R., Sachsenhofer, R.F., Bechtel, A., Coric, S., Harzhauser, M., Piller, W.E. and Sperl, H., 2013. Early Burdigalian infill of the Puchkirchen Trough (North Alpine Foreland Basin, Central Paratethys): facies development and sequence stratigraphy. Marine and Petroleum Geology, doi:http://dx.doi.org/10.1016/j.marpetgeo.2012.08.009.

Gusterhuber, J., Dunkl, I., Hinsch, R. Linzer, H.-G. and Sachsenhofer, R.F., 2012. Neogene uplift and erosion in the Alpine Foreland basin (Upper Austria and Salzburg). Geologica Carpathica, 63, 295-305.

Hantschel, T., Kauerauf, A., Wygrala, B., 2000. Finite element analysis and ray tracing modeling of petroleum migration. Marine and Petroleum Geology, 17, 7, 815-820.

Hantschel, T., Kauerauf, A., 2009. Fundamentals of Basin Modeling. Springer Verlag, 425 pp.

Hinsch, R., 2008. New Insights into the Oligocene to Miocene Geological Evolution of the Molasse Basin of Austria. Oil & Gas European Magazine, 34 (3), 138-143.

Hinsch, R., 2013. Laterally varying structure and kinematics of the Molasse fold and thrust belt of the Central Eastern Alps:implications for exploration. AAPG Bulletin, 97, 10, 1805-1831.

Hubbard, S.M., De Ruig, M.J. and Graham, S.A, 2009. Confined channel-levee complex development in an elongate depo-center: Deep-water Tertiary strata of the Austrian Molasse basin. Marine and Petroleum Geology, 26, 85-112.

Janoschek, R., 1961. Über den Stand der Aufschlussarbeiten in der Molassezone Oberösterreichs. Erdoel-Zeitschrift, 77, 161-175.

Jarvie, D., Claxton, B., Henk, F. and Breyer, J., 2001. Oil and shale gas from the Barnett Shale, Fort Worth Basin, Texas (abs): AAPG Annual Meeting Program, 10, p. A100.

Kollmann, K., 1977. Die Öl- und Gasexploration der Molassezone Oberösterreichs und Salzburgs aus regional-geologischer Sicht. Erdoel-Erdgas-Zeitschrift, 93, 36-49.

Krenmayer, H. G., 1999. The Austrian sector of the North Alpine Molasse: A classic foreland basin: FOREGS (Forum of Euopean Geological Surveys) Dachstein-Hallstatt- Salzkammergut Region, Vienna, 22-26.

Kuhlemann, J. and Kempf, O., 2002. Post-Eocene evolution of the North Alpine Foreland Basin and its response to Alpine tectonics. Sedimentary Geology, 152, 45-78.

Linzer, H.-G., 2002. Structural and stratigraphic traps in channel systems and intraslope basins of the deep-water molasse foreland basin of the Alps. AAPG 2002 Annual Convention & Exhibition, Houston, Texas.

Mackenzie, A.S. and McKenzie, D., 1983. Isomerization and aromatization of hydrocarbons in sedimentary basins formed by extension. Geology Magazine, 120, 417-470.

Malzer, O., Roegl, F., Seifert, P., Wagner, L., Wessely, G. and Brix, F., 1993. Die Molassezone und deren Untergrund. In: F. Brix and O. Schultz (eds.), Erdöl und Erdgas in Österreich. Naturhistorisches Museum Wien und F. Berger, 281–358.

Nachtmann, W. and Wagner, L. 1987. Mesozoic and Early Tertiary Evolution of the Alpine foreland in Upper Austria and Salzburg, Austria. Tectonophysics, 137, 61-76.

Parra, M., Sanchez, G., Montilla, L., Guzman, O., Namson, J. and Jacome, M., 2011. The Monagas Fold-Thrust Belt of Eastern Venezuela. Part I: Structural and thermal modeling. Marine and Petroleum Geology, 28, 40-69.

Peters, K. and Moldowan, J., 1993. The biomarker guide; interpreting molecular fossils in petroleum and ancient sediments. Prentice Hall, 363 pp.

Peters, K., Walters, C. and Moldowan, J., 2005. The biomarker guide, 2nd edition. Cambridge University Press, 1155 p.

Peters, K. E., Schenk, O. and Wygrala, B., 2009. Exploration Paradigm Shift: The Dynamic Petroleum System Concept. Swiss Bulletin fuer Angewandte Geologie, 14/1+2, 65-71.

Poelchau, H., Baker, D., Hantschel, T., Horsfield, B. and Wygrala, B., 1997. Basin simulation and the design of the conceptual basin model. In: D.H. Welte, B Horsfield and D. Baker (eds.), Petroleum and Basin Evolution. Springer, 70 pp.

Pohl, W., 1968. Zur Geologie und Paläogeographie der Kohlemulden des Hausruck (O.Ö.). PhD Thesis, University of Vienna 17, 70 pp.

Radke, M. and Welte, D. H., 1983. The methylphenanthrene index (MPI). A maturity parameter based on aromatic hydrocarbon.In: M. Bjoroy, C. Albrecht and C. Cornford (eds.), Advances in Organic Geochemistry, John Wiley and Sons, New York, 504-512.

Reischenbacher, D. and Sachsenhofer, R., 2011. Entstehung von Erdgas in der oberösterreichischen Molassezone: Daten und offene Fragen. BHM, 156 (11), 463-468.

Roeder, D. and Bachmann, G., 1996. Evolution, structure and petroleum geology of the German Molasse Basin, In: P. Ziegler and F. Horvath, (eds.), Peri-Tethys Memoir 2, Structure and Prospects of Alpine Basins and Forelands. Mèmoire du Museum National d'Histoire naturelle, 170, 263-284.

Roegl, F., 1998. Palaeogeographic Considerations for Mediterranean and Paratethys Seaways (Oligocene to Miocene). Annalen des Naturhistorischen Museums in Wien, 99A, 279–310.

Roegl, F., 1999. Mediterranean and Paratethys. Facts and Hypothesis of an Oligocene to Miocene Paleogeography (short overview). Geologica Carpathica, 50, 339-349.

Rullkoetter, J. and Marzi, R., 1989. New aspects of the application of sterane isomerization and steroid aromatization to petroleum exploration and the reconstruction of geothermal histories of sedimentary basins. Reprint Division of Petroleum Geochemistry, American Chemical Society, 34, 126-131.

Rupp, C., Hofmann, T., Jochum, B., Pfleiderer, S., Schedl, A., Schindlbauer, G., Schubert, G., Slapansky, P., Tilch, N., van Husen, D., Wagner, L. and Wimmer-Frey, I., 2008. Geologische Karte der Republik Österreich 1:50.000, Blatt 47 Ried im Innkreis. Erläuterungen zu Blatt 47 Ried im Innkreis. Geological Survey of Austria, Vienna.

Sachsenhofer, R. and Littke, R., 1993. Characterization of organic matter in the Styrian basin (Austria, Pannonian basin system). In: K. Oygard (ed.): Organic Geochemistry, 26-30, Falch Hurtigtrykk, Oslo.

Sachsenhofer, R.F. and Schulz, H.-M., 2006. Architecture of Lower Oligocene source rocks in the Alpine Foreland Basin: a model for syn- and post-depositional source - rock features in the Paratethyan realm. Petroleum Geoscience, 12, 363-377.

Sachsenhofer, R. F., Gratzer, R., Tschelaut,W. and Bechtel, A., 2006. Characterisation of non-producible oil in Eocene reservoir sandstones (Bad Hall Nord field, Alpine Foreland Basin, Austria). Marine and Petroleum Geology, 23, 1-15.

Sachsenhofer, R.F., Leitner, B., Linzer, H.-G., Bechtel, A., Coric, S., Gratzer, R. Reischenbacher, D. and Soliman, A., 2010. Deposition, Erosion and Hydrocarbon Source Potential of the Oligocene Eggerding Formation (Molasse Basin, Austria). Austrian Journal of Earth Sciences, 103, 76-99.

Schmidt, F. and Erdogan, L. T., 1993. Basin modelling in an overthrust area of Austria. In: A.G. Doré, E. Holter, J.H. Augustson, W. Fjeldskaar, S. Hanslien, Ch. Hermanrud, B. Nyland, D. J. Stewart and O. Sylta, (eds.), Basin Modelling: Advances and Applications. NPF Special Publications, 3, 573-581.

Schulz, H.-M., Sachsenhofer, R.F., Bechtel, A., Polesny, H. and Wagner L., 2002. Origin of hydrocarbon source rocks in the Austrian Molasse Basin (Eocene-Oligocene transition). Marine and Petroleum Geology, 19, 683-709.

Schulz, H.-M., Bechtel, A., Rainer, T., Sachsenhofer R.F. and Struck, U, 2004. Paleoceanography of the western Central Paratethys during Early Oligocene nannoplankton zone NP23 in the Austrian Molasse Basin. Geologica Carpathica, 55, 4, 311-323.

Schulz, H.-M. and van Berk, W., 2009. Bacterial methane in the Atzbach-Schwanenstadt gas field (Upper Austrian Molasse Basin), Part II: Retracing gas generation and filling history by mass balancing of organic carbon conversion applying hydrogeochemical modelling. Marine and Petroleum Geology, 26, 1180-1189.

Schulz, H.-M., van Berk, W., Bechtel, A., Struck, U. and Faber, E., 2009. Bacterial methane in the Atzbach-Schwanenstadt gas field (Upper Austrian Molasse Basin), Part I: Geology: Marine and Petroleum Geology, 26, 1163-1179.

Sissingh, W., 1997. Tectonostratigraphy of the North Alpine Foreland Basin: Correlation of Tertiary depositional cycles and orogenic phases. Tectonophysics, 282, 223-256.

SRTM 2004: Void-filled seamless SRTM data V1 (2004) International centre for tropical agriculture (CIAT). Available from the CGIAR-CSI SRTM 90 m Database: http://srtm.csi.cgiar.org and http://www.ambiotek.com/topoview.

Stach, E., Mackowsky, M., Teichmueller, M., Taylor, G. and Chandra, D., 1982. Coal Petrology. Gebrueder Bontraeger.

Sweeney, J.J. and Burnham, A.K., 1990. Evaluation of a simple model of vitrinite reflectance based on chemical kinetics. AAPG Bull., 74, 10, 1559-1570.

Taylor, G., Teichmüller, M., Davies, A., Diessel, C. F. K., Littke, R. and Robert, P., 1998. Organic Petrology. Gebr. Borntraeger, Berlin, 704 pp.

Teichmueller, M., 1982. Application of coal petrological methods in geology including oil and natural gas prospecting. In: E. Stach, M. Mackowsky, M. Teichmueller, R. Teichmueller, G. Taylor and D. Chandra (eds.). Stach's Textbook of Coal Petrology, Gebrueder Bontraeger, 381-413.

Teichmueller, M., 1987. Recent advances in coalification studies and their applications to geology. In: A. Scott (ed.), Coal and coal bearing strata: Recent advances, Blackwell Scientific Publications, 127-169.

Tissot, B.P. and Welte, D.H., 1984. Petroleum Formation and Occurrence. 2nd ed., Springer-Verlag, Berlin, 699 pp.

Veron, J., 2005. The Alpine Molasse Basin – Review of petroleum geology and remaining potential. Bulletin fuer Angewandte Geologie, 10, 75-86.

Vetö, I., 1987. An Oligocene sink for organic carbon: Upwelling in the Paratethys. Palaeogeography, Palaeoclimatology, Palaeoecology, 60, 143–153.

Wagner, L., 1980. Geological Characteristic of the Main Oil and Gas Producing Formations of the Upper Austrian Molasse Basin – Part 1. The Eocene Sandstones. Erdoel-Erdgas-Zeitschrift, 96, 338-345.

Wagner, L., Kuckelkorn, K. and Hiltmann, W., 1986. New results on the Alpine Orogeny in Upper Austria based on the Oberhofen 1 Well – Stratigraphy, Facies, Maturity and Tectonics. Erdöl, Erdgas, Kohle, 102, 1, 12-19.

Wagner, L.R., 1996. Stratigraphy and hydrocarbons in the Upper Austrian Molasse Foredeep (active margin). In: G. Wessely and W. Liebl (eds.), Oil and Gas in Alpidic Thrustbelts and Basins of Central and Eastern Europe. EAGE Special Publications, 5, 217-235.

Wagner, L.R, 1998. Tectono-stratigraphy and hydrocarbons in the Molasse foredeep of Salzburg, Upper and Lower Austria. In: A. Mascle, C.Puigdefàbregas, H.P.Luterbacher and M.Fernandez (eds.), Cenozoic Foreland Basins of Western Europe. Geological Society, Special Publications, 134, 339-369.

Wehner, H., and Kuckelkorn, K., 1995. Zur Herkunft der Erdöle im nördlichen Alpen-/Karpatenvorland. Erdöl, Erdgas, Kohle, 111, 12, 508–514.

Welte, D. H. and Yukler, M. A., 1981. Petroleum origin and accumulation in basin evolution - A quantitative model. AAPG Bulletin, 65, 1387-1396.

Welte, D. and Yalcin, M., 1987. Formation and occurrence of petroleum in sedimentary basins as deduced from computer-aided basin modeling. In S. P. Kumar, P. Dwivedi, V.Banerjie and V. Gupta (eds.), Petroleum geochemistry and exploration in the Afro-Asianregion, 17-23.

Welte, D. H. and Yalcin, M.N., 1988. Basin modelling - A new comprehensive method in petroleum geology. Organic Geochemistry, 13, 141-151.

Welte, D. H., Horsfield, B. and Baker, D.R., 1997. Petroleum and Basin Evolution. Springer Verlag, 535 pp.

Wygrala, B., 1988. Integrated computer-aided basin modeling applied to analysis of hydrocarbon generation history in a Northern Italian oil field. Organic Geochemistry, 13, 187-197.

Wygrala, B., 1989. Integrated study of an oil field in the southern Po Basin, northern Italy. PhD thesis, University of Cologne, 226pp.

Yalcin, M., Littke, R. and Sachsenhofer, R., 1997. Thermal history of sedimentary basins. In: D.H. Welte, B. Horsfield and D. Baker (eds.), Petroleum and Basin Evolution. Springer, 3–70.

Yuekler, A., Cornford, C. and Welte, D., 1978. One-dimensional model to simulate geologic, hydrodynamic and thermodynamic development of a sedimentary basin. Geologische Rundschau, 67, 3, 960–979.

Ziegler, P. A. and Roure, F., 1999. Petroleum systems of Alpine-Mediterranean foldbelts and basins. In: B. Durand, L. Loivet, F. Horváth and M. Séranne (eds.), Geological Society Special Publications, 156, 517–540.

6 Publications

6.1 Publications included in this Thesis and Author Contributions

Publication I

Neogene Uplift and Erosion in the Alpine Foreland Basin (Upper Austria and Salzburg)

Juergen Gusterhuber, István Dunkl, Ralph Hinsch, Hans-Gert Linzer, Reinhard F. Sachsenhofer

Geologica Carpathica, 63, 4, August 2012, 295-305.

doi: 10.2478/v10096-012-0023-5

Author contributions

The author reviewed geophysical well log data, conducted investigations on shale compaction and wrote the manuscript. Fission track analyses were provided by I. Dunkl. R. Hinsch helped with the interpretation of 2D seismic data and on creating the structure maps. R. Sachsenhofer helped to outline the manuscript, provided fruitful discussions particularly on coal data and proof read the manuscript. G. Linzer contributed with discussions on seismic data.

Publication II

Evaluation of hydrocarbon generation and migration in the Molasse fold and thrust belt (Central Eastern Alps; Austria) using structural and thermal basin models

Juergen Gusterhuber, Ralph Hinsch, Reinhard F. Sachsenhofer

AAPG Bulletin, 2013/2014, in press.

doi: 10.1306/06061312206

Author contributions

The author evaluated the calibration data, prepared polished sections for vitrinite reflectance measurements, conducted vitrinite measurements on the microscope, performed the basin and petroleum systems model and wrote the manuscript. The structural forward model as well as the corresponding interpretation was provided by

R. Hinsch. R. Sachsenhofer helped during interpretation of the modeling results and proof read the manuscript.

Publication III

Hydrocarbon generation and migration from sub-thrust source rocks to foreland reservoirs: The Austrian Molasse Basin.
Juergen Gusterhuber, Ralph Hinsch, Hans-Gert Linzer, Reinhard F. Sachsenhofer
Austrian Journal of Earth Sciences, 2013/2014, submitted manuscript.
Author contributions
The author reviewed the calibration data and conducted vitrinite reflectance measurements. J Gusterhuber also performed all basin and migration models including interpolation work on reservoir structure maps and wrote the manuscript. R. Hinsch designed the structural forward model and provided the interpretation of relevant data. R. Sachsenhofer provided valuable insights on gas migration, was helpful during interpretation of the results and proof read the manuscript. G. Linzer contributed with helpful discussions.

6.2 Abstracts and Posters (not included in this thesis)

Gusterhuber, J., Sachsenhofer, R.F. and Linzer, H.-G., 2010. 2D Becken/Kohlenwasserstoffsystem Modellierung der westlichen Molassezone Österreichs. Geosciences, PANGEO Conference 2010, Fundamentals and Applications, 130-131.

Gusterhuber, J., Sachsenhofer, R.F. and Linzer, H.-G., 2011. A 2D Basin and Petroleum Systems Modelling Study in an Overthrust Setting– the Alpine Molasse Basin, Austria. 73rd EAGE Conference & Exhibition incorporating SPE EUROPEC 2011, Vienna.

Gusterhuber, J., Hinsch, R., Linzer, H.-G. and Sachsenhofer, R.F, 2011. A multidimensional basin and petroleum systems modelling study in an overthrust setting – the Alpine Molasse basin (Austria). International Association for Mathematical Geosciences (IAMG) Conference 2011, Salzburg.

Neogene Uplift and Erosion in the Alpine Foreland Basin (Upper Austria and Salzburg)

Geologica Carpathica, 63, 4, August 2012
doi: 10.2478/v10096-012-0023-5

Juergen Gusterhuber[1], István Dunkl[2], Ralph Hinsch[3], Hans-Gert Linzer[3], Reinhard F. Sachsenhofer[1]

[1]Department Applied Geosciences and Geophysics, Chair of Petroleum Geology, Peter-Tunner-Strasse 5, A-8700 Leoben, Austria.
juergen.gusterhuber@unileoben.ac.at; reinhard.sachsenhofer@unileoben.ac.at
[2]Sedimentology & Environmental Geology, Geoscience Center, University of Göttingen, Goldschmidtstraße 3, D-37077 Göttingen, Germany.
istvan.dunkl@geo.uni-goettingen.de
[3]RAG Rohöl-Aufsuchungs Aktiengesellschaft, Schwarzenbergplatz 16, A-1015 Vienna, Austria
ralph.hinsch@rag-austria.at; hans-gert.linzer@rag-austria.at

Abstract

In the present paper we apply a multi-technique approach (shale compaction data, seismic stratigraphy, isopach maps, moisture content of lignite, fission track data) to assess timing and amount of uplift and erosion of the Alpine Foreland Basin. The combination of the different techniques allows us to discriminate the effects of two different erosion events during the Neogene: (1) Seismic stratigraphy and isopach maps indicate a Karpatian (Early Miocene) regional tilting of the basin to the west (slope of about 0.5 %) and a minor erosion phase. (2) Moisture content of lignite combined with fission track data provides evidence for extensive regional uplift after deposition of Late Miocene

fluvial deposits. It is estimated that sediments, 500 to 900 m thick, have been eroded. Shale compaction data derived from sonic logs indicates additional uplift of the eastern part of the basin (near river Enns). Here, 300 to 1000 m of sediments were additionally eroded (giving a total erosion of about 1000 to 1900 m!), with a general increase of erosion thickness towards the northeast. While the regional uplift is probably related to isostatic rebound of the Alps after termination of thrusting, the local uplift in the east could be affected by Late Neogene E-W compressional events within the Alpine-Pannonian system. Both, tilting and erosion influence the hydrocarbon habitat in the Molasse Basin (tilting of oil-water contacts, PVT conditions, biodegradation).

Key words: Neogene, Alpine Foreland Basin, uplift, erosion, shale compaction, seismic stratigraphy, fission track data.

1 Introduction

Extensive oil and gas exploration activities in the Austrian and German sectors of the Alpine Foreland Basin contributed greatly to a detailed image of the subsurface. But while the stratigraphy, architecture and evolution of the basin fill are reasonably well understood (e.g. Nachtmann & Wagner 1987; Bachmann et al. 1987; Wagner 1996; 1998; Kuhlemann & Kempf 2002) knowledge on Neogene uplift and erosion processes within the basin is largely missing (Genser et al. 2007).

This is in contrast to the Swiss sector of the Alpine Foreland Basin, where several authors, including Schegg & Leu (1998) and Cederbom et al. (2011) investigated amount and timing of erosion. Beside this difference in knowledge a significant higher amount of erosion in the western part of the Alpine Foreland Basin is proven.

The investigation of erosional events in the eastern part of the Alpine Foreland has been initiated in the course of a basin and petroleum systems modelling study in Upper Austria and Salzburg (Gusterhuber et al. 2011) which showed that erosion and uplift may have strong effects on timing of generation, charging and preservation of hydrocarbons.

Different techniques, including shale compaction, lignite compaction, and low temperature thermochronology are applied in the present paper with the objective to assess the timing and magnitude of Neogene uplift and erosion.

2 Geological Setting

The Alpine Foreland Basin (Molasse Basin) of Salzburg and Upper Austria represents a part of the Alpine-Carpathian Foredeep (Figure 1). It was formed due to the collision of the Alpine orogenic system with the southern margin of the European platform in the middle Paleogene. The basin displays a typical asymmetric peripheral foreland basin in terms of an increasing basin depth towards the Alpine thrust front in the south and a gradual shallowing and narrowing trend from west to east towards the spur of the Bohemian Massif (Malzer et al. 1993).

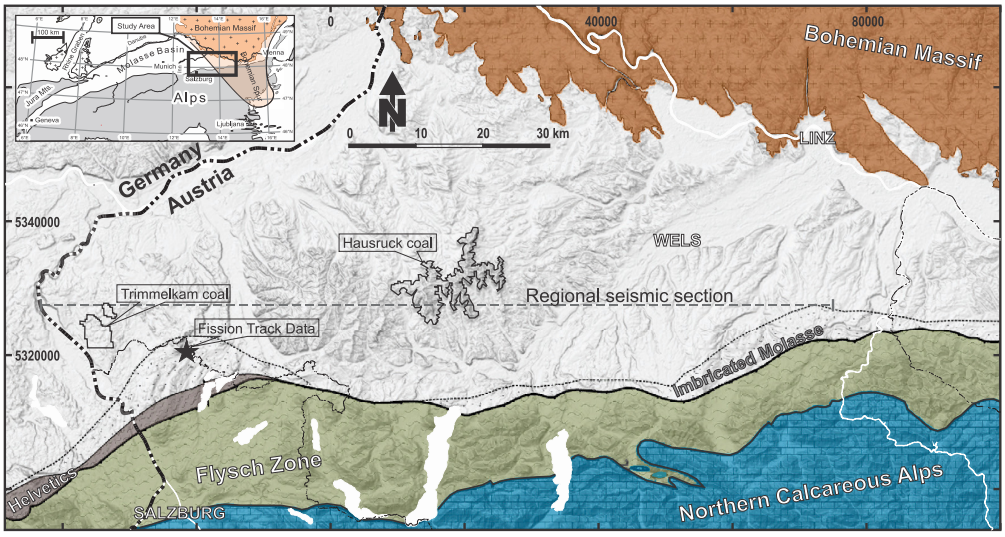

Figure 1: Simplified geological map of the study area superposed on shaded relief digital elevation model created from SRTM data (SRTM 2004). The positions of data discussed in the paper are given: The regional seismic section (Figure 5), the well position of the Fission Track samples (Per-001) and the outlines of coal mining areas (samples for Lignite digenesis analysis; Figure 6). The inset map (top left) shows the position of the study area in the frame of the Northern Alpine Foreland.

The crystalline basement of the Molasse Basin is overlain by an incomplete cover of Late Paleozoic and Mesozoic rocks (Figure 2). Erosion during latest Cretaceous time left a peneplain on which the Tethyan Sea progressively

transgressed during latest Eocene and earliest Oligocene times. At this stage the Molasse basin was formed and became the pelagic Alpine Foredeep. The area rapidly subsided to deep water conditions accompanied by the development of an E-W trending fault network due to downward bending of the European Plate (Wagner 1996; 1998).

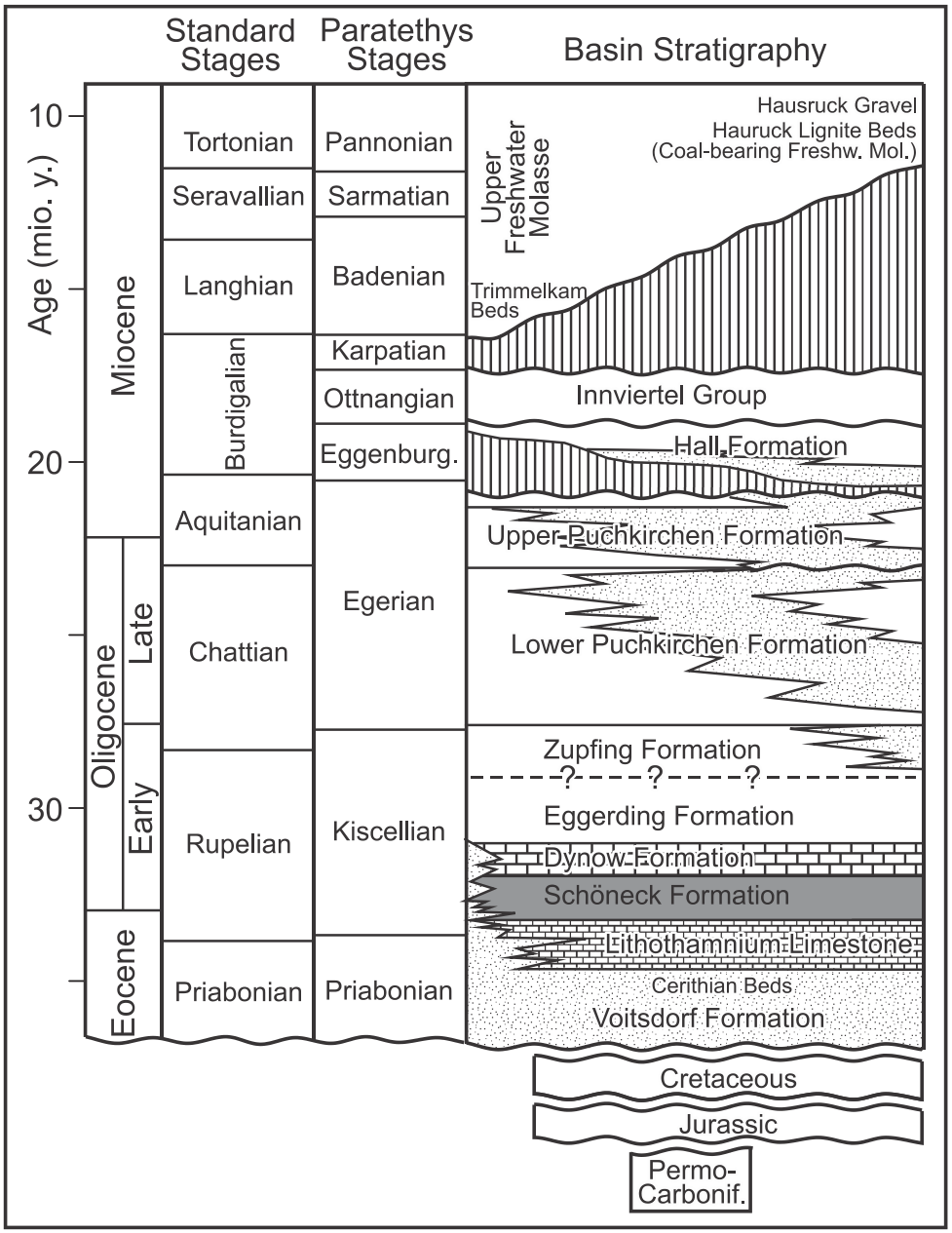

Figure 2: Stratigraphy of the Austrian part of the Alpine Foreland Basin (modified after Wagner 1998).

Approximately at the Eocene-Oligocene boundary, strong tectonic activities changed the Eurasien configuration and separated the Tethyan Sea into the Paratethys in the north and the Mediterranean in the south. The closure of the Indo-Pacific connection caused the first isolation of the Paratethys. Deep basins with reduced circulation and oxygen deficient bottom conditions led to the deposition of marine organic matter-rich rocks, which are the source for thermogenic hydrocarbons in the Molasse Basin (Schoeneck, Dynow, Eggerding Formations; Schulz et al. 2002; 2005; Sachsenhofer et al. 2010). Thereafter new seaways opened from the Mediterranean and the Indian Ocean to the Paratethys causing normal marine oxygenated bottom conditions (Roegl 1999). In the Late Oligocene and earliest Miocene, uplift of the Alps caused increased sediment discharge from the south correlating with a distinct eustatic sea-level fall and the incision of a slope-parallel (E-W) trough by strong bottom currents (Krenmayer 1999) and corresponding widespread deposition of deepwater channels (Linzer 2002; De Ruig & Hubbard 2006). Contemporaneous sediments of the deep water Lower and Upper Puchkirchen Formation (Egerian) are represented by coal-bearing continental to brackish clays and sands along the northern margin of the study area (Krenmayer 1999). In the Early Burdigalian (Eggenburgian), deep water conditions persisted during deposition of the Hall Formation when a gradual transition to shallow-water sedimentation occurred with continental slope-delta progradation across the area (Hinsch 2008; Hubbard et al. 2009).

Marine conditions continued during Ottnangian time with the deposition of the Innviertel Group (e.g. Faupl & Roetzel 1987; Grunert et al. 2010). While fully-marine, tidal dominated silts and sands represent Early and Middle Ottnangian transgressive and highstand phases, brackish-fluvial sediments of the Oncophora Beds were deposited during a Late Ottnangian regressive phase (Roegl 1998; Grunert et al. 2011). Based on their brackish character, a separation of the Oncophora Beds from the Innviertel Group is under discussion (Rupp et al. 2008).

Following a major hiatus, a thick succession of coal-bearing clays, sands and fluviatile gravels was deposited (Upper Freshwater Molasse). In Upper Austria, freshwater deposition commenced in Early Badenian time in the western Trimmelkam area (Rein in Weber & Weiss 1983; see Figure 1 for location) and became gradually younger towards the east. In the Hausruck area Badenian and Sarmatian deposits are missing and Pannonian coal measures directly overlie Ottnangian deposits (Czurda 1978). This indicates that sedimentation proceeded

eastwards on a tilted surface and agrees with the observation that coal-bearing beds in the Hausruck area were deposited in erosional depressions within a generally southwestward dipping peneplain (Pohl 1968; Groiss 1989). The youngest preserved deposits in the Upper Austrian part of the Molasse Basin are fluviatile Hausruck Gravels. These are poorly dated, but generally attributed to the Pannonian (Rupp et al. 2008). Obviously, today the Molasse Basin is an erosional domain.

Badenian lignite seams have been mined in the western Trimmelkam district, whereas Pannonian lignite was exploited in the Hausruck mining district (Weber & Weiss 1983).

3 Data and Methods

The study is based on seismic data, well log data, moisture content of lignite and fission track data.

3.1 Seismic data

Large parts of the Upper Austrian part of the Molasse basin are covered by high quality 3D seismic data. These data have been used to outline progradational patterns within the Hall Formation. In addition, stratigraphic information from the wells was used to map the base of the Innviertel Group (representing a significant part of the Upper Marine Molasse) and the base of the Upper Freshwater Molasse, as well as thickness of sediments between both. These shallow stratigraphic markers are often picked from mud logging or well log response and not always confirmed by micropaleontology. Thus, some uncertainties in the order of 10th of meters might be regarded to the individual picks. To moderate uncertainties, the created surfaces have been smoothed on a 1*1km grid. The created surface therefore reflects the trends of the stratigraphic surfaces.

3.2 Shale compaction / Log data

Shale compaction is irreversible and directly related to overburden stress (burial depth) if pore pressure is hydrostatic. Obviously, deeply buried shales which reached a given depth will be more strongly compacted after uplift and erosion than shales at the same depth in an area without erosion. Thus, in an area with

hydrostatic pressure shale compaction trends can be used to estimate the thickness of eroded rocks (Magara 1976; 1980). The amount of compaction can be quantified from the sonic log because sonic transit time is a result of interaction between porosity and rock matrix in a uniform lithology like shales. In the present study sonic logs from 80 boreholes have been used to quantify erosion.

3.3 Moisture content of lignite

Similar to shale, the compaction of low-rank coal is mainly controlled by burial depth and increasing overburden pressure. The moisture content of lignite (on an ash free basis, af) provides a great tool to monitor this process. A data set from (as received) lignite in the Lower Rhine Embayment (Kothen & Reichenbach 1981) confirms this relation (Figure 6). Because the ash yield of lignite from the Lower Rhine Embayment is typically only 1 to 2 %, the difference between moisture contents on an as received and an ash free basis is negligible. Thus, in the present paper the moisture depth trend in Figure 6 is used to estimate the thickness of overburden rocks in the Hausruck and Trimmelkam areas. Analytical data from 31 pillar samples from the Pannonian-age Hausruck lignite have been reported by Pohl (1968). Data from the Badenian-age Trimmelkam lignite have been provided by Weber & Weiss (1983). Both data sets have been used to calculate moisture contents (af).

3.4 Low temperature thermochronology

In order to detect the magnitude and timing of the post-depositional burial temperature we have performed low temperature thermochronology using apatite fission track and apatite (U-Th)/He methods (AFT and AHe, respectively). Several samples from different stratigraphic horizons have been investigated, but only one sample from well Per-001 (see Figure 1; 1600 m depth) yielded suitable contents of apatite

3.5 AFT

The apatite crystals were embedded in epoxy resin and the crystal mounts were polished by diamond using a five-step procedure. In order to reveal the spontaneous tracks the apatite mounts were etched by 5.5 N nitric acid at 21°C for 20 seconds (Donelick et al. 1999). Neutron irradiations were performed at the nuclear reactor of Oregon State University, USA. The external detector

method was used (Gleadow 1981); after irradiation the induced fission tracks in the mica detectors were revealed by etching in 40 % HF for 35 min. Track counts were made with a Zeiss-Axioskop microscope – computer-controlled stage system (Dumitru 1993), with a magnification of 1000. The FT ages were determined by the zeta method (Hurford & Green 1983) using age standards listed in Hurford (1998).

3.6 AHe

Only single crystal aliquots were dated; and only inclusion and fissure-free specimens with a well-defined external morphology were used. The shape parameters were determined and archived by multiple digital microphotographs. The ejection correction factor (Ft) was determined for the single crystals by the method of Farley (2002). The crystals were wrapped in ca. 1x1 mm sized platinum capsules and degassed by heating an infrared diode laser. The extracted gas was purified using a SAES Ti-Zr getter at 450 °C. The chemically inert noble gases and a minor amount of other rest gases were expanded into a Hiden triple-filter quadrupole mass spectrometer equipped with a positive ion counting detector. No analysed crystal exhibited residual gas >1% after the first extraction. Following degassing, samples were retrieved from the gas extraction line, spiked with calibrated 230Th and 233U solutions and dissolved in a 2% HNO3 + 0.05% HF acid mixture in teflon vials. Each sample batch was prepared with a series of procedural blanks (including Pt tube blanks) and spiked normals to check the purity and calibration of the reagents and spikes. Spiked solutions were analysed as 0.5 or 0.8 ml of ~ 0.5 ppb U-Th solutions by isotope dilution on a Perkin Elmer Elan DRC II ICP-MS with a APEX micro-flow nebulizer. Procedural U and Th blanks by this method are usually very stable and below 1.5 pg. Sm, Pt and Ca were determined by external calibration.

4 Results

4.1 Shale compaction

Figure 3 shows the depth trend of the sonic transit times for the Eggerding Formation. In order to minimise effects due to lithology variations, only the shaly upper part of the Eggerding Formation, which is typically characterized

by uniform transit times, is considered (see inset in Figure 3). The data, which are from wells located in different parts of the study area (Figure 4a), follow a well-defined exponential trend, which reflects increasing shale compaction with burial depth. Actually exponential relations are the most widely accepted equation for describing shale compaction (Issler 1992), although linear shale compaction trends have also been reported (e.g. Wells 1990).

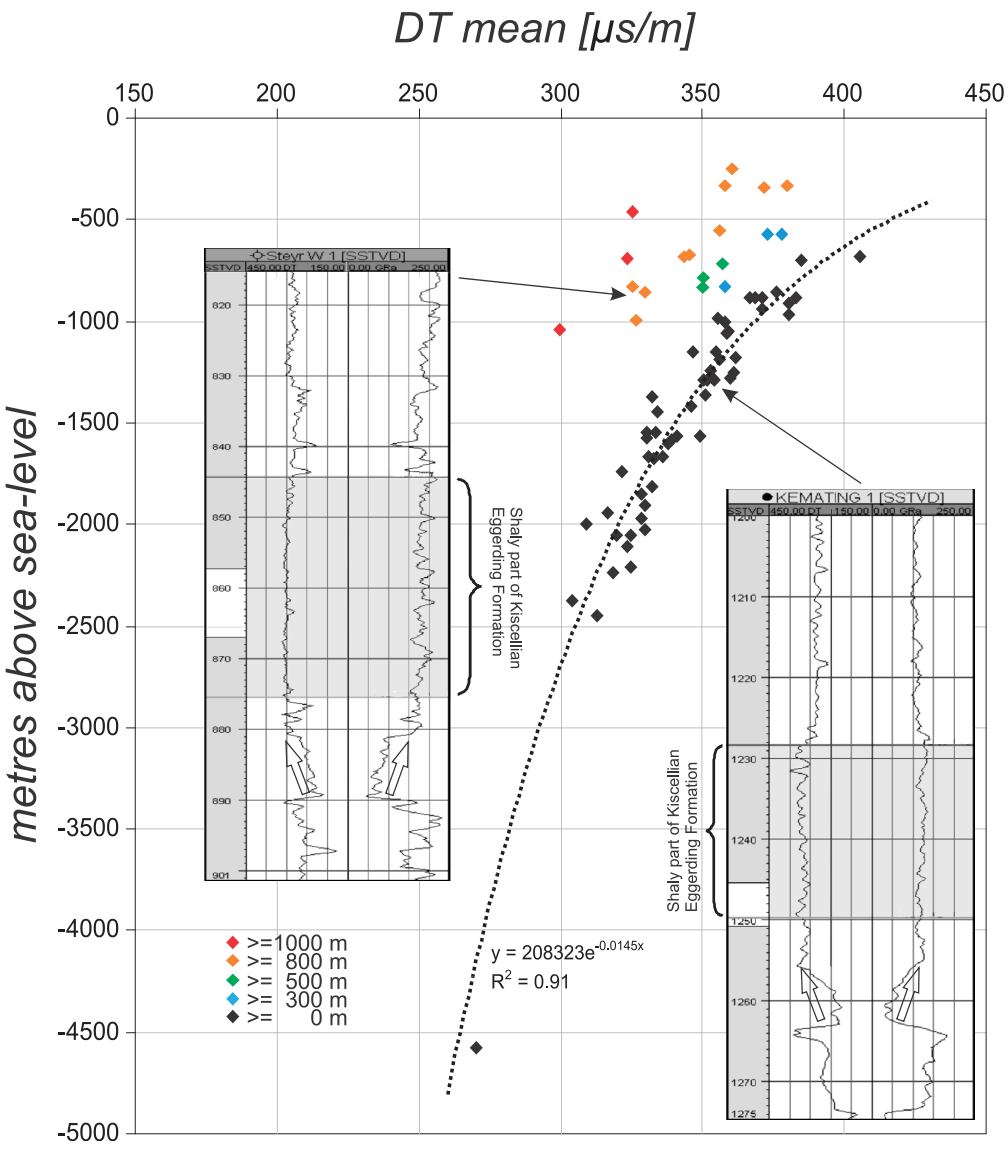

Figure 3: Transit-time of the shaly interval of the Oligocene Eggerding Formation vs. metres above sea-level for several wells.

It is important to note, that the Eggerding Formation shows relatively low transit times and significant deviations from the "normal" exponential

compaction curve in some shallow wells. All “abnormal” wells are located in the eastern part of the study area. A comparison of the gamma ray logs from the “abnormal” Steyr W 1 and the “normal” Kemating 1 wells (inset in Figure 3) suggests that this is not due to an eastward increase in sand content, but due to overcompaction. Consequently, we conclude that the easternmost part of the study area experienced more uplift and erosion than its main part. The vertical deviation of the measured data points from the normal compaction trend allows a quantification of the additional amount of erosion. These data range from 300 to 1000 m and are mapped in Figure 4a.

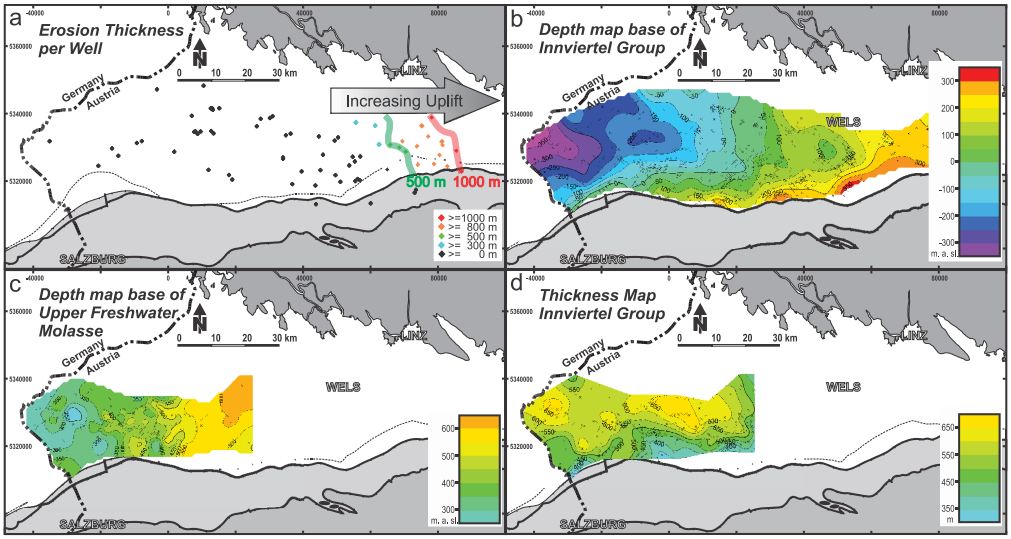

Figure 4: Results from different analysis, displayed on a study area map (for background geology see Figure 1). a) Estimated amount of erosion from shale compaction analysis of the Eggerding Formation in several wells (small diamonds). Hand-contoured isolines mark 500 m (green) and 1000 m (red). b) Interpolated present day depth map (metres above sea-level – m.a.sl) of the base of Innviertel Group from well data (small dots). c) Interpolated present day depth map of the base of Upper freshwater Molasse from well data (small dots). d) Interpolated thickness of the Innviertel Group from well data (small dots). In order to determine the thickness of the Innviertel Group before deposition of the Upper Freshwater Molasse, only areas where the Innviertel Group is overlain by the latter are considered.

4.2 Seismic stratigraphic aspects of the Hall Formation

Eggenburgian sediments of the Hall Formation exhibit progradational patterns, which indicate eastward sediment transport (Figure 5). It is reasonable to assume that during progradation, the top of the sedimentary package (toplap-surface) was horizontal. Thus, the observed present-day inclination of the toplap surface was horizontal during its formation. Consequently, the observed

pattern implies a distinct eastward tilting of the basin since Eggenburgian time. The seismic section flattened to the base of the Innviertel Group (= top Hall Fm.) displays the original geometry before the tilting event (Figure 5).

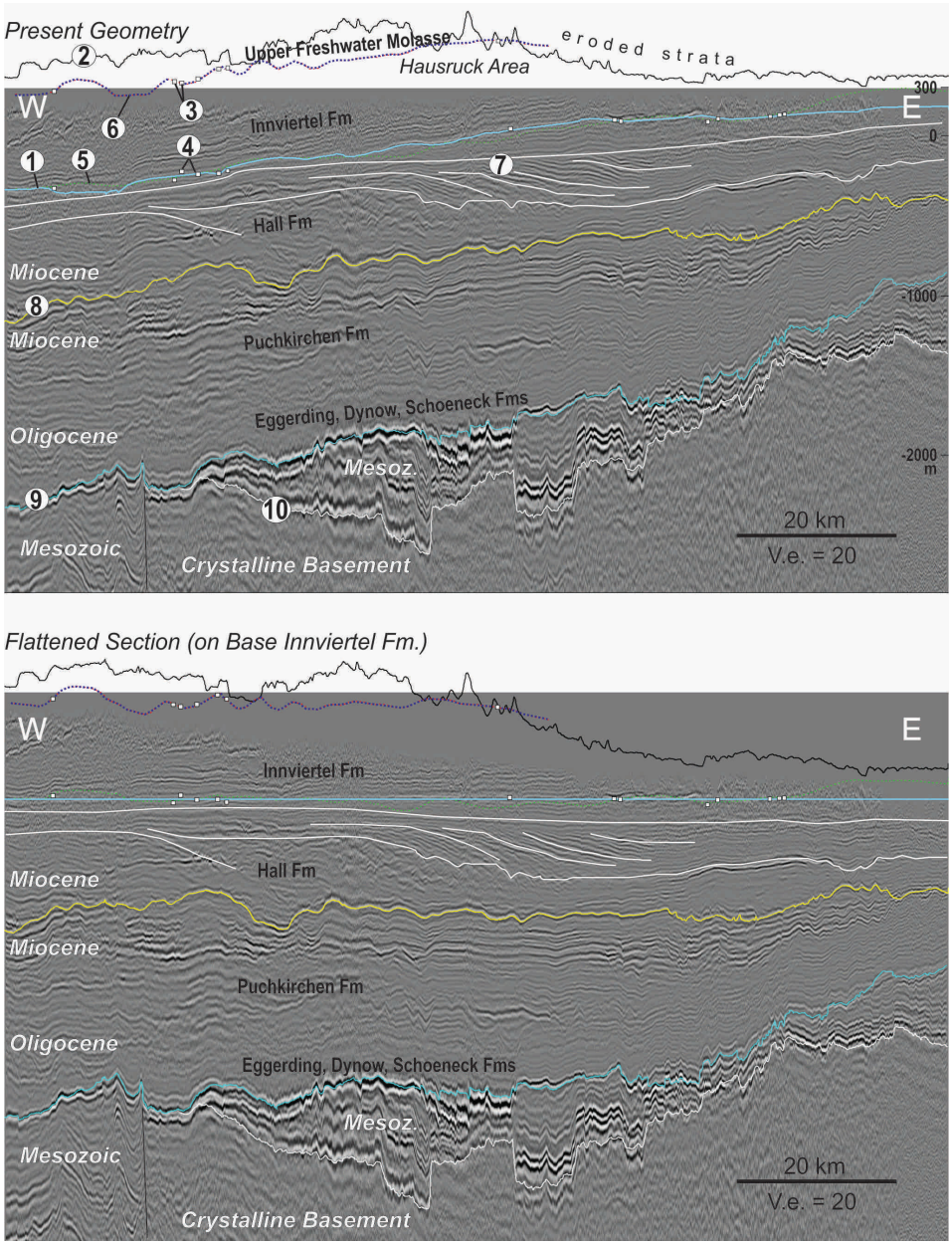

Figure 5: Regional W-E 3D-reflection-seismic section in depth (vertical exaggeration 20 times, for position see Figure 1) showing the present day geometry (upper section) and the geometry "flattened" on the interpreted base of Innviertel Group (point 1) in the lower section. The morphology (point 2) is created from SRTM 2004 data. Small squares represent projected well-tops of Base of Upper Freshwater Molasse and Base of Innviertel Group (Points 3 and 4 respectively) as well as the interpolated surfaces (dotted lines, points 5 and 6, cf. Figure 4b, c)). The prograding system in Hall Formation is indicated (point 7). Additional regional horizons marked are Base of Hall unconformity (point 8), Top of Eocene (point 9) and Top of Crystalline Basement (point 10).

4.3 Elevation of base Innviertel Group and base Upper Freshwater Molasse

Based on 3D seismic data and information from 698 wells depth-maps of base Innviertel Group (=top Hall Fm.), base Upper Freshwater Molasse (=top Innviertel Group) and a thickness-contour-map of the Innviertel Group have been compiled (Figure 4b-d).

Figure 4b shows the elevation of the smoothed base of the Innviertel Group. The general trend of this surface reflects the morphological evolution reasonably. The elevation increases gradually from west to east from -300 m to +300 m a.sl. (above sea-level). The Upper Freshwater Molasse is only preserved in the eastern part of the study area. There the elevation of its base shows a similar trend as the base of the Innviertel Group and increases eastwards from +300 m to +600 m a.sl. (Figure 4c). The intersection of both horizon maps with the seismic line is also displayed in Figure 5.

The thickness-contour-map of the Innviertel Group shows a rather uniform thickness of 550 to 600 m along the basin axis (W-E direction; Figure 4d).

This suggests that (1) the effect of erosion during Karpatian time before deposition of the Upper Freshwater Molasse was minor and (2) that the Ottnangian Innviertel Group was tilted together with the Hall Formation.

4.4 Moisture content of Hausruck and Trimmelkam lignite

The average moisture content of Pannonian-age Hausruck lignite is 44.2 %(af) (standard deviation: 2.05 %; Pohl, 1968). Considering the moisture depth trend for the Lower Rhine Embayment (Figure 6), this value suggests burial of the Hausruck lignite beneath about 650 m thick overburden. The present-day elevation of the Hausruck lignite seams varies between 580 and 650 m a. sl. This suggests a Late Miocene paleo-land-surface at about 1250 m a. sl., which is in contrast to the highest present-day elevation in the Hausruck area of 801 m a. sl. (Goebelberg). Uncertainties of the erosion estimate are related to the influence of coal facies on moisture depth trends and the role of erosion in the Lower Rhine Embayment. In any case, the moisture content in the Hausruck lignite implies extensive uplift and erosion.

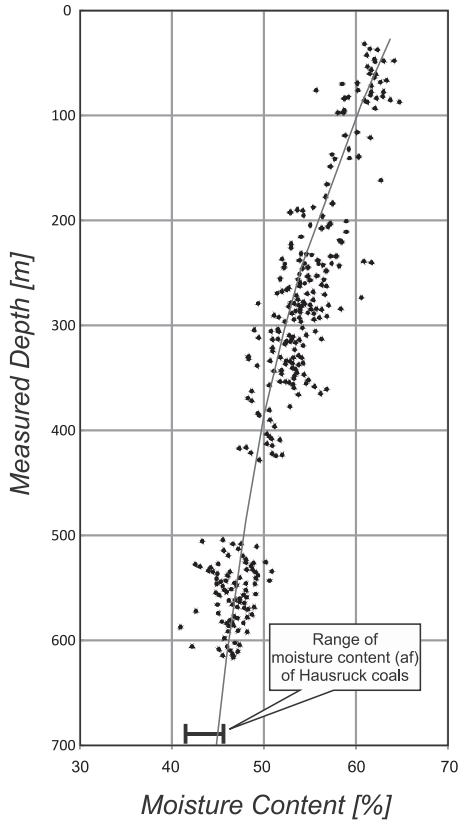

Figure 6: Moisture depth trend of lignite from the Lower Rhine Embayment (after Kothen & Reichenbach 1981).

Lignite in the Trimmelkam area is characterized by even lower moisture contents of (~35 % af; Weber & Weiss, 1983). Unfortunately, Figure 6 cannot be used to estimate the thickness of the original overburden. However, the lower moisture content well agrees with the lower elevation of the Trimmelkam lignite (300-350 m a. sl.) and might be a result of burial beneath nearly 1000 m of overburden. Note, that the low moisture content of the Trimmelkam lignite has been previously explained by the pressure effect of the Pleistocene Salzach glacier. However, the Salzach glacier only reached a maximum thickness of 600 m in the Trimmelkam area (van Husen 1987).

4.5 Fission track data (U-Th/He; AFT, AHe)

The AFT and AHe data of sample Per-001 (1600 m; Upper Puchkirchen Fm.) are rather consistent (Table 1). The apparent AFT age is older than the age of deposition (55 Ma vs. 22 Ma), but the mean track length shows significant shortening (12.8 μm). This is an indication of a young thermal overprint. The

AHe ages also prove thermal reset; they are clearly younger than the age of deposition (single-grain ages are between 4.6 and 7.9 Ma).

Sample	aliq.	He vol. [ncc]	He s.e. [ncc]	U238 mass [ng]	U238 s.e. [%]	U238 conc. [ppm]	Th232 mass [ng]	Th232 s.e. [%]	Th232 conc. [ppm]	Th/U ratio	Sm mass [ng]	Sm s.e. [%]	Sm conc. [ppm]	Ejection correct. (Ft)	*Uncorr. He-age [Ma]*	Ft-Corr. *He-age* [Ma]	1s [Ma]	Sample unweighted aver. & s.e.	
Per1 1598.5-	#1	**0.023**	4.691	**0.040**	2.1	7.0	**0.048**	2.5	8.4	1.203	**0.104**	7.6	18	**0.720**	*3.7*	**5.1**	0.3		
-1601.5 K7 Ki2	#3	**0.042**	3.497	**0.042**	2.1	11.1	**0.173**	2.4	46.2	4.160	**0.693**	7.4	185	**0.598**	*4.0*	**6.6**	0.5		
	#5	**0.142**	2.274	**0.090**	1.9	8.1	**0.339**	2.4	30.4	3.767	**2.942**	7.7	264	**0.767**	*6.0*	**7.9**	0.4		
	#6	**0.005**	10.140	**0.011**	4.3	5.0	**0.012**	3.0	5.5	1.096	**0.089**	8.5	42	**0.588**	*2.7*	**4.6**	0.6	**6.1**	0.7

Amount of helium is given in nano-cubic-cm in standard temperature and pressure
Amount of radioactive elements are given in nanograms
Ft: alpha-ejection correction (according to Farley, 2002)
Error on sample average age is 1σ, as (SD)/(n)$^{1/2}$; where SD=standard deviation of the age replicates and n =number of age determinations.

Sample	Cryst.	Spontaneous ρs (Ns)	Induced ρi (Ni)	Dosimeter ρi (Ni)	$P(\chi^2)$ [%]	Disp.	FT age* [Ma ± 1s]	Track length [µm, n]	Dpar [µm]
Per1 1598.5-									
-1601.5 K7 Ki2	20	7.09 (571)	13.0 (1044)	6.29 (4638)	64	0.02	**55.4** **3.1**	12.8 ± 1.1 (53)	1.99 ± 0.25

Cryst: number of dated apatite crystals.
Track densities (ρ) are as measured (x10^5 tr/cm^2); number of tracks counted (N) shown in brackets.
P (χ^2): probability obtaining Chi-square value for n degree of freedom (where n = no. crystals-1).
Disp.: Dispersion, according to Galbraith and Laslett (1993).
*: Central ages.

Table 1: Apatite fission track and apatite (U-Th)/He (AFT and AHe, respectively) results from the Per-001 borehole (measured depth 1600 m; position in Figure 1).

For the proper interpretation of the detected rejuvenations in the thermochronometers several modelling runs of the thermal history were performed. For the modelling we have used the computer program of HeFTy (Ketcham 2005). This forward modelling algorithm considers the apparent AFT age, track length distribution (Figure 7), the angle of confined tracks relatively to the crystallographic C-axis, kinetic parameters (Dpar), AHe ages and the geometry and actinide concentrations of the dated apatite crystals. For the modelling we only considered the age of sedimentation (22 Ma @ 16 °C) and the current borehole temperature (ca. 55 °C) as invariable time-temperature points. The pre-depositional cooling age of the apatite grains was assumed to be between 100 and 60 Ma, because it is a dominant cooling age phase in the Eastern Alps, which is the major source area of the sediment.

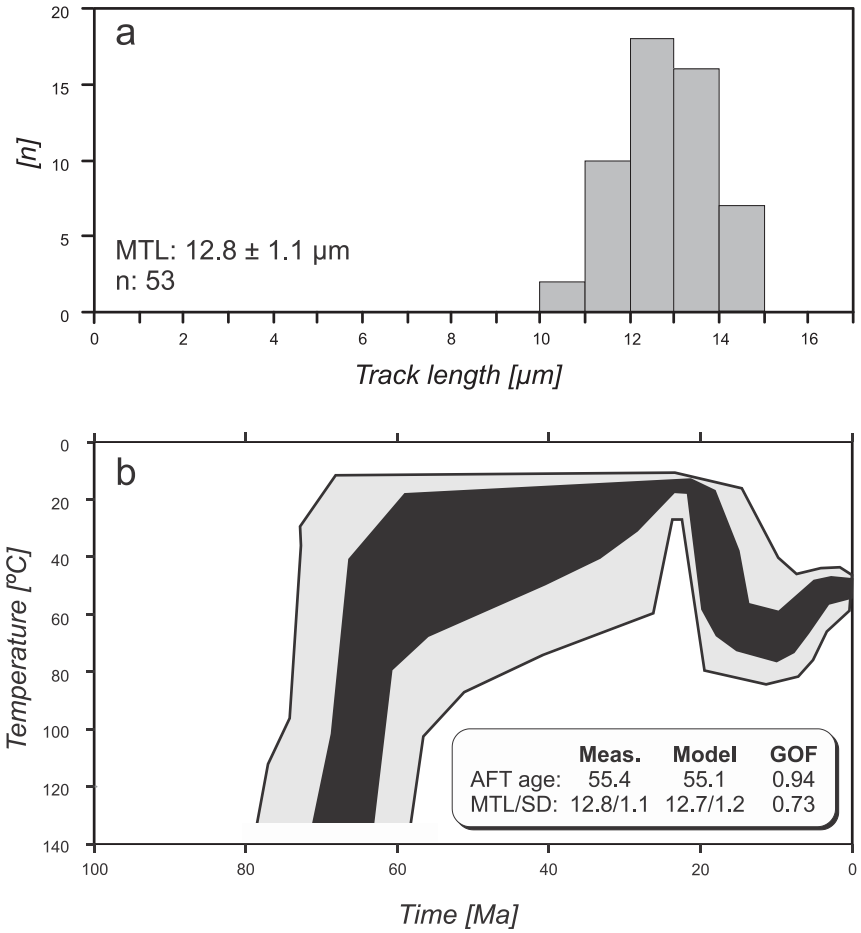

Figure 7: a) Confined horizontal track lengths in the apatite crystals from the Per-001 borehole, measured depth 1600 m. (position in Figure 1) b) Time - temperature plot showing the results of the thermal modelling performed with HeFTy software (Ketcham, 2005).

The thermal modelling indicates a remarkable turn in the post-depositional thermal history. The rather rapid increase of the burial temperature was terminated around 10 Ma ago and since ca. 8 Ma the temperature decreases. Another less pronounced turn can also be observed at ca. 5 Ma. Since that time the temperature conditions are rather stable. However we should consider that this last turn is already in the less sensitive time-temperature range of the thermochronometers, thus this turn is much less constrained than the turn in the trend at ca. 10 Ma ago.

The enveloping of the acceptable tT paths (goodness of fit: GOF >0.05) is represented by a light grey field (Figure 7) and the envelope of 'good fits' (GOF >0.5) by a black belt. These areas do not include those individual paths that offer numerically correct solutions, but tT paths, which are geologically meaningless. For example, paths showing extremely quick rate of post-depositional warming or indicating sharp turns (running in zigzags) were not considered.

5 Discussion

The integration of the different data sets allows the separation of at least two tectonic events during Neogene times:

5.1 Karpatian/Badenian westward tilting

A regional Miocene westward tilting event affecting the Austrian part of the Molasse Basin is strongly evidenced by the tilting of progradational patterns within the Hall Formation (Eggenburigan). The uniform thickness of Ottnangian sediments of the Innviertel Group along the basin axis suggests that the tilting occurred after Ottnangian time. The onlap relation of Lower Badenian to Pannonian rocks of the Upper Freshwater Molasse and the top of the Innviertel Group suggests that tilting occurred before the Badenian. Thus, the tilt of about 0.5 % can be attributed to the Karpatian. There is no regular change of the amount of Karpatian erosion along the E-W trending basin axis. This suggests that tilting postdates erosion.

5.2 Late Miocene regional uplift

Moisture contents of lignite in the Hausruck mining district suggest that the hypothetical Late Miocene paleo-land-surface is located at about 1250 m a. sl. This implies major erosion after deposition of the Upper Freshwater Molasse in post-Early Pannonian time. Erosion removed 450 (Goebelberg area) to 800 m (valley areas between Trimmelkam and Hausruck) thick sediments.

Late Miocene to Pliocene cooling, as indicated by thermochronological data, supports regional exhumation after 10 million years before present. Although the amount of cooling is poorly constrained, its most likely value of about 20 °C (Figure 7) fits well with an erosion in the order of 500 to 700 m (in consideration of typical geothermal gradients for this part of the basin of about 3.0 °C/100 m; Kamyar 2000). Moreover, the modelling results suggest that cooling reached a peak before 5 Ma.

5.3 Local uplift in the eastern Molasse Basin

Shale compaction data suggest that erosion in the eastern part of the study area removed sediments, which are up to 1000 m thicker than in the main part. Thus sediments in the order of 1500 to 1800 m thick were probably eroded. Although thermochronological data are missing, we assume that uplift was contemporaneous with regional uplift in Late Miocene time.

5.4 Comparison with Neogene uplift in the Swiss part of the Molasse Basin

For the Swiss part of the Alpine Foreland Basin eroded rocks of at least 2 km are related to a Late Miocene uplift event is approved (Kuhlemann & Kempf 2002). Schegg & Leu (1998) clarify the thicknesses of eroded Neogene sediments with values of 700 m in the northeast and 1500-3000 m near the Alpine front to the south. Numerous analyses on mineral cooling ages demonstrate that the basin underwent the erosion during Pliocene times. Concerning to the reason of uplift it is proposed that accelerated erosional unroofing of the Swiss Alps triggered isostatic rebound and erosion of the foreland basin after 5 Ma. Additionally a change in climate and/or drainage reorganization is suggested (Cederbom et al. 2004; 2011). Andeweg & Cloetingh (1998) propose that the Late Cenozoic uplift, which superimposes the former flexural process due to loading, might be caused by breaking up or delamination of part of the subsided European crust.

5.5 Consequences for hydrocarbon systems in the Molasse Basin

Changes in basin geometry have an influence on both thermogenic and biogenic hydrocarbon systems. Tilting of the basin shifts oil water contacts and controls migration paths. Basin uplift and erosion may cause termination of hydrocarbon generation if the system leaves the oil window (due to temperature decrease) along the way. Cooling favors biodegradation processes and biogenic gas generation. Decreasing pressure changes the gas-oil ratio. Upcoming basin and petroleum systems modelling based on structural forward modelled sections will provide information about these issues.

5.6 Possible mechanism for Neogene tectonic activity

A main extensional phase captured the region during Late Ottnangian or Karpatian to Early Badenian times. East of the Tauern window a number of intramontane pull-apart basins were formed along major stike-slip fault zones (e.g. Mur-Mur-Mürz-valley, Enns-valley) Due to these tectonic movements, stress regimes and sedimentation patterns significantly changed in the central and eastern part of the Eastern Alps (Frisch et al. 1998) and may have affected also the foreland basin even though in a minor way.

Peresson & Decker (1997) proposed that a Late Miocene (after 9 Ma and prior to 5.3 Ma) compressional event along the entire Alpine-Pannonian system terminated the former eastward lateral extrusion and reversed the stress regime.

The cause for prominent Neogene uplift in the Alpine region is still intensively discussed. It is probably related to isostatic rebound of the Alps after termination of thrusting. Cederbom et al. (2004) suggest that erosional unroofing of the Swiss part of the North Alpine Foreland Basin occurred due to isostatic rebound of the mountain belt in response to a wetter climate (driven by increased precipitation) post 5 Ma.

The strong local uplift in the eastern Molasse Basin parallels the southwestern margin of the Bohemian Spur. This spur exhibiting thickened crystalline crust extends some 100 km to the southeast below the Eastern Alps (see inset in Figure 1 for location of the Bohemian Spur) (e.g. Tari 2005). Thus, isostatic uplift of the Bohemian Spur might have caused the observed differential uplift. Within this context, uplift data from the eastern margin of the Bohemian Spur would be interesting. According to our knowledge such data are not available.

6 Conclusion

The combination of geophysical, petrophysical and thermochronological techniques provides new insights into the timing and dimension of uplift and erosion events in the Austrian part of the Northern Alpine Foreland Basin. The most important conclusions drawn from the present study include:

- An inclined toplap surface within the Hall Formation and the geometry of Innviertel Group provide evidence for regional westward tilting of the study area. The gradient of the slope is about 5 m per kilometer (0.5 %). Tilting occurred during Karpatian time (~17 Ma before present) and postdates the Late Ottnangian filling of the marine basin. Tilting might be related to the contemporaneous onset of continental escape within the Eastern Alps. As a result of tilting, Badenian to Pannonian sediments of the Upper Freshwater Molasse onlap onto the inclined top Innviertel unconformity.
- Moisture contents of lignite in the Hausruck mining district and thermochronological (apatite fission track and (U-Th)/He) data from a sample in the western part of the study area indicate uplift and erosion after deposition of the Upper Freshwater Molasse. Erosion estimates are in the order of 500 to 900 m. Major erosion probably commenced at about 8 Ma and slowed down about 4 Ma before present. Although poorly constrained, this time interval excellently fits with the time constraints of Cederbom et al. (2004) and Genser et al. (2007) although the thicknesses of eroded rocks reach greater dimensions in the Swiss part of the basin.
- Shale compaction data have been derived from sonic logs of the Eggerding Formation (Lower Oligocene). Most data follow a regular depth trend. Deviations from this trend indicate that uplift along a narrow zone at the easternmost part of the study area was significantly higher (up to 1000 m) than in the rest of the study area. Considering the regional uplift of 500 to 900 m, it is concluded that sediments, up to 1500 or even 1900 m thick, have been eroded along the narrow eastern zone. It is reasonable to assume that eastern uplift was contemporaneous with regional uplift (i.e. Late Miocene). Uplift in the east is probably related to differential isostatic rebound of the crystalline rocks along the Bohemian Spur compared to clastic basin fill or to a compressional event (Peresson & Decker 1997).
- It can be expected that both Karpatian tilting and Late Miocene erosion have major influence on the petroleum systems. For example, tilting probably

influenced oil water contacts in E-W-elongated hydrocarbon deposits. Moreover uplift and erosion probably stopped hydrocarbon generation and influenced gas to oil ratios in existing accumulation.

Acknowledgments

We thank RAG AG for their permission to publish the data. Special thanks go to geologic RAG personnel for constructive discussion inputs. For helpful comments concerning the moisture content of coal we are notable thankful to Bernhard Salcher (ETH Zürich). The manuscript benefited from the useful comments of the reviewers, Gabor Tari (OMV) and Nestor Oszczypko (Jagiellonian University Krakow).

References

Andeweg B. & Cloetingh S.A.P.L 1998: Flexure and ‚unflexure' of the North Alpine German-Austrian Molasse Basin: constraints from forward tectonic modelling: In: Mascle A., Puigdefàbregas C., Luterbacher H.P. & Fernandez M. (Eds.): Cenozoic Foreland Basins of Western Europe. *Geological Society Special Publications* 134, 403-422.

Bachmann G.H., Mueller M. & Weggen K. 1987: Evolution of the Molasse Basin (Germany, Switzerland). *Tectonophysics* 137, 77-92.

Cederbom C.E., Sinclair H.D., Schlunegger F. & Rahn M.K. 2004: Climate induced rebound and exhumation of the European Alps. *Geology* 32, 709-712.

Cederbom C.E., Van der Beek P., Schlunegger F., Sinclair H.D. & Oncken O. 2011: Rapid extension erosion of the North Alpine foreland basin at 5-4 Ma. *Basin Research* 23, 528-550.

Czurda K. 1978: Sedimentologische Analyse und Ablagerungsmodell der miozänen Kohlemulden der oberösterreichischen Molasse. *Jb. Geol. B.-A.* 121, 123-154.

De Ruig M.J. & Hubbard S.M. 2006: Seismic facies and reservoir characteristics of a deep marine channel belt in the Molasse foreland basin: *AAPG Bulletin* 90, 735-752.

Donelick R.A., Ketcham R.A. and Carlson W.D. 1999: Variability of apatite fission-track annealing kinetics; II, Crystallographic orientation effects. *American Mineralogist* 84(9), 1224-1234.

Dumitru T.A. 1993: A new computer-automated microscope stage system for fission-track analysis. *Nucl. Tracks Radiat. Meas* 21, 575-580.

Farley K.A. 2002: (U-Th)/He dating: techniques, calibrations and applications, Reviews in *Mineralogy and Geochemistry* 47, 819-844.

Faupl P. & Roetzel R. 1987: Gezeitenbeeinflusste Ablagerungen der Innviertler Gruppe (Ottnangian) in der österreichischen Molassezone. *Jb. Geol. B.-A.* 130, 415-447.

Frisch W., Kuhlemann J., Dunkl I. & Brügel A. 1998: Palinspastic reconstruction and topographic evolution of the Eastern Alps during late Tertiary tectonic extrusion. *Tectonophysics* 297, 1-15.

Genser J., Cloetingh S.A.P.L. & Neubauer F. 2007: Late orogenic rebound and oblique Alpine convergence: New constraints from subsidence analysis of the Austrian Molasse basin. *Global and Planetary Change* 58, 214-223.

Gleadow A.J.W. & Duddy I.R. 1981: A natural long-term track annealing experiment for apatite. *Nuclear Tracks* 5, 169-174.

Groiss R. 1989: Geologie und Kohlebergbau im Hausruck (Oberösterreichische Molasse). *Arch. f. Lagerst. Forsch. Geol. B.-A. Wien* 11, 167-178.

Grunert P., Soliman A., Harzhauser M., Müllegger S., Piller W. E., Roetzel R. & Rögl F. 2010: Upwelling conditions in the Early Miocene Central Paratethys sea. *Geologica Carpathica* 61,129–145.

Grunert P., Soliman A., Coric S., Roetzel R., Harzhauser M. & Piller W. E. 2011: Facies development along the tide-influenced shelf of the Burdigalian Seaway: An example from the Ottnangian stratotype (Early Miocene, middle Burdigalian). *Marine Micropaleontology* Accepted Manuscript.

Gusterhuber J., Sachsenhofer R.F. & Linzer H.-G., 2011. A 2D Basin and Petroleum Systems Modelling Study in an Overthrust Setting – The Alpine Molasse Basin, Austria. *73rd EAGE Conference & Exhibition incorporating SPE EUROPEC 2011 Vienna*, 257 S.

Hinsch R. 2008: New Insights into the Oligocene to Miocene Geological Evolution of the Molasse Basin of Austria. *Oil & Gas European Magazine* 34 (3), 138-143.

Hubbard S.M., De Ruig M.J. & Graham S.A. 2009: Confined channel-levee complex development in an elongate depo-center: Deep-water Tertiary strata of the Austrian Molasse basin. *Marine and Petroleum Geology* 26, 85-112.

Hurford A.J. 1998: Zeta: the ultimate solution to fission-track analysis calibration or just an interim measure? In: Van den Haute P.& De Corte F. (Eds.): Advances in fission-track geochronology. *Kluwer Academic Publishers*, 19-32.

Hurford A.J. & Green P.F. 1983: The zeta age calibration of fission-track dating. *Chem. Geol., Isot. Geosci.* 41, 285-312.

Issler D.R. 1992: A New Approach to Shale Compaction and Stratigraphic Restoration, Beaufort-Mackenzie Basin and Mackenzie Corridor, Northern Canada. *The AAPG Bulletin* 76, 1170-1189.

Kamyar H.R. 2000: Verteilung der Untergrundtemperarturen an den Beispielen der Bohrlochtemperatur (BHT) – Messungen in den RAG Konzessionen, Oberösterreichs und Salzburgs, (Molasse- und Flyschzone). *PhD thesis University of Vienna*, 145 S.

Ketcham R.A. 2005: Forward and Inverse Modeling of Low-Temperature Thermochronometry Data. *Reviews in Mineralogy and Geochemistry* 58, 275-314.

Kothen H. & Reichenbach K. 1981: Teufenabhängigkeit und gegenseitige Beziehungen von Qualitätsparametern der Braunkohle der Niederrheinischen Bucht. *Fortschr. Geol. Rheinland. Westfalen* 29, 353-380.

Krenmayer H.G. 1999: The Austrian sector of the North Alpine Molasse: A classic foreland basin. *FOREGS (Forum of Euopean Geological Surveys)* Dachstein-Hallstatt-Salzkammergut Region, Vienna, 22-26.

Kuhlemann J. & Kempf O. 2002: Post-Eocene evolution of the North Alpine Foreland Basin and its response to Alpine tectonics. *Sedimentary Geology* 152, 45-78.

Linzer H.-G. 2002: Structural and Stratigraphic Traps in Channel Systems and Intraslope Basins of the Deep-Water Molasse Foreland Basin of the Alps. *AAPG Search and Discovery Article #90007* AAPG Annual Meeting Houston, Texas, 2 S.

Magara K. 1976: Thickness of Removed Sedimentary Rocks, Paleopore Pressure, and Paleotemperature, Southwestern Part of Western Canada Basin. *The AAPG Bulletin* 60, 554-565.

Magara K. 1980: Comparison of porosity-depth relationships of shale and sandstone. *Journal of Petroleum Geology* 3, 175-185.

Malzer O., Rögl F., Seifert P., Wagner L., Wessely G. & Brix F. 1993: Die Molassezone und deren Untergrund. In: Brix F. & Schultz O. (Eds.): *Erdöl und Erdgas in Österreich*. Naturhistorisches Museum Wien und F. Berger, 281–358.

Nachtmann W. & Wagner L. 1987: Mesozoic and Early Tertiary evolution of the Alpine foreland in Upper Austria and Salzburg, Austria. *Tectonophysics* 137, 61-76.

Peresson H. & Decker K. 1997: Far-field effects of Late Miocene subduction in the Eastern Carpathians: E-W compression and inversion of structures in the Alpine-Carpathian-Pannonian region. *Tectonics* 16, 38-56.

Pohl W. 1968: Zur Geologie und Paläogeographie der Kohlemulden des Hausruck (O.Ö.). *PhD Thesis, University of Vienna* 17, 70 S.

Roegl F. 1998: Palaeogeographic Considerations for Mediterranean and Paratethys Seaways (Oligocene to Miocene). *Annalen des Naturhistorischen Museums in Wien* 99A, 279–310.

Roegl F. 1999: Mediterranean and Paratethys. Facts and Hypothesis of an Oligocene to Miocene Paleogeography (short overview). *Geologica Carpathica* 50, 4, 339-349.

Rupp C., Hofmann T., Jochum B., Pfleiderer S., Schedl A., Schindlbauer G., Schubert G., Slapansky P., Tilch N., Husen D. van, Wagner L., & Wimmer-Frey I. 2008: Geologische Karte der Republik Österreich 1:50.000, Blatt 47 Ried im Innkreis. Erläuterungen zu Blatt 47 Ried im Innkreis. *Geological Survey of Austria*, Vienna.

Sachsenhofer R.F., Leitner B., Linzer H.-G., Bechtel A., Coric S., Gratzer R., Reischenbacher D. & Soliman A. 2010: Deposition, erosion and hydrocarbon source potential of the Oligocene Eggerding Formation (Molasse Basin Austria). *Austrian Journal of Earth Sciences* 103, 76-99.

Schegg R. & Leu W. 1998: Analysis of erosion events and palegeothermal gradients in the North Alpine Foreland Basin of Switzerland. In: Düppenbecker S.J. & Iliffe J.E. (Eds.) Basin Modelling: Practice and Progress. *Geological Society London* 141, 137-155.

Schulz H.-M., Sachsenhofer R.F., Bechtel A., Polesny H. & Wagner L. 2002: Origin of hydrocarbon source rocks in the Austrian Molasse Basin (Eocene-Oligocene transition). *Marine and Petroleum Geology* 19 (6), 683-709.

Schulz H.-M., Bechtel A. & Sachsenhofer R.F. 2005: The birth of the Paratethys during the Early Oligocene: From Tethys to an ancient Black Sea analogue? *Global and Planetary Change* 49, 163-176.

Tari G. 2005: The Divergent Continental Margins of the Jurassic Proto-Pannonian Basin: Implications for the Petroleum Systems of the Vienna Basin and the Moesian Platform. 25th Annual Bob F. Perkins Research Conference: Petroleum Systems of Divergent Continental Margins, Houston.

SRTM 2004: Void-filled seamless SRTM data V1 (2004) International centre for tropical agriculture (CIAT). Available from the CGIAR-CSI SRTM 90 m Database: http://srtm.csi.cgiar.org and http://www.ambiotek.com/topoview

Van Husen D. 1987: Die Ostalpen in den Eiszeiten. *Populärwissenschaftliche Veröffentlichungen der Geologischen Bundesanstalt*, (Map 1:500.000),Vienna.

Wagner L.R. 1996: Stratigraphy and hydrocarbons in the Upper Austrian Molasse Foredeep (active margin). In: Wessely G. & Liebl W. (Eds.): *Oil and Gas in Alpidic Thrustbelts and Basins of Central and Eastern Europe*. EAGE Special Publications 5, 217-235.

Wagner L.R. 1998: Tectono-stratigraphy and hydrocarbons in the Molasse foredeep of Salzburg, Upper and Lower Austria. In: Mascle A., Puigdefàbregas C., Luterbacher H.P. & Fernandez M. (Eds.): Cenozoic Foreland Basins of Western Europe. *Geological Society Special Publications* 134, 339-369.

Weber L. & Weiss A. 1983: Bergbaugeschichte und Geologie der österreichischen Braunkohlevorkommen. *Arch. f. Lagerst. Forsch. Geol. B.-A*. Wien 4, 317 S.

Wells P.E. 1990: Porosities and seismic velocities of mudstones from Wairarapa and oil wells of North Island, New Zealand, and their use in determining burial history. *New Zealand Journal of Geology and Geophysics* 33, 29-39.

Evaluation of hydrocarbon generation and migration in the Molasse fold and thrust belt (Central Eastern Alps; Austria) using structural and thermal basin models

Manuscript in press, AAPG Bulletin, 2013/2014
doi: 10.1306/06061312206

Juergen Gusterhuber[1, 2], Ralph Hinsch[3, 4], Reinhard F. Sachsenhofer[1]

[1]Montanuniversitaet Leoben, Department Applied Geosciences and Geophysics, Chair of Petroleum Geology, Peter-Tunner-Strasse 5, A-8700 Leoben, Austria, reinhard.sachsenhofer@unileoben.ac.at
[2]Present address: Santos Ltd., 60 Flinders Street, Adelaide SA 5000, Australia, juergen.gusterhuber@gmx.at
[3]RAG Rohöl-Aufsuchungs Aktiengesellschaft, Schwarzenbergplatz 16, A-1015 Vienna, Austria.
[4]Present address: OMV Exploration & Production GmbH, Trabrennstrasse 6-8, 1020 Vienna,
ralph.hinsch@omv.com

Acknowledgements

The authors thank RAG AG for the kind permission to publish the data and the scientific staff of GFZ Potsdam for determining bulk kinetic parameters. Research was supported by the Schlumberger PetroMod Group in Aachen via a generous software grant to the Montanuniversitaet Leoben. Special thanks in this regard go to Wolf Rottke (Schlumberger Aachen) for his kind support and constructive inputs. For helpful comments on oil-oil and oil-source rock correlations we are thankful to

Reinhard Gratzer and Achim Bechtel (Montanuniversitaet Leoben). The authors thank also Hans-Gert Linzer (RAG) for inspiring discussions which helped to improve the paper. An earlier version of the manuscript benefited from constructive comments by R. Tscherny, B. Katz, and two other anonymous reviewers.

Abstract

The Molasse Basin represents the northern foreland basin of the Alps. After decades of exploration it is considered to be mature in terms of hydrocarbon exploration. However, geological evolution and hydrocarbon potential of its imbricated southernmost part (´Molasse fold-and-thrust belt´) are still poorly understood. In the present study structural and petroleum systems models are integrated to explore the hydrocarbon potential of the Perwang imbricates in the western part of the Austrian Molasse Basin.

The structural model shows that total tectonic shortening in the modeled N-S section is at least

32.3 km (20.1 mi) and provides a realistic input for the petroleum systems model. Formation temperatures show present-day heat flows decreasing towards the south from 60 to 41 mW/m². Maturity data indicate very low paleo-heat flows decreasing southwards from 43 to 28 mW/m². The higher present-day heat flow probably indicates an increase in heat flow during Pliocene and Pleistocene times.

Apart from oil generated below the imbricated zone and captured in autochthonous Molasse rocks in the foreland area, oil stains in the Perwang imbricates and oil-source rock correlations argue for a second migration system based on hydrocarbon generation inside the imbricates. This assumption is supported by the models presented in this study. However, the model-derived low transformation ratios (<20 %) indicate a charge risk. In addition, the success for future exploration strongly depends on the existence of migration conduits along the thrust planes during charge and on potential traps retaining their integrity during recent basin uplift.

Introduction

The Molasse Basin is a Cenozoic Foreland Basin located north of the Alps (Figure 1a). The Eocene to Miocene Molasse sedimentary rocks overlie Cretaceous to

Jurassic units and crystalline basement of the Bohemian Massif (e.g. Malzer et al., 1993). After decades of petroleum exploration and almost 200 discoveries, the Molasse Basin is considered to be mature in terms of hydrocarbon exploration (Véron, 2005). The Austrian part of the basin includes two reasonably well understood petroleum systems (Wagner, 1996, 1998): (1) a thermogenic oil system based on Oligocene source rocks, which reach the oil window beneath the Alpine nappes (Schmidt and Erdogan, 1993; Schulz et al., 2002; Sachsenhofer and Schulz, 2006; Gratzer et al., 2011), and (2) a biogenic dry gas system which is restricted to Oligocene and Miocene units (Schulz and van Berk, 2009; Schulz et al., 2009; Reischenbacher and Sachsenhofer, 2011).

In contrast to the mainly undeformed part of the Molasse Basin, its folded and imbricated southernmost part (Figure 1) is still poorly understood and its hydrocarbon potential is not yet fully explored. Recently drilled wells, 3D seismic data and the application of balancing techniques considerably increase the understanding of the structure of the Molasse imbricates (Linzer, 2001, 2002, 2009; Covault et al., 2009). Based on timing of tectonic processes, the position of the detachment horizon and the geometry of the imbricates, three different imbricate systems can be distinguished along strike within the Austrian part of the basin (Hinsch and Linzer, 2010). The decollement of the western Perwang imbricates (for location see Figure 1a) is located within Upper Cretaceous marls. In the two eastern imbricate systems the decollement is located in a position above the Oligocene source rock interval. Therefore, occurrence of source rocks within the thrust sheets is restricted to the Perwang imbricates.

The main goal of the present study is to focus on the impact of the fold-and-thrust belt on the petroleum system within and beneath the Molasse imbricates at the southern basin margin. To reach this goal, a two-dimensional thermal basin model was established along a north-south cross-section located at the eastern margin of the Perwang imbricates (Figure 1a). In order to take the complex kinematic evolution of the thrust sheets into account, the thermal basin model is based on a structural forward model. Recent uplift and erosion of the Molasse Basin provide an additional complexity. This effect was considered in the thermal basin model using uplift data from Gusterhuber et al. (2012).

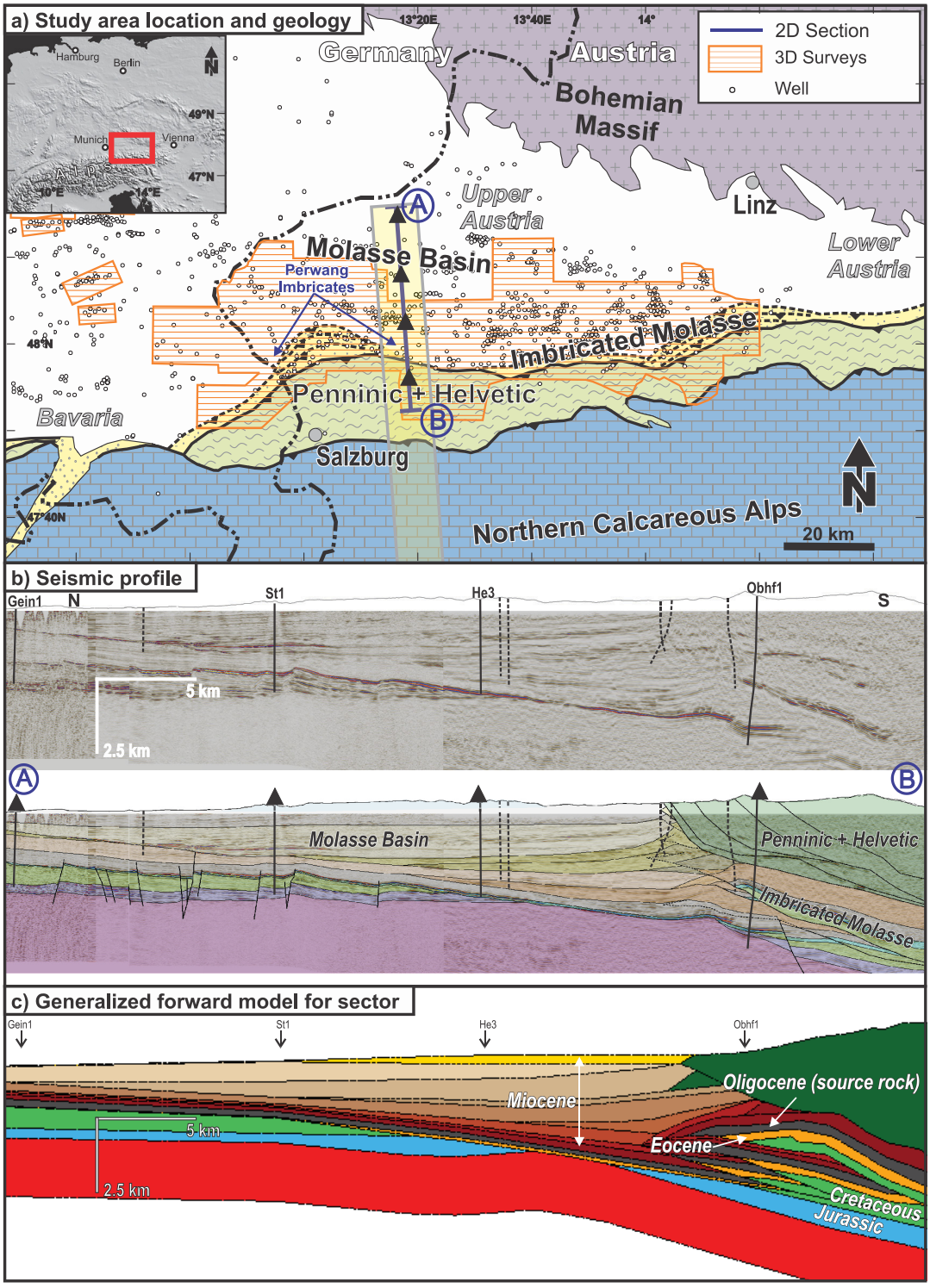

Figure 1: a) Simplified geological map of the study area (outline of the imbricated Molasse from the subsurface); course of the 2D section (A – B) near the Perwang imbricates as well as the area for which we suppose that the structural model is valid and where the thermal model may have significance to meet the thermal history (yellow shading); wells (approx. status 2010); the inset map (top left) shows the position of the study area on a shaded relief in the frame of Central Europe. Black triangles mark calibration well

positions. b) 2D seismic section; interpretation overlay including calibration wells and main geotectonic units c) generalized structural forward model considered to be valid for the specified corridor and important stratigraphic units (e.g. Eocene reservoir rocks: orange; source rocks: dark grey)

Geological Setting

Basin Evolution

The Molasse Basin was formed due to the collision of the Alpine orogenic system with the southern margin of the European platform during the Middle Paleogene (Roeder and Bachmann, 1996; Sissingh, 1997). The basin represents a typical asymmetric foreland basin in terms of an increasing basin depth towards the Alpine thrust front in the south. The basement of the Molasse sequence is formed by crystalline rocks of the Bohemian Massif overlain by Jurassic sandstones and platform carbonates as well as Upper Cretaceous sandstones and marls. Locally Permian-Carboniferous graben deposits underlie the Mesozoic succession (Figure 2).

The Cenozoic succession can be structurally subdivided into autochthonous Molasse units and allochthonous Molasse units (Steininger et al., 1986). The autochthonous units overlie crystalline basement or Mesozoic rocks and are relatively undisturbed. The allochthonous units, including the Molasse imbricates, are composed of rocks which are incorporated in the Alpine thrusts and subsequently moved tectonically into and above the southern parts of the autochthonous units.

Uplift and erosion left a peneplain on which the Paratethys Sea progressively transgressed during latest Eocene and earliest Oligocene times. At this stage the area subsided rapidly to deep water conditions accompanied by the development of E-W and NNW-SSE trending fault systems due to downward bending of the European Plate (Wagner, 1996, 1998). Fine-grained, often organic matter rich sediments were deposited during Rupelian times in a deep-water environment (approx. 800 m; Dohmann, 1991).

In the Late Oligocene and earliest Miocene the northward movement of the Alpine wedge caused formation of the Molasse imbricates and increased sediment discharge from the south (Kuhlemann and Kempf, 2002). Deep water channel systems formed along the axis of the Molasse Basin (Puchkirchen trough; Linzer, 2002; De Ruig and Hubbard, 2006). Deep marine sediments graded northwards into brackish clays, sands and coal-bearing successions (Krenmayer, 1999). Contemporaneously, terrestrial conglomerates and sandstones have been deposited on top of the Alpine wedge

(Augenstein Formation). Today these sediments are only preserved in small remnants on plateaus of the Northern Calcareous Alps (Frisch et al., 2001).

Deep water conditions along the basin axis continued during deposition of the lower part of the Hall Formation in Early Burdigalian time. Later, prograding deltas initiated the infill of the basal Hall Trough (Hinsch, 2008; Hubbard et al., 2009; Grunert et al., 2013). Upper Burdigalian sediments of the Innviertel Group are represented by tide dominated silts and brackish-fluvial sands (Roegl, 1998; Grunert et al., 2012). This succession indicates the termination of marine development in the basin.

Following on a major hiatus (Figure 2), a several hundred meters thick succession composed of coal-bearing clays, sands and fluvial gravels (Upper Freshwater Molasse) was deposited. Today these Middle to Upper Miocene rocks are largely eroded due to major uplift starting approximately 9 million years BP (Gusterhuber et al., 2012).

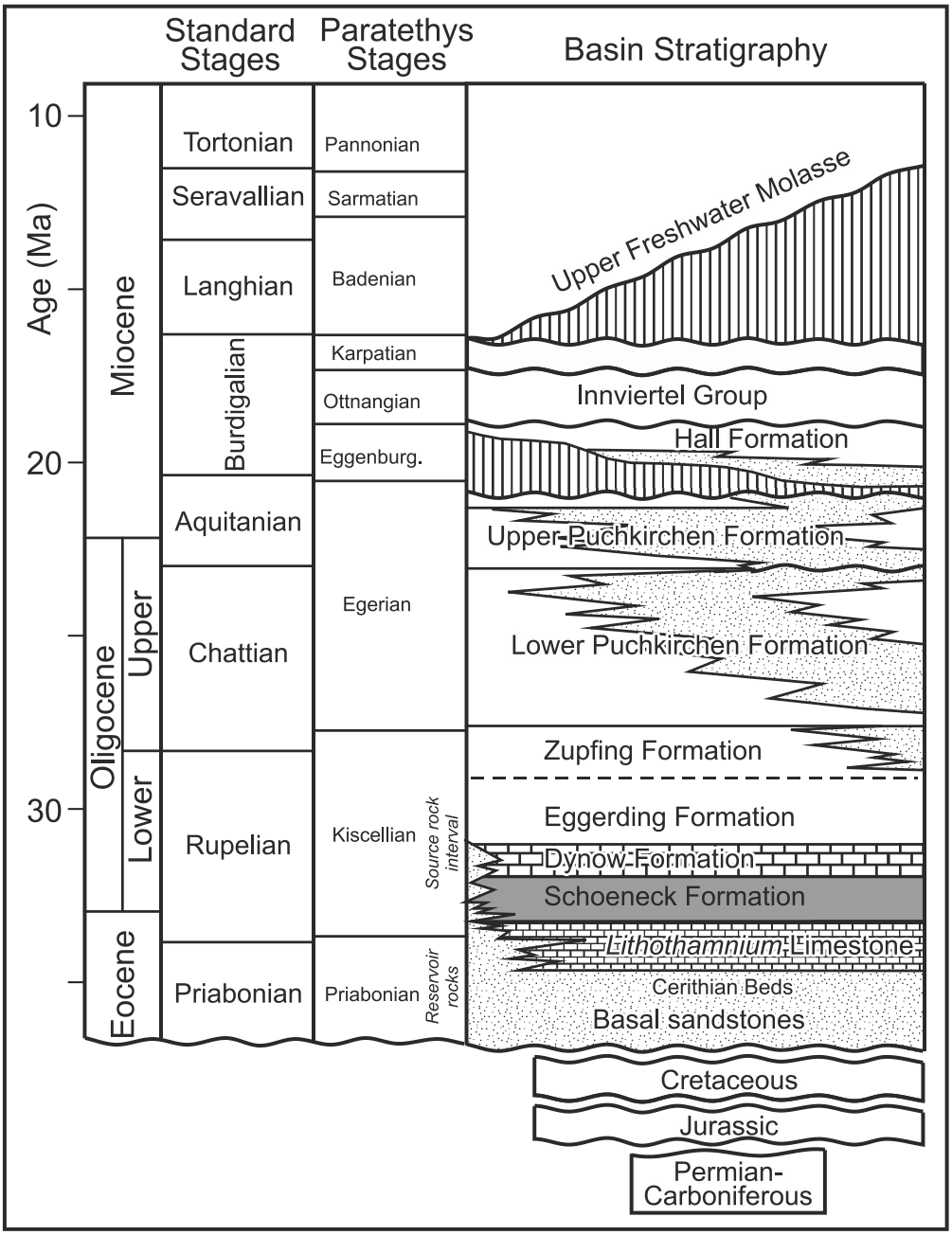

Figure 2: Stratigraphy of the Austrian part of the Molasse Basin (modified after Wagner, 1998).

Petroleum Systems

Two petroleum systems are traditionally distinguished in the Molasse Basin east of Munich: (1) a Lower Oligocene to Mesozoic thermogenic oil system and (2) an Oligocene-Miocene biogenic gas system (Wagner, 1996, 1998). The latter is mentioned here for the sake of completeness but not treated in the scope of the present study.

(1) The most important reservoirs for oil and minor thermal gas are Upper Eocene basal sandstones (Figure 2). Additional hydrocarbons are trapped in Eocene carbonates as well as in Mesozoic and Lower Oligocene successions (Malzer et al., 1993). Almost all thermal oil and gas traps in the Molasse Basin are bound to the described fault systems featuring vertical throws of several hundred meters (Nachtmann, 1995).

Potential source rocks in the Molasse Basin are restricted to the Lower Oligocene succession and comprise from bottom to top: Schoeneck Formation, Dynow Formation and Eggerding Formation (Table 1; Schulz et al., 2002; Sachsenhofer and Schulz, 2006; Sachsenhofer et al., 2010). The deep-water organic rich shales and marls of the Schoeneck Formation have the highest source potential. The overlying Dynow Formation is composed of three sedimentary cycles, each starting with marlstones and grading into organic-rich shales (Schulz et al., 2004). The Eggerding Formation is composed of grey laminated pelites (Sachsenhofer et al., 2010).

Formation		**Av. Thickness [m]**	**TOC [%]**	**HI [mgHC/gTOC]**
Eggerding Formation	Merged SR interval	35 - 50	1.5 - 6.0	250 - 400
Dynow Formation		5 - 15	0.5 - 3.0	500 - 600
Schoeneck Formation		10 - 20	2.0 - 12.0	400 - 600
Merged source rock interval			3	450
‚Oberhofen facies‘		~50	~1.3	400

Table 1: Characteristics of Lower Oligocene source rocks (Schulz et al., 2002; Sachsenhofer and Schulz, 2006; Sachsenhofer et al., 2010). TOC: total organic carbon; HI: hydrogen index.

The present-day distribution of Lower Oligocene rocks is controlled by submarine mass movements which affected the northern passive slope of the foreland basin, and by tectonic erosion. Mass movements climaxed shortly before the end of deposition of the source rock interval when locally Oligocene successions of up to 70 m thickness (Sachsenhofer et. al., 2010) were removed gravitationally from the northern slope, re-deposited along the lower basin slope and are now located beneath the Alpine nappes. Such re-deposited source rocks (termed Oberhofen facies) predominate west of the Lindach Fault (see Figure 3a). In contrast Lower Oligocene units with a ‘normal’ source rock facies have been drilled in autochthonous units east of this fault but also in the western Perwang Imbricates (Sachsenhofer and Schulz,

2006; Sachsenhofer et al., 2011). It is important to note that the source rock potential of the Oberhofen facies is lower compared to that of the 'normal' source rock facies (Table 1; Sachsenhofer and Schulz, 2006).

The different source rock facies in the autochthonous Molasse basin sequence (west of Lindach Fault: Oberhofen facies; east of Lindach Fault: normal facies) are reflected by the biomarker and isotopic compositions of crude oil in the foreland. Gratzer et al. (2011) showed that the oil generated beneath the thrust (and discovered in foreland reservoirs) in the western part of the study area is slightly more enriched in sulfur-bearing biomarkers and its carbon is slightly enriched in ^{13}C. This oil is termed Type A oil in the present paper, whereas oil generated from the normal facies is termed Type B (Figure 3a). Type B is characterized for instance by very low DBT/Ph (Dibenzothiophene versus phenanthrene) ratios indicating the limited availability of reduced sulphur for incorporation into organic matter (Hughes et al., 1995).

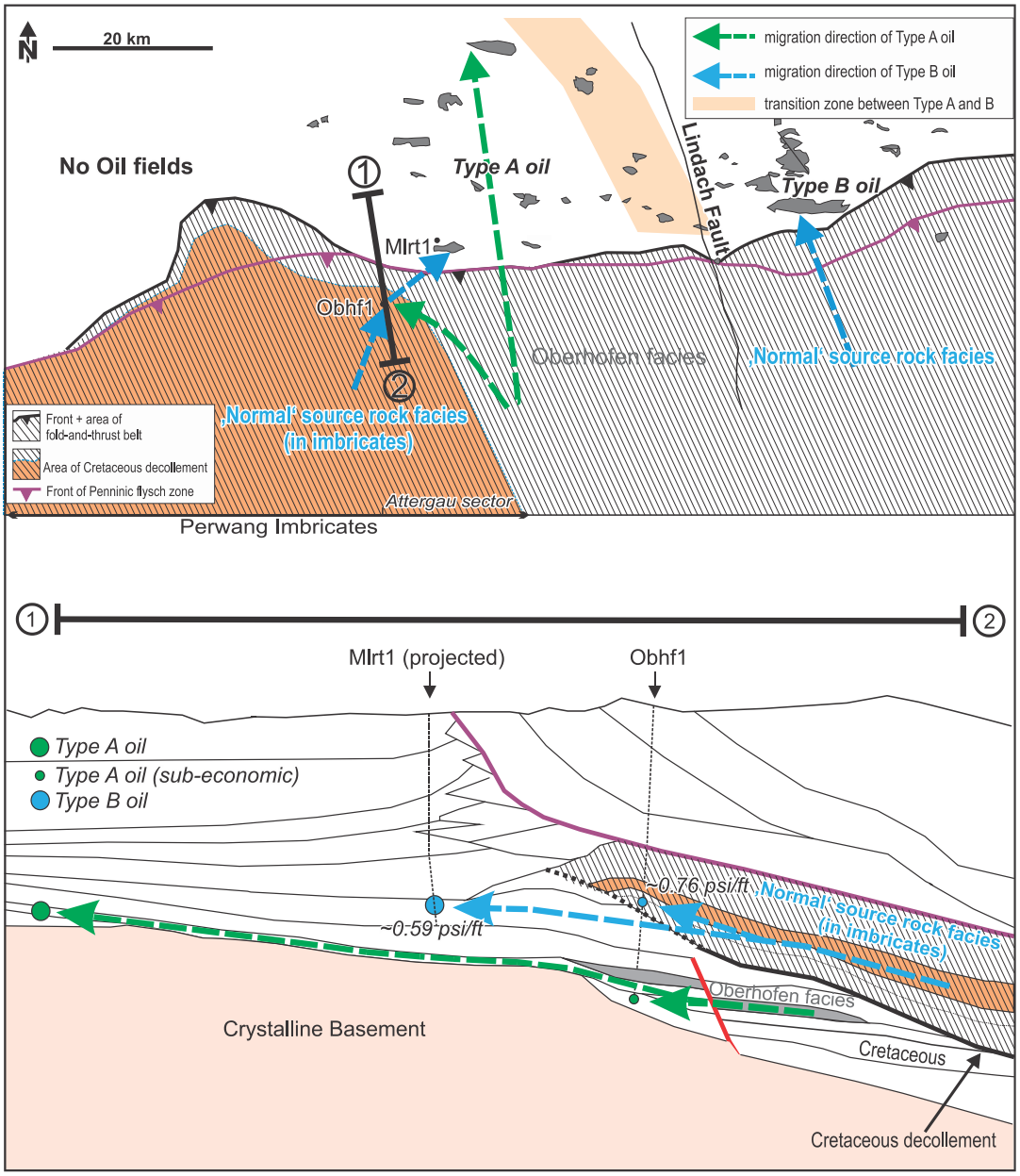

Figure 3: a) Spatial distribution of biomarker parameters from crude oils (grey shaded areas mark investigated oil fields) in the Austrian part of the Molasse Basin (modified after Gratzer et al., 2011); course of the 2D section; b) Sketch adopted from the seismic profile shown in Figure 1b; approx. reservoir gradient [psi/ft].

Exceptions from the west-east trend include the Mlrt 1 (Figure 3a-b) oil, accumulated in Lower Oligocene sandstones just north of the Molasse imbricates, as well as oil stains within the Perwang imbricates (Oberhofen1 (Obhf)1 well; Figure 3a-b; Gratzer et al., 2011; R. Gratzer, 2012, personal communication). These oils exhibit characteristics of a Type B oil.

(2) Isotopically light gas in Oligocene to Miocene Puchkirchen and Hall formations was probably generated by bacterial activity (Malzer et al., 1993; Schulz and van Berk, 2009; Schulz et al., 2009). Productive reservoirs are found in different subfacies of the Puchkirchen and Hall channel systems (De Ruig and Hubbard, 2006; Hubbard et al., 2009).

Data and Methods

Cross-Section Forward Modeling

Based on 3-D seismic and well data interpretation as well as section balancing the structure and kinematic evolution of the imbricated Molasse has been evaluated (Hinsch and Linzer, 2010; Hinsch, in press). Results from cross section restoration have been used to constrain a forward model that mimics the structural evolution of the Perwang imbricates, especially the Attergau sector (Figure 3a). A forward model approach has been chosen to allow a slight simplification of the structural evolution over a wider area. Additionally, this approach allowed to include eroded sediments and early evolutionary stages that otherwise would not be represented by a balanced and restored section. The software package LithoTect (Version 5000.0.1.0; Halliburton-Landmark, 2010) is used for forward modeling, utilizing standard integrated fault-slip algorithms. Forward modeling with LithoTect was done for the timespan lower Oligocene to present. The individual modeled steps represent either deformation increments or important time steps in the evolution of the orogenic front. Manual editing of the intermediate model increments was done to mimic subsidence, erosion and syntectonic sedimentation.

Section modeling was performed on a kinematical basis only. However, the individual deformation increments are manually adapted to reflect a more realistic, pseudo-dynamic evolution. Subsidence, erosion, and syntectonic deposition are added after each deformation increment to reflect known or plausible paleogeographic conditions like facies distribution. Some reasoning behind this is given below. Thus, the presented models act as kinematic models with geodynamic background. Fully geodynamic modeling is far beyond the scope of this study. In addition, too many parameters are unknown or uncertain (e.g. distribution of mechanical parameters through accretionary prism, facies distribution and basement) and results would probably not be more useful for the purpose of this study.

The individually modeled increments followed, in general the subsequent scheme: 1) slight adaption of the shape of the flexurally loaded foreland plate, 2) re-establishing a relative sea level, 3) assessing erosion and deposition. Several constraints were used for the manual adaption. 1) The flexurally loaded foreland plate is approximated to the shape described in Andeweg and Cloetingh (1998). Their section C corresponds approximately to the position of our study area. After every deformation increment the flexed foreland plate in our model was adapted to show a slight northward migration of the bulge and some increase in the local dip gradient underneath the advancing wedge. Hence the shape of the modeled section by Andeweg and Cloetingh (1998) acted as rough guide which had to be achieved in the finite deformation state (present day). 2) Care was taken to give the shape of the orogenic wedge a visually reasonable geometry and the newly gained paleo-sea level and the basin morphology were in accordance to known facies distribution of the time step (cf. Wagner, 1996; Roegl, 1998; Kuhlemann and Kempf, 2002; De Ruig and Hubbard, 2006; Bernhardt et al., 2012; Grunert et al., 2012; 2013). 3) Morphological peaks, reaching the sea level or areas showing steep slopes were manually eroded. Approximately the same amount of sediments eroded is deposited in the deep marine troughs.

Thermal Basin Modeling

Basin modeling integrates geological, geophysical and geochemical properties. By means of these properties, temperature and pressure evolution as well as generation and migration of hydrocarbons can be calculated (Welte and Yukler, 1981; Hantschel and Kauerauf, 2009). The study was performed using PetroMod TecLink v11 (SP4) software package developed by the Schlumberger PetroMod Group. In order to model complex tectonic environments like thrust belts, they need to be restored structurally and kinematically. In the present study several balanced paleo-sections were used to forward-model the temperature and maturity history of the section. With the PetroMod TecLink-concept, the finite element simulator is able to handle multiple z-values on one vertical grid line. Hence every paleo-section is split into several blocks specified by its boundaries and a characteristic layer stack.

Model Input

The precondition for basin modeling is the conversion of a consistent geological concept into numerical form (Welte and Yalcin, 1988). To process the evolution of the basin by the simulator it has to be subdivided into uninterrupted and discrete sequences, named events (Wygrala, 1988). An event represents a time span during

which geological processes (deposition, erosion, hiatus) occur (Bueker, 1996). Different geological processes can happen in various parts of the basin at the same time. In TecLink a paleo time step (section) may combine several geological events. Physically existing sedimentary units at a certain time are called layers. Each layer is deposited during a single event and may be eroded during a later erosional event (Wygrala, 1988). The model in this study comprises numerous original layers. Based on core analysis, facies were assigned to each layer using synthetic lithology mixtures provided by the software and featuring different properties like thermal conductivity (Table 2). As thermal conductivity values for the rock matrix are shown in Table 2, it is important to note that porosity affects thermal conductivity to an important degree, because pore fluids have lower thermal conductivities than the rock matrix.

Lithostratigraphic unit	Lithology mixture ratio	Thermal conductivity (matrix)	
	[%]	[W/(mK)] at 20 °C	[W/(mK)] at 100 °C
Basin fill			
Innviertel Group	40 Sandst./40 Shale/20 Marl	2.48	2.07
Hall Fm.	60 Siltst./20 Sandst./20 Marl	2.37	2.03
Up. Puchkirchen Fm.	40 Siltst./40 Marl/20 Shale	1.97	1.89
Low. Puchkirchen Fm.	40 Shale/40 Marl/20 Siltst.	1.86	1.85
Source rock interval	75 Shale/25 Marl	1.91	1.86
Eocene Sandst. (reservoir rock)	80 Sandst./10 Limest./10 Marl	3.75	2.52
Mesozoic			
Cretaceous	90 Marl/10 Sandst.	2.17	1.96
Jurassic	40 Limest./40 Dolom./20 Sandst.	3.79	2.54
Thrust			
Flysch	80 Shale/10 Sandst./10 Marl	1.83	1.83
North. Calc. Alps	50 Limest./50 Dolom.	3.71	2.51

Table 2: Assigned thermal conductivities of rock matrix (at 20 °C and 100 °C) for the various facies in the model. Calculated thermal properties are based on comprehensive literature review published in Hantschel and Kauerauf (2009).

A decompaction routine is integrated by default in PetroMod in order to reconstruct the initial thickness of each layer from present day data. The TecLink concept of the software uses predefined paleo-section geometries to determine porosity change. Therefore, compaction of autochthonous sediments was first computed in a preliminary model, where thrusting was simulated by increasing thicknesses of nappes through time (using PetroMods ´salt movement tool´). The achieved compaction data were later integrated in the thermal basin model built with the TecLink tool.

The Schoeneck, Dynow and Eggerding Formations are considered to be the source rocks (Schulz et al., 2002; Sachsenhofer et al., 2010). Due to scaling problems caused

by limited thicknesses of these layers, the three formations are merged to one source rock interval (Table 1). The entire interval has a net-thickness of about 70 m and is featured with an average initial TOC of 3 % and a HI of 450 mg HC/g TOC (Schulz et al., 2002; Sachsenhofer et al., 2010). Conversion of kerogen to hydrocarbons is driven by temperature and time dependent kinetic reaction processes (Tissot and Welte, 1984). Bulk kinetic parameters including an activation energy distribution and a single frequency factor of five immature Lower Oligocene source rocks samples from the Molasse Basin were determined at GFZ Potsdam (GeoS4 GmbH) using non-isothermal open system pyrolysis at four different laboratory heating rates (0.7, 2.0, 5.0 and 15 °C/min) and a Source Rock Analyzer©. The kinetic parameters of these samples differ only slightly (Figure 4). A corresponding kinetic data set ('Molasse kinetic') was assigned to the source rock unit.

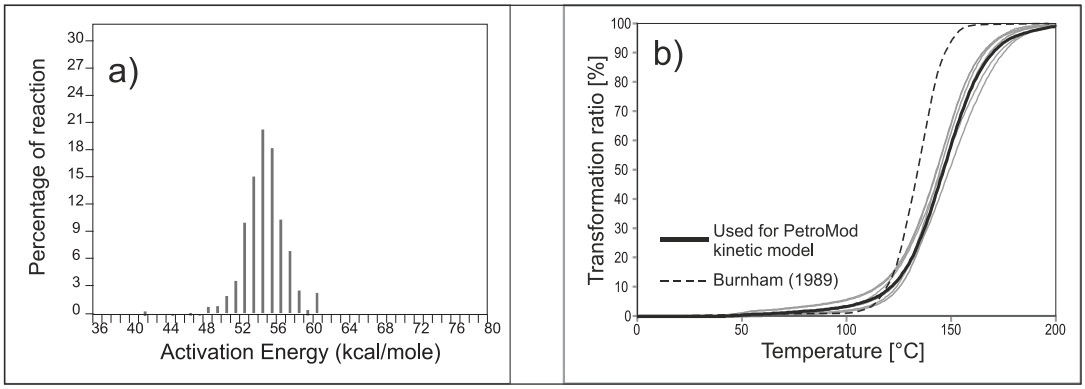

Figure 4: a) Kinetic parameters which were used to model petroleum generation; b) Predictions of transformation ratio for five different Lower Oligocene source rock samples based on kinetic parameters and a heating rate of 3.3 °C/million years. The prediction for the sample selected for modeling (see Figure 9) is shown by a thick black line. The dashed line represents predictions for a Type II kerogen (Burnham, 1989), which was used in the frame of a sensitivity analysis.

Boundary conditions

Paleo-water depth was chosen according to the general understanding of basin evolution (Wagner, 1996). The sediment water interface (SWI) temperature specifies the upper boundary condition for heat transfer in the basin. Mean surface temperature values over time are considered in PetroMod based on paleotemperature distribution maps after Wygrala (1989) and the paleo-water depth. The heat flow evolution at the base of the modeled section represents the lower thermal boundary condition.

Calibration Data

Temperature-sensitive parameters, such as vitrinite reflectance, sterane (20S / (20S + 20 R)) and hopane (22S / (22S + 22R)) isomerization ratios (MacKenzie et al., 1980, 1981; Mackenzie and McKenzie, 1983) as well as formation temperature have been used to calibrate the thermal evolution of the basin.

The calculation of vitrinite reflectance is based on the kinetic EASY%RO-algorithm (Sweeney and Burnham, 1990). The calculation of sterane and hopane isomerisation ratios uses the kinetics of Rullkötter and Marzi (1989).

Wagner et al. (1986) provided a wealth of vitrinite reflectance data for well Obhf1. Only reliable data (taken from core samples, high number of measurements) from the autochthonous Mesozoic and Cenozoic succession were considered. Data from wells Gein1, St1, He3 have been taken from Xu (1991).

In order to support the older data, vitrinite reflectance of some additional core samples has been determined within the frame of the present study following established procedures (Taylor et al., 1998). All new data, as well as those from Xu (1991) have been determined either on coal or macroscopically visible driftwood. These data are therefore considered highly reliable, show comparable results to the older published data and are integrated in the calibration plots.

The methylphenanthrene index (MPI-1; Radke and Welte, 1983) and the RockEval parameter Tmax (Espitalie et al., 1977) were used for a coarse estimation of maturity and to support measured vitrinite reflectance data but were not used for model calibration. A relation between MPI-1 and vitrinite reflectance (Ro (calculated) = 0.60 x MPI-1 + 0.40) for Type III kerogen was suggested by Radke et al. (1984). However, the applicability of the empirical relationship to Type II kerogen has been discussed controversially (Cassani et al., 1988).

With the formula Ro (calculated) = 0.0180 x Tmax – 7.16 it is possible to convert Tmax to reflectance (Peters et al., 2005). The equation was derived from a collection of shales and can be applied for low sulphur type II and type III kerogen.

Sterane and hopane isomerization ratios, Tmax and MPI-1 data have been taken from Schulz et al. (2002).

For the calibration of the present-day heat flow, three different data sets were used: (1) uncorrected bottom-hole temperatures (BHT; Kamyar, 2000), (2) corrected temperatures considering information on the time since circulation of the drilling fluid stopped (Horner-Plot; Horner, 1951), (3) temperature data from formation tests in well Obhf1 and He3.

All available calibration data for wells Gein1, St1, He3 and Obhf1 are plotted versus depth in Figure 5 (for position of wells see Figure 1).

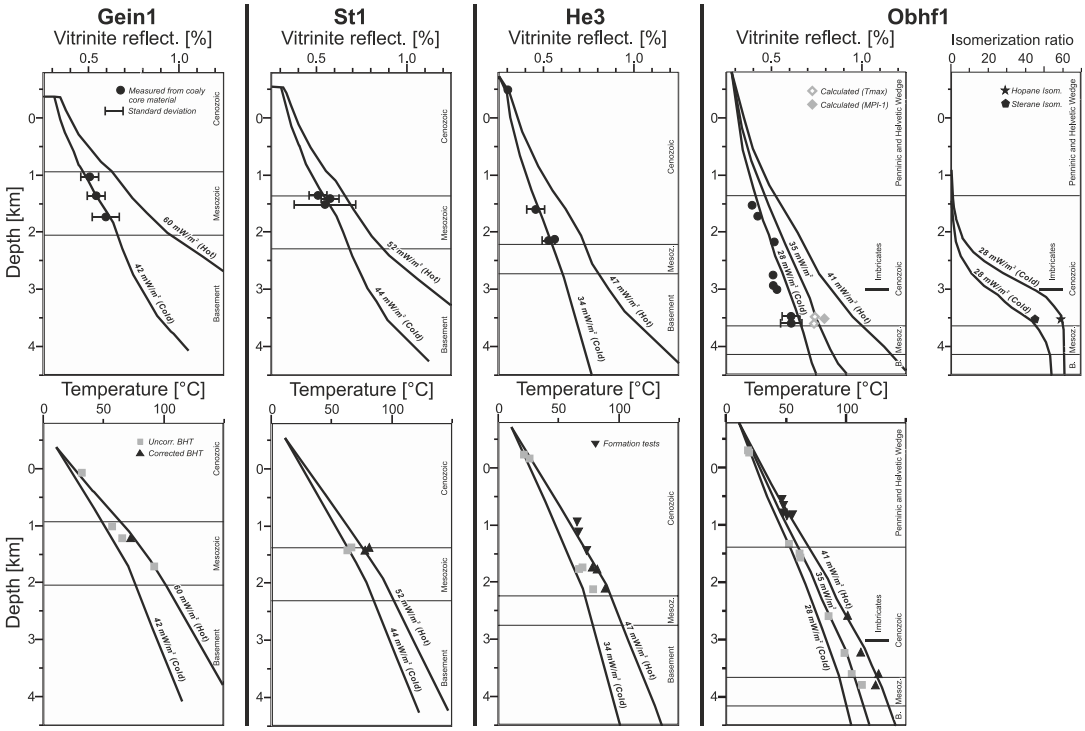

Figure 5: Maturity (vitrinite reflectance, steranes isomerization, hopanes isomerization) and temperature plots versus depth. Gein1 is the northernmost well, Obhf1 the southernmost well. Calculated trends of different heat flow scenarios are shown by different lines.

Results

In order to model the petroleum system in the Perwang imbricates, a kinematic forward model for the Attergau sector has been constructed in a way that it resembles in a simplified manner the structure imaged in the seismic interpretation (Figure 1b and c). In addition to the imaged structure in Figure 1b, the model features two small frontal thrust sheets in order to be comparable with the Perwang imbricates further to the west, where additional thrust sheets have evolved. The section crosses the deep Obhf1 well, which reached Molasse imbricates beneath the Penninic flysch and Helvetic wedge. Thus, the section can be calibrated against well data. Moreover the results allow extrapolation towards the main part of the Perwang imbricates.

Cross Section Forward Modeling

Figure 6 a-j shows 10 time / deformation increments along the modeled north-south section which reflect the kinematic evolution of the Perwang imbricates since Late Oligocene times (25 Ma; initiation of thrusting). Before onset of frontal accretion, the Molasse Basin units are overridden by the Penninic and Helvetic wedge (Figure 6b). Thereafter a large thrust sheet (Oberhofen thrust sheet; Figure 6c) is accreted and syntectonic sedimentation occurs along the deformation front. Additional frontal accretion of a smaller thrust is shown in Figures 6d, e. Then deformation steps back within the wedge which is moved towards the foreland on an out-of-sequence thrust (Figures f-i). Subsequent uplift affects both foreland and alpine wedge (Figure j) Derived minimal tectonic shortening in the forward modeled section is minimum 32.3 km (20.1 mi), which can be deduced from the position of the front of the Penninic and Helvetic wedge. Considering only the shortening affecting the Molasse imbricates, 15.1 km (9.4 mi) [L0-L] (L= deformed length; L0= undeformed length) corresponding to 39% of shortening is documented. The southern termination of the thrust sheet beneath the Penninic and Helvetic wedge and thus its footwall cut-off are unknown.

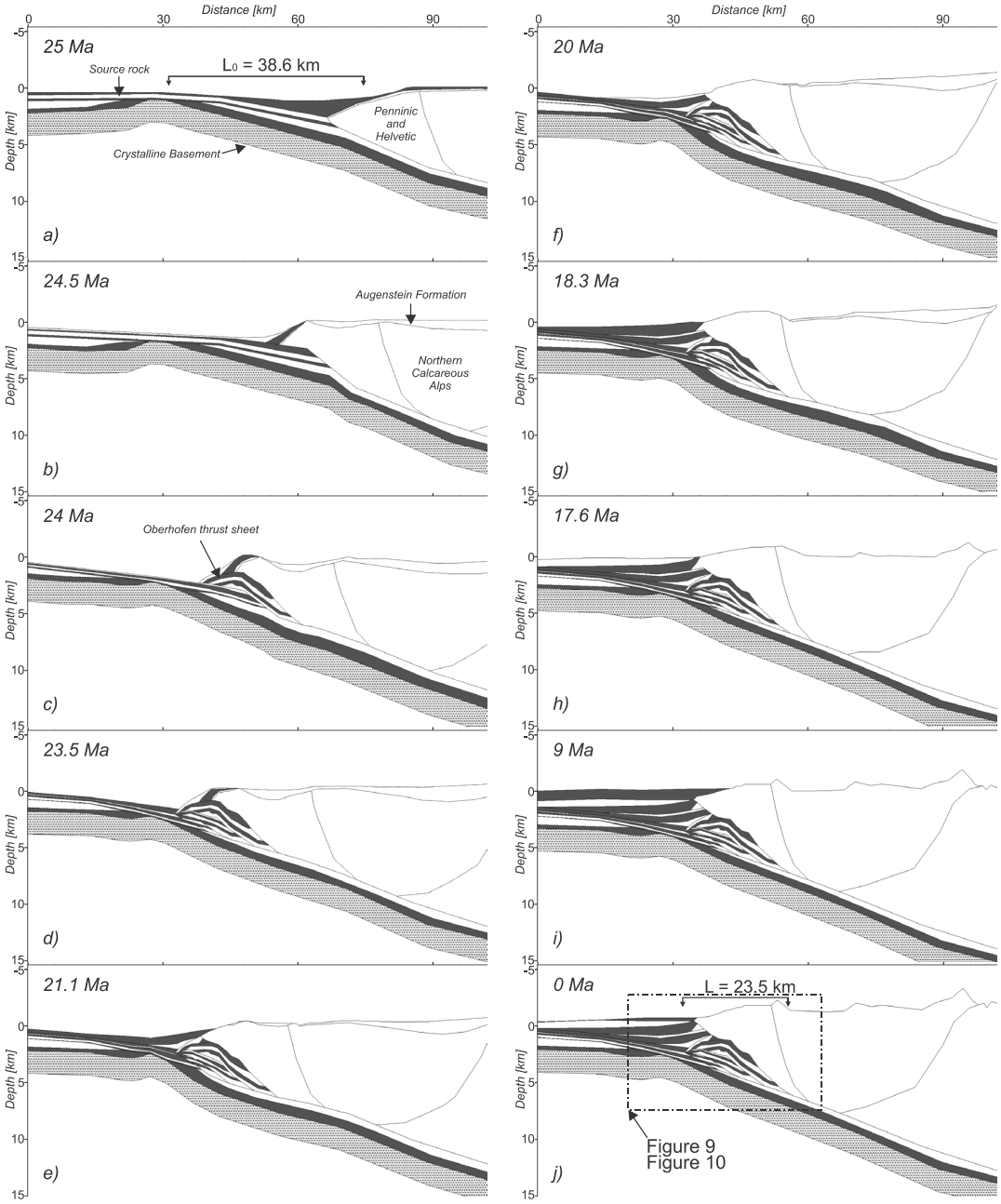

Figure 6: 2D basin evolution on a N-S section at the border of the Perwang imbricates (see Figure 1). The length between reference points for calculation of tectonic shortening is displayed on the oldest (Figure 6a) as well as on the Present Day section (Figure 6j; black arrows). Figure 6j shows also the section outline of Figures 9 and 10.

Thermal Modeling

Heat flow scenarios

Based on the calibration process, different heat flow scenarios have been used to model the thermal history along the section (Figure 7). In the first scenario ('hot'), a time-constant heat flow trend has been chosen to obtain a fit with corrected BHT and formation test temperatures (HF 1 in Figure 7). In this scenario heat flow decreases from north to south from 60 mW/m² to 41 mW/m². Obviously this heat flow scenario significantly overestimates all maturity data (Figure 5). This is also true for vitrinite values calculated from geochemical parameters.

In the second scenario ('cold'), a time-constant heat flow decreases from north to south from 40 to 45 mW/m² to 28 mW/m² (HF 2 in Figure 7). This scenario results in a good fit with measured vitrinite reflectance and isomerization data, but underestimates present-day formation temperatures (even when uncorrected BHT values are considered). Additional runs have been performed along the southern part of the section in order to find a fit in the Obhf1 well with vitrinite reflectance obtained from Tmax and MPI-1 (35 mW/m²). This heat flow results in a fit with uncorrected BHT data, but not with the corrected data which are considered to be more reliable.

In a third scenario ('best fit'), we tried to gain a fit for both maturity and present-day temperature data. This can be reached by accepting heat flow scenario HF 2 until the time of maximum burial (9 million years) in order to meet the maturity data and by increasing the heat flow in the recent past (since 2.5 million years) to heat flow scenario HF 1.

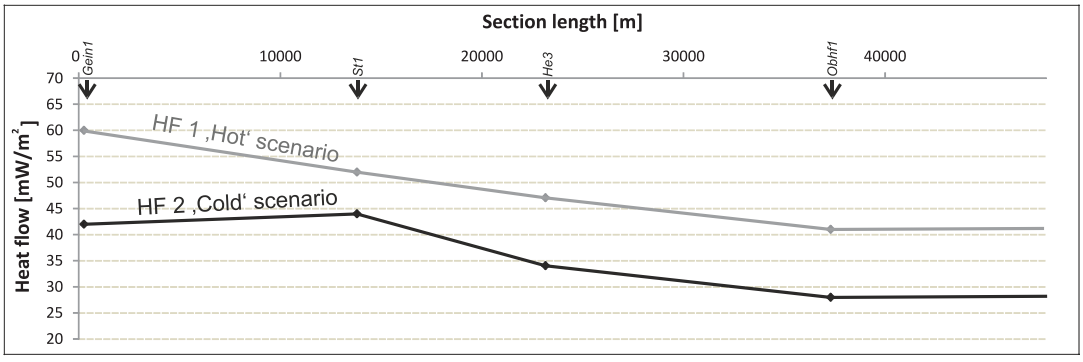

Figure 7: Assigned heat flow scenarios along the section. The later applied "best fit" scenario is a combination of HF 1 and HF 2 (see text for discussion.).

Sensitivity analysis

It is difficult to decide whether the recent increase in heat flow is a fact or an artifact. Therefore, different aspects which may bias the heat flow reconstructions are considered in this chapter:

- Quality of calibration data

  Recent heat flow is calibrated with formation temperature values whereas paleo-heat flow is calibrated with measured or calculated vitrinite reflectance data applying the EASY %RO algorithm. Therefore, apart from geological reasons, discrepancies between paleo- and present-day heat flow could be due to biased vitrinite and temperature data or due to inaccuracies of the applied algorithm.

  In order to exclude the eventuality that increase in heat flow is due to biased vitrinite data (e.g. Carr, 2000), some samples were re-measured. These samples yielded identical results and did not show indications of suppression. In addition to measured vitrinite data, vitrinite reflectance calculated using Tmax and MPI-1 values has been considered. The calculated values are slightly higher than the measured ones resulting in slightly higher reconstructed heat flow values (35 mW/m). However, a heat flow of 35 mW/m² still underestimates (corrected) temperature data.

  Temperature data derived from formation test measurements are considered to be most reliable, but are available only for wells Obhf1 and He3. Measured BHT temperatures have been corrected using the approach of Horner (1951). Although measured BHT data are considered as minimum estimates, the corrected temperatures are considered more reliable. Additionally it has to be noted that previous studies (e.g. Hermanrud et al., 1990) claimed that the Horner plot method will generally underestimate formation temperatures, if the time since circulation stopped is short.

- Impact of erosion estimates on the reconstructed thermal history

  In order to avoid uncertainties related to thrusting, well He3 located north of the thrust front has been selected for the sensitivity analysis (Figure 1). Based on Gusterhuber et al. (2012), erosion of the upper part of the Miocene Freshwater Molasse, 600 m thick, has been adopted in the conceptual model (Figure 8a). Considering this assumption, a good fit with calibration data is obtained with the 'best fit' heat flow scenario and a 13 mW/m² heat flow increase (Figure 8a). Obviously the amount of heat flow increase depends on the erosion estimate. In order to test an extreme model, erosion was set to a minimum value of only 80 m (difference between a nearby mountain top and the elevation of the He3 well) in a sensitivity run. Figure 8b shows that even in this model time-constant heat flows

either underestimate present-day temperatures (38 mW/m²) or overestimate maturity (42 mW/m²).

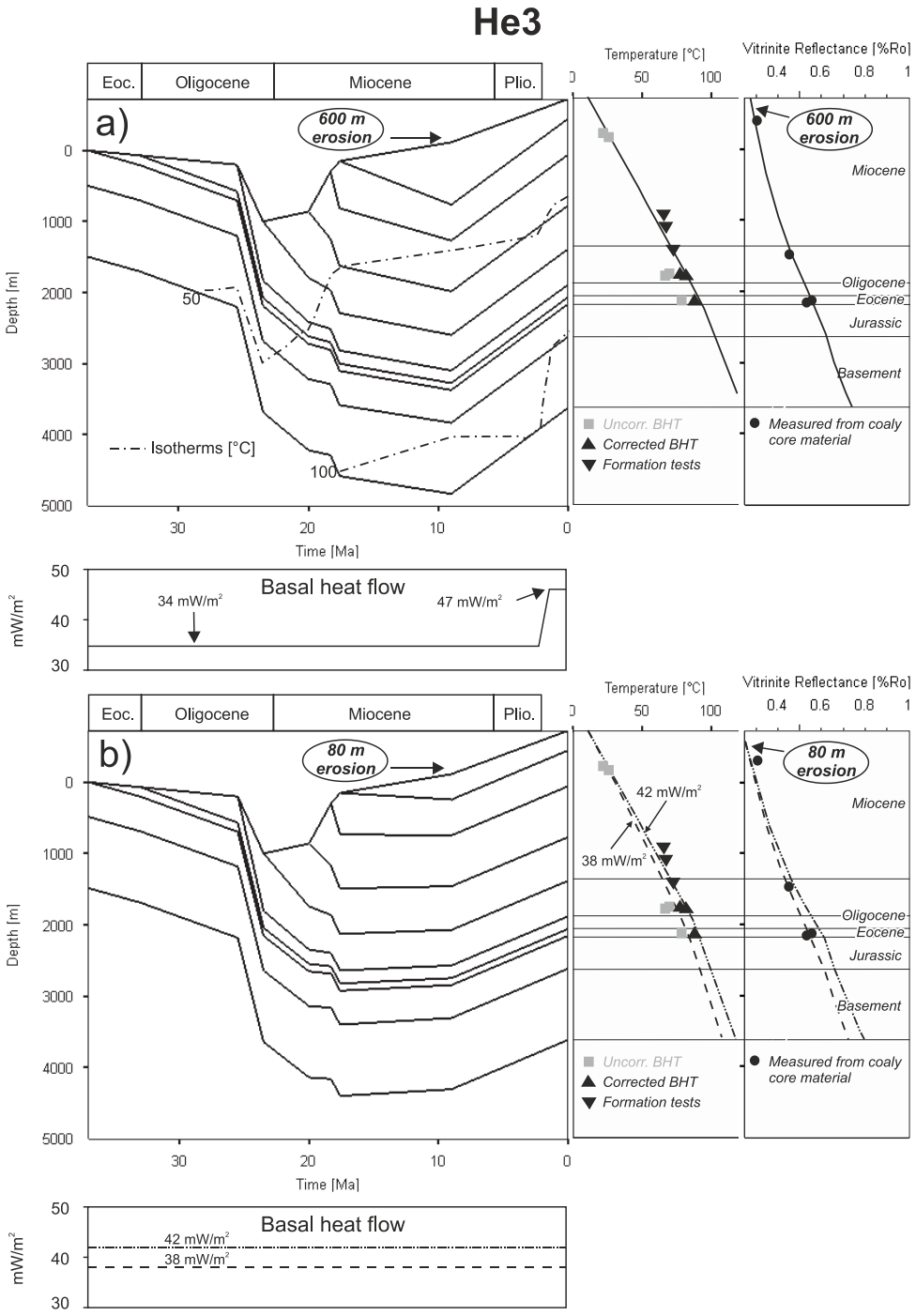

Figure 8: (a) Burial history of borehole He3 (see Figure 1 for position) based on the input parameters from the 2D conceptual model including erosion of 600 m. The 'best fit' heat flow scenario results in a good fit between measured and calculated calibration data. (b) Burial history plot considering erosion of rocks, 80 m thick. The calibration data show that a time-constant heat flow of 38 mW/m² underestimates formation

temperatures, whereas a time-constant heat flow of 42 mW/m² overestimates maturity. This result indicates that even if an unrealistic low thickness of eroded rocks is applied, a time-constant heat flow does not result in a successful fit.

- Overpressure

  It is assumed that overpressure is able to retard the maturity of organic matter (Carr, 1999, 2000; Zou and Peng, 2001). This may explain the misfit for heat flow derived from maturity and temperature data. Actually, the southernmost well (Obhf1) penetrates Molasse imbricates with an overpressured pore fluid system (1.7-1.8 bar/10m; 0.74-0.78 psi/ft). However, all northern wells show hydrostatic conditions. Thus, the observed discrepancy between heat flows derived from maturity and temperature data, cannot (solely) be attributed to overpressuring.

Petroleum Systems Modeling

Hydrocarbon Generation

Based on the above discussion, the heat flow scenario 'best fit' is considered the most likely one and has been used to model hydrocarbon generation. Models based on heat flow scenarios ´cold´ and ´hot´ are also presented in order to show the sensitivity of the model results.

As the present study focuses on the thermal evolution and the generation potential of the Molasse imbricates, Figure 9 highlights enlargements of the specific area (see limits in Figure 6 j). In Figure 9, generation zones for each heat flow scenario based on calculated vitrinite reflectance are shown for three different time slices (20 Ma, 9 Ma, present-day). Although vitrinite reflectance isolines (red lines) are shown for all rock units, blue to green colored generation zones are indicated only for the source rock formations. In addition, temperature, thermal maturity and generation history plots are shown on Figure 9 for two points (X: shallow imbricate; Y: deeper imbricate) representing the deepest zones of two different Molasse imbricates.

In the '**best fit**' scenario (Figure 9) the Molasse imbricates reach a first thermal maximum about 19 million years BP (Early Miocene). Thereafter temperatures remain constant or decrease slightly. Hydrocarbon generation commenced as a result of early Miocene heating only in the deepest part of the higher Molasse imbricates (point Y) and at a very low rate. Despite uplift, temperatures increased in both Molasse imbricates at about 20 °C during the last 2.5 million years. This is clearly a consequence of increasing heat flow. The recent heating event had a minor effect on vitrinite reflectance, but restarted hydrocarbon generation. However, the transformation ratio remains very low (<20%). Thus, in this scenario two phases of

hydrocarbon generation (both minor and confined to the deepest part of the imbricated zone) can be distinguished.

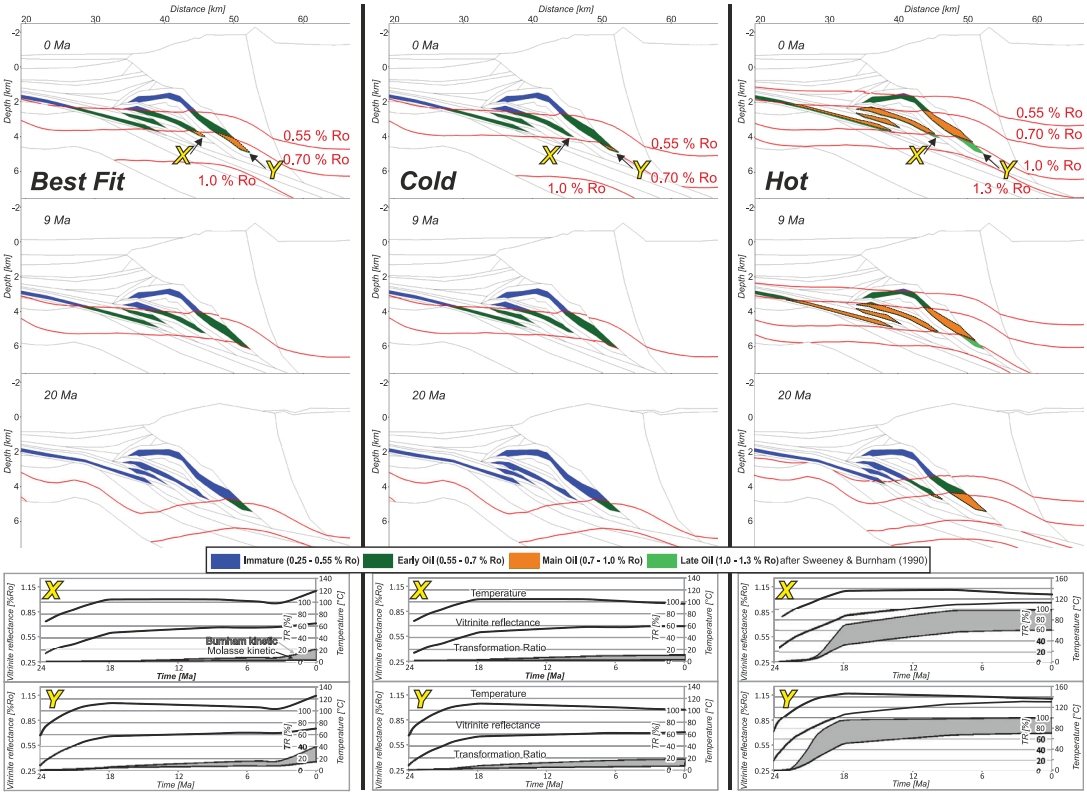

Figure 9: Petroleum generation history focused on the Perwang imbricates. Specific sector extracted from the structurally forward modeled section (see position in Figure 6j). Red lines indicate the separation of the different maturity stages. Time plots (below) show temperature, vitrinite reflectance (Ro) and transformation ratio (TR) evolution over the time for the deepest zones of two different imbricates (X and Y). Orange shaded areas in the time plots mark the difference between the applied 'Molasse kinetic' and the kinetic from Burnham (1989) which is shown as boundary condition.

Sensitivity analysis

- Alternative kinetic data set

  Uncertainty arises from the fact that the kinetic parameters were determined from rock samples in the foreland, whereas the source kitchen is located beneath the Alpine nappes. Therefore, an alternative kinetic data set (Type II kerogen of Burnham, 1989) was considered for sensitivity analysis (Figure 4). In the alternative model hydrocarbon generation starts at the same time, but continued at a very low rate during the Middle and Late Miocene. Young heating results in a transformation ratio of 40 and 20% for the positions Y and X respectively. This

suggests that the prediction of the total amount of generated hydrocarbons strongly depends on the applied kinetic data set.

- Heat flow scenarios 'cold' and 'hot'

  The '**cold**' scenario (Figure 9) is similar to the best fit scenario, but the recent increase in heat flow is missing. Consequently, the more recent generation phase is absent and some early oil is generated only with the Burnham kinetic in the deeper parts of the Molasse imbricates.

  In the '**hot**' scenario (Figure 9) major hydrocarbon generation in the Molasse imbricates started as early as 23 Ma and reached 60-80 % of transformation ratio already during Late Miocene time. Running this scenario with the Burnham kinetic, there is no hydrocarbon potential left regardless if the shallow or the deep imbricate are considered.

- Alternative topography of the paleo-Penninic flysch surface

  In the conceptual model, the wedge forms a prominent topographic high (Figure 6). However, the precise elevation of the surface is unknown. In order to test the influence of the precise topography on the thermal and hydrocarbon generation histories in the Molasse imbricates, the model '**wedge slope**' was performed. In this model the topography formed a gently northward dipping slope just above base level (Figure 10), with the present day topography (Figure 6) forming only since 3 million years BP. Obviously the removal of the topographic high results in a decrease in temperatures. Figure 10 shows the effect for the time-step 17. 6 million years BP which can be considered representative for the time-interval between 20 and 2.5 million years. For this time step the maximum decrease in temperature is 7 °C.

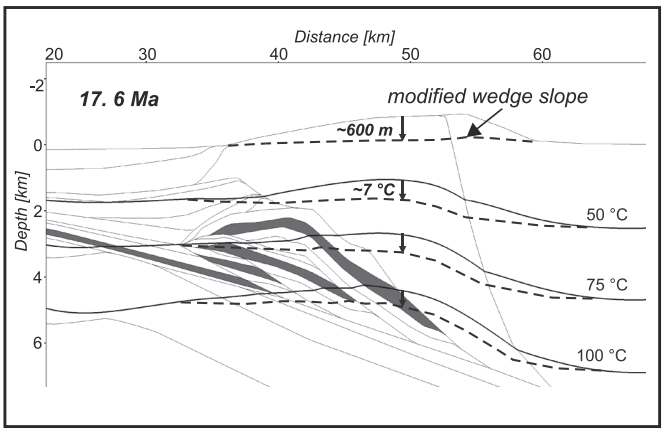

Figure 10: Detail of the Perwang imbricates (see position in Figure 6j) showing the effect of different elevations of the paleo-wedge surface on isotherms. The original model considers a significant topographic

high in the area of the Penninic flysch Zone. Dashed lines refer to the model "wedge slope", where the wedge surface is near sea level. The latter model results in lower temperatures in the Perwang imbricates and a downward shift of isotherms.

Based on the 'best fit' heat flow scenario, Figures 11 and 12 show the effects of the modified flysch wedge surface on the depth (below sea-level) of two points of interest (X and Y; Figure 9) and their thermal and maturity histories. The figures show that the effect on temperature (5-10 °C cooling) and maturity (0.03-0.05 % Ro decrease) is minor. The subtle cooling effect allows increase of paleo-heat flow to 30 mW/m² in the '**wedge slope**' model without overestimating present-day maturity (Figures 11, 12).

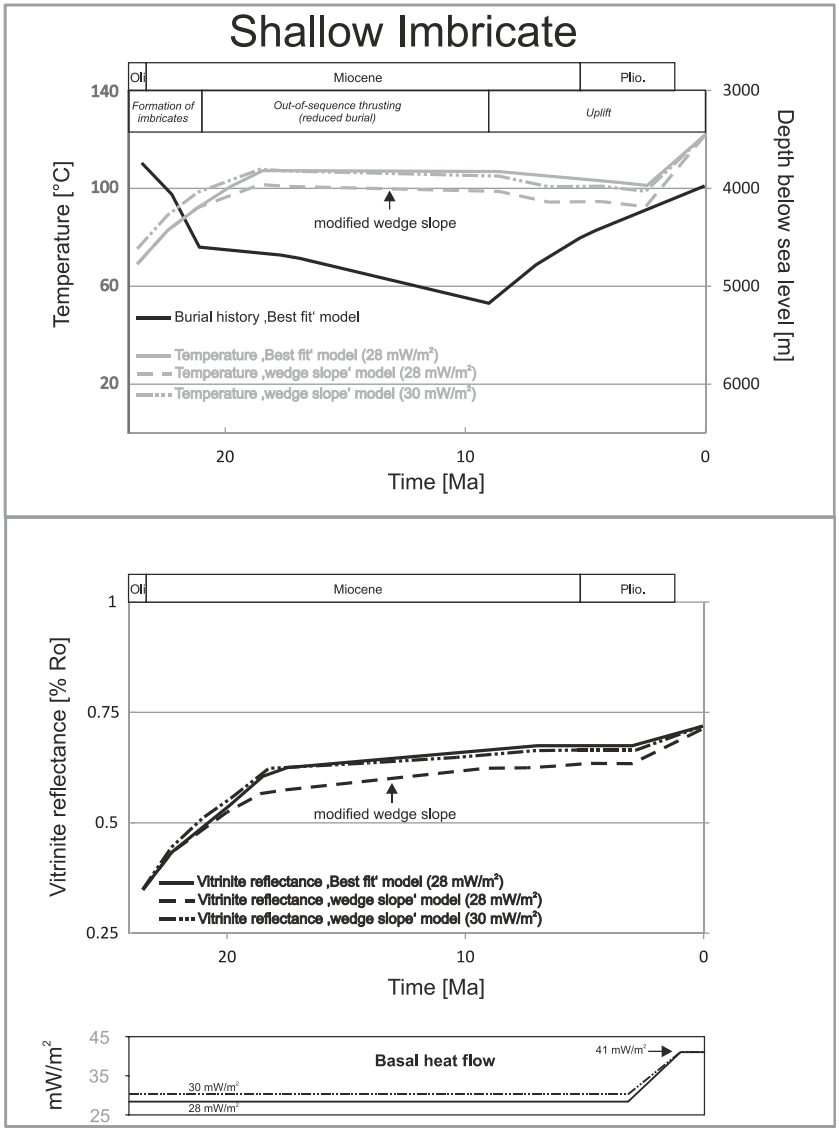

Figure 11: Burial history, temperature (above) and vitrinite reflectance (below) development of point X (shallow imbricate; Figure 9) for different models. Continuous lines represent the results of the conceptual

model applying the 'best fit 'heat flow scenario; dashed lines mark the results of the model "wedge slope" (see Figure 10) using the 'best fit 'heat flow scenario; dashed-dotted lines show the model "wedge slope" with a paleo-heat flow of 30 mW/m².

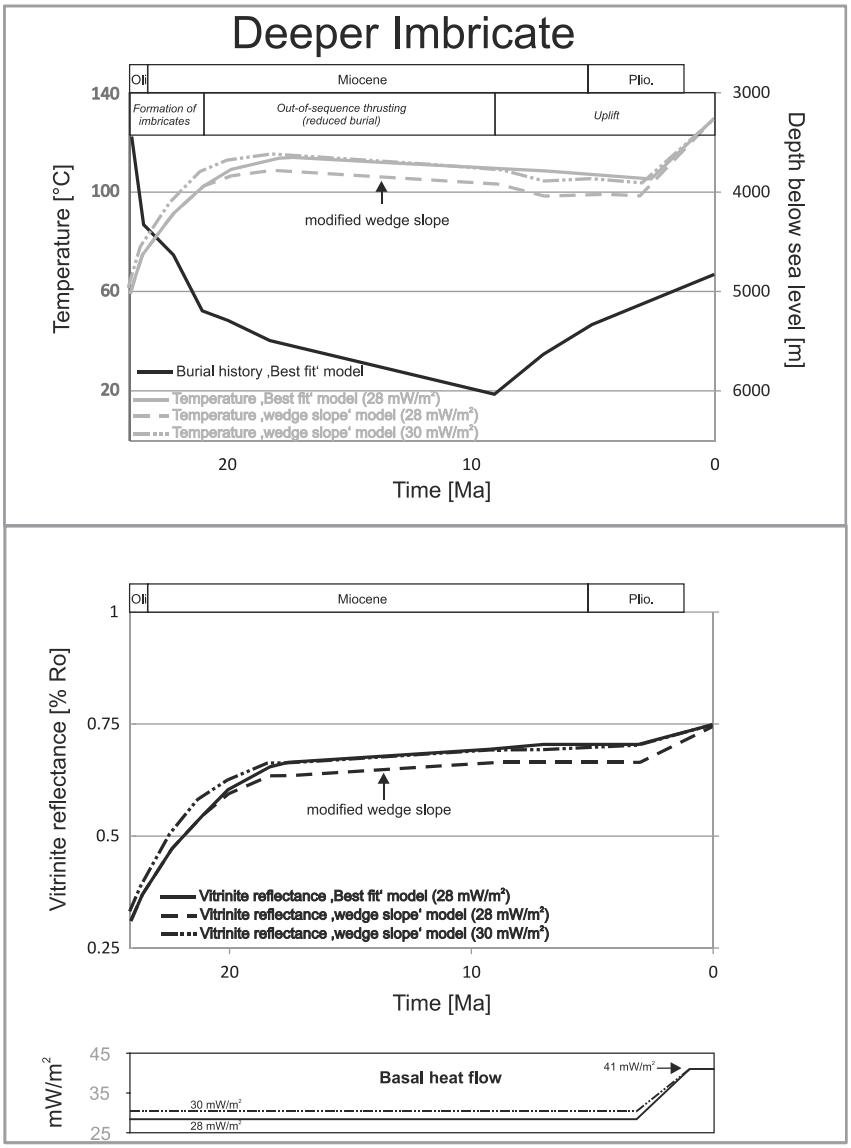

Figure 12: Burial history, temperature (above) and vitrinite reflectance (below) development of point Y (deeper imbricate; Figure 9) for different models. Continuous lines represent the results of the conceptual model applying the 'best fit 'heat flow scenario; dashed lines mark the results of the model "wedge slope" (see Figure 10) using the 'best fit 'heat flow scenario; dashed-dotted lines show the model "wedge slope" with a paleo-heat flow of 30 mW/m².

The effect on hydrocarbon generation is minor, because of the late increase in temperature and maturity, all hydrocarbons are formed during the last 2.5 million years in the scenario with 28 mW/m² paleo-heat flow ('best fit').

Discussion

Heat flow history

The heat flow evolution of the study area is characterized by (1) very low Oligocene and Miocene heat flows, (2) an increase in heat flow during the Pliocene and the Pleistocene, (3) a southward decrease, both, in paleo-heat flow and in present-day heat flow, and (4) present-day heat flow, which is slightly lower than that shown in a new heat flow map of Europe (Majorowicz and Wybraniec, 2011).

(1) Oligocene and Miocene heat flows

The reconstructed Oligocene and Miocene heat flows are very low (28-44 mW/m²) resulting in low average paleo-geothermal gradients reaching 25 °C/km in the foreland and 20 °C/km in the imbricated zone. Similar conditions have been observed in wells in the Swiss (Rybach, 1984; Schegg, 1994; Schegg and Leu, 1996; Schegg et al., 1997), German (Jacob and Kuckelkorn, 1977; Teichmueller and Teichmueller, 1986) and Austrian Molasse Basin and its fold-and-thrust belt (Sachsenhofer, 2001).

(2) Increase in heat flow during Pliocene and Pleistocene times

The sensitivity analysis suggests that the increase in heat flow is not an artifact. However, the geological reasons for it are still poorly understood. Possible reasons include

- a change in hydrodynamics caused by a Pleistocene change in the stress field (Schmidt and Erdogan, 1993; Horvath and Cloetingh, 1996),
- a topography-induced perturbation of the shape of isotherms e.g. due to high exhumation rates in the Eastern Alps. However, present-day exhumation rates are clearly below values which are considered to affect the shape of isotherms (450 m Ma^{-1}; Glotzbach et al., 2009).
- a large scale increase in mantle heat flow, which should have affected major parts of the Alps. Without more and better heat flow data from the central Eastern Alps, the latter possibility remains pure speculation, and
- Pleistocene glaciation, which has affected considerably the southern part of the section (Van Husen, 1987). Majorowicz and Wybraniec (2011) have shown that glaciation has led to a substantial reduction in temperature at shallow depth (mainly <1 km) resulting in an underestimation of present-day heat flow. Important to note that the minimum present-day heat (41 mW/m²) is based on formation temperature data from more than 3 km depth in the Obhf1 well. Thus, these data are supposed to be unaffected by glaciation (Majorowicz and

Wybraniec, 2011). Moreover, the application of paleoclimatic corrections would enlarge the difference between Neogene and present-day heat flow.

(3) Southward decrease in heat flow

Both, reconstructed paleo-heat flow and present-day heat flow decrease towards the south. Similar heat flow patterns have also been observed by Rybach (1984), Teichmueller and Teichmueller (1986) and Sachsenhofer (2001) in the Swiss, Bavarian and Austrian parts of the Molasse Basin, respectively. The southward decrease in heat flow may have different causes: (I) thermal disequilibrium due to downbending of the Mohorovicic (MOHO) -discontinuity and thickening of the crust (Teichmueller and Teichmueller, 1986); (II) a thermal blanketing effect driven by the fast approach of the already compacted nappe system; (III) deep infiltration of cold surface water in the karstified rocks of the Northern Calcareous Alps (Wessely, 1983); (IV) elevated heat flows in the northern part of the Molasse Basin due to heat transfer by northward migrating fluids from beneath the Alpine nappes (Schmidt and Erdogan, 1993), which influenced the temperature field in the upper few kilometers of the crust (Rybach, 1984); (V) or any combination of the above.

(4) Present-day heat flow

The reconstructed present-day heat flow varies between 41 and 60 mW/m². As discussed earlier, the heat flow is probably not affected by glaciation. Nevertheless, the heat flow range is slightly lower than that suggested in a new heat flow map of Europe for the same area (50-70 mW/m²; Majorowicz and Wybraniec, 2011). Maybe the difference is due to different estimates of thermal conductivities. For lack of measured data, matrix conductivities predefined by the software for each of the drilled lithologies were used.

Implications for the prospectivity of the Perwang imbricates

The numeric models suggest that some hydrocarbons were generated within the Molasse imbricates. However, adopting kinetic data from the Lower Oligocene source rock interval, hydrocarbon generation remains at a low level (transformation ratio <20 %). Based on the '**best fit**' heat flow scenario (Figure 9), it is likely that hydrocarbons within the imbricates were generated only recently during Pliocene and Pleistocene times. An earlier hydrocarbon generation phase during Early Miocene time (18 to 20 million years BP) occurred if the kinetic data of the organic matter are similar to those of Type II kerogen of Burnham (1989).

Independent support for hydrocarbon generation within the Molasse imbricates is provided by oil in the thrust sheet tested by the Obhf1 well. This oil exhibits characteristics of a Type B oil (e.g. very low DBT/Ph ratios) arguing for a source

with ´normal´ facies, which occurs within the Perwang imbricates, but not in the autochthonous section west of the Lindach Fault.

Thus, two different migration systems can be recognized (Figures 3):

(1) Oil generated in autochthonous Molasse rocks west of the Lindach Fault (´Oberhofen´ facies) migrated north(west)wards beneath the imbricates and filled the reservoirs in the western part of the study area (Type A oil; Figure 3a). Biomarker data from oil stains detected in autochthonous Jurassic rocks in the Obhf1 well (Figure 3b; R. Gratzer, 2012, personal communication) suggest a similar source.

(2) Type B oil generated within the Molasse imbricates caused the oil show in the Perwang imbricates of the Obhf1 well and filled reservoirs in nearby autochthonous Oligocene sediments (Mlrt1; Gratzer et al., 2011). The lack of Type B oil north of the Perwang imbricates suggests that lateral hydrocarbon migration from the Perwang imbricates was minor with the exception of the discovered economic reservoir in Mlrt1. Mlrt1 exhibits a reservoir gradient of approx. 1.3-1.4 bar/10 m; 0.57-0.61 psi/ft). Obviously this overpressure gradient is lower than in nearby Perwang imbricates (1.7-1.8 bar/10 m; 0.74-0.78 psi/ft; Figure 3b). Mlrt 1 is located in a proto thrust zone where constricting deformation by the thrust belt has already started but no proper thrust has been formed. Hence, developing thrust faults might be subseismically and no transport of stata can be observed. Pressure difference could have caused leakage of reservoirs located in the Perwang imbricates into the virtually undeformed foreland. Even though there is no precise evidence on timing, a likely explanation is that charging of Mlrt took place at time of sub-recent regional uplift involving the Perwang imbricates. Uplift or exhumation in respect to the hydrostatic datum may increase relative pressure gradients inside the imbricate reservoirs with a strong probability of seal-breach. It is important to point out that oil shows inside the Perwang imbricates were only detected in the deeper part of the thrust belt (Oberhofen thrust sheet) which extends beneath the flysch wedge. No oil shows are known in the small wedges situated in a shallower position in front of the accretionary wedge (Figure 3b). This means that these thrust slices have never been charged because they were not connected to migration pathways to the oil kitchen in larger and deeper thrust sheets. Alternatively, these small imbricates lost all their charge due to seal-breach (in the younger uplift history). Future investigations will have to show, whether seal integrity of potential traps remained intact during recent basin uplift. Whereas hydrocarbon generation within the Molasse imbricates is proven (e.g. by the Mlrt oil and oil stains in the Obhf well), the low transformation ratio constitutes an exploration risk.

Conclusions

The structural model, a kinematic model with geodynamic background, provides realistic input for the petroleum systems model. Furthermore, it supposes that total tectonic shortening in the modeled section is at least 32.3 km (20.1 mi).

Formation temperatures indicate present-day basal heat flows decreasing southwards from 60 to 41 mW/m². Maturity data argue for very low paleo-heat flows along the modeled section decreasing in the same direction from 44 to 28 (or 30) mW/m². This higher present-day heat flow probably indicates an increase in heat flow during Pliocene and Pleistocene times. The cause of the increase in heat flow is not yet understood. In order to account for the uncertainty, three different heat flow scenarios ('best fit', 'cold', 'hot') were applied and different sensitivity runs were performed.

In the 'best fit' scenario and considering kinetic data from the Lower Oligocene source rock interval, minor hydrocarbon generation (transformation ratio <20 %) occurred only in the deeper parts of the Molasse imbricates and was caused by a Pliocene and Pleistocene increase in heat flow. Models considering different amounts of erosion in the foreland and different positions of the paleo-wedge surface have little influence on this result.

The 'cold' scenario is similar to the best fit scenario but the recent increase in heat flow is missing. Therefore no significant hydrocarbon generation occurs in this scenario. In the 'hot' scenario, which is considered most unlikely, major hydrocarbon generation in the Molasse imbricates started as early as 23 Ma (Early Miocene) and the transformation ratio reached 60 % even in the shallow imbricate applying the kinetic data determined on the Oligocene source rocks.

Hydrocarbon generation in the deeper parts of the Perwang imbricates is proven by oil stains and supported by the presented models. The low transformation ratio indicates a charge risk. However, deeper parts of the imbricates are assumed to have a have a higher hydrocarbon potential and a lower charge risk than smaller frontal imbricates In matters of oil migration out of the imbricates, incorporation of recent insights in oil families and oil-source rock correlations (Gratzer et al., 2011) provides at least evidence for oil migration from the deep Oberhofen thrust sheet into nearby autochthonous units. This lateral migration from the overpressured Perwang imbricates towards the north was probably only limited.

If there was any oil migration upward into the smaller frontal imbricates or even further into the foreland, remains uncertain. This means that the potential for future oil exploration strongly depends on the existence of migration pathways along the

thrust planes during charge as well as on potential traps retaining their integrity during recent basin uplift.

References cited

Andeweg, B., and S. Cloetingh, 1998, Flexure and 'unflexure' of the North Alpine German-Austrian Molasse Basin: constraints from forward tectonic modelling: Geological Society of London, Special Publications, v. 134, no. 1, p. 403-422.

Bernhardt, A., L Stright, and D. R Lowe, 2012, Channellized debris-flow deposits and their impact on turbidity currents: the Puchkirchen axial channel belt in the Austrian Molasse Basin: Sedimentology, DOI: 10.1111/j.1365-3091.2012.01334.x.

Bueker, C, 1996, Absenkungs-, Erosions- und Waermeflussgeschichte des Ruhrbeckens und des nordoestlichen Rechsrheinischen Schiefergebirges: PhD thesis., University of Bochum, Forschungszentrum Juelich, 3319, 212 p.

Burnham, A. K., 1989, A simple kinetic model of petroleum formation and cracking: Lawrence Livermore National Laboratory Report, UCID-21665, 11 p.
Carr, A. D., 1999, A vitrinite reflectance kinetic model incorporating overpressure retardation: Marine and Petroleum Geology, v. 16, p. 355-377.

Carr, A. D, 2000, Suppression and retardation of vitrinite reflectance, part 1. Formation and significance for hydrocarbon generation: Journal of Petroleum Geology, v. 23, p. 313–343.

Cassani, F., O. Gallango, S. Talukdar, C. Vallejos, and U. Ehrmann, 1988, Methylphenanthrene maturity index of marine source rock extracts and crude oils from the Maracaibo Basin: Organic Geochemistry, v. 13, p. 73-80.

Covault, J. A., S. M Hubbard, S. A Graham, R. Hinsch, and H. Linzer, 2009, Turbidite-reservoir architecture in complex foredeep-margin and wedge-top depocenters, Tertiary Molasse foreland basin system, Austria: Marine and Petroleum Geology, v. 26, p. 379-396.

De Ruig, M. J., and S. M. Hubbard, 2006, Seismic facies and reservoir characteristics of a deep marine channel belt in the Molasse foreland basin: AAPG Bulletin, v. 90, p. 735-752.

Dohmann, L., 1991, Die unteroligozaenen Fischschiefer im Molassebecken: PhD thesis, Ludwig-Maximilian-Universitaet, Munich, 365 p.

Espitalié, J., J. L. LaPorte, M. Madec, F. Marquis, P. Leplat, J. Poulet, and A. Boutefeu, 1977, Méthode rapide de charactériasation des roches mères de leur potential pétrolier et de leur degré d´evolution: Revue de l´Institut Francais du Pétrole, v. 32, p. 23-42.

Frisch, W., J. Kuhlemann, and I. Dunkl, 2001, The Dachstein paleosurface and the Augenstein Formation in the Northern Calcareous Alps – a mosaic stone in the geomorphological evolution of the Eastern Alps: International Journal of Earth Sciences, v. 90, p. 500-518.

Glotzbach, C., C. Spiegel, J. Reinecker, M. Rahn, and W. Frisch, 2009, What perturbs isotherms? An assessment using fission-track thermochronology and thermal modelling along the Gotthard transect, Central Alps: Geological Society of London, Special Publications, v. 324, p. 111-124.

Gratzer, R., A. Bechtel, R. F Sachsenhofer, H.-G Linzer, D. Reischenbacher, and H.-M Schulz, 2011, Oil-oil and oil-source rock correlations in the Alpine Foreland Basin of Austria: Insights from biomarker and stable carbon isotope studies: Marine and Petroleum Geology, v. 28, p. 1171-1186.

Grunert, P., A. Soliman, S. Coric, R. Roetzel, M. Harzhauser, and W. E. Piller, 2012, Facies development along the tide-influenced shelf of the Burdigalian Seaway: An example from the Ottnangian stratotype (Early Miocene, middle Burdigalian): Marine Micropaleontology, v. 84-85, p. 14-36.

Grunert, P., R. Hinsch, R. F. Sachsenhofer, A. Bechtel, S. Coric, M. Harzhauser, W. E. Piller, and H. Sperl, 2013, Early Burdigalian infill of the Puchkirchen Trough (North Alpine Foreland Basin, Central Paratethys): Facies development and sequence stratigraphy: Marine and Petroleum Geology, http://dx.doi.org/10.1016/j.marpetgeo.2012.08.009.

Gusterhuber, J., I. Dunkl, R. Hinsch, H.-G. Linzer, and R. F. Sachsenhofer, 2012, Neogene uplift and erosion in the Alpine Foreland basin (Upper Austria and Salzburg): Geologica Carpathica, v. 63, p. 295-305.

Halliburton, 2010, LithoTect Software, v. 5000.01, Landmark Software and Services.
Hantschel, T., and A. Kauerauf, 2009, Fundamentals of Basin and Petroleum Systems Modeling: Springer-Verlag Berlin Heidelberg, 476 p.

Hermanrud, C., S. Cao, and I. Lerche, 1990, Estimates of virgin rock temperature derived from BHT measurement: Bias and errors: Geophysics, v. 55, no. 7, p. 924-931.

Hinsch, R., 2008, New Insights into the Oligocene to Miocene Geological Evolution of the Molasse Basin of Austria: Oil & Gas European Magazine, v. 34, no. 3, p. 138-143.

Hinsch, R., and H.-G. Linzer, 2010, Along-strike variations of structural styles in the imbricated Molasse of Salzburg and Upper Austria: a 3D seismic perspective: EGU General Assembly, Geophysical Research Abstracts, vol. 12, EGU2010-4966-3.

Hinsch, R., in press, Laterally varying structure and kinematics of the Molasse fold-and-thrust belt of the Central Eastern Alps:implications for exploration: AAPG Bulletin.

Horner, D. R., 1951, Pressure buildup in wells, in: E. J. Brill, ed., Proceedings of the Third World Petroleum Congress, The Hague Section II, Cologne, p. 503-521.

Horvath, F., and S. Cloetingh, 1996, Stress-induced late-stage subsidence anomalies in the Pannonian basin: Tectonophysics, v. 266, p. 287-300.

Hubbard, S. M., M. J. De Ruig, and S. A Graham, 2009, Confined channel-levee complex development in an elongate depo-center: Deep-water Tertiary strata of the Austrian Molasse basin: Marine and Petroleum Geology, v. 26, p. 85-112.

Hughes, W. B., A. G. Holba, and L. I. P. Dzou, 1995, The ratios of dibenzothiophene to phenanthrene and pristan to phytan as indicators of depositional environment and lithology of petroleum source rocks: Geochimica et Cosmochimica Acta, v. 59, p. 3581-3598.

Jacob, H., and K. Kuckelkorn, 1977, The carbonization profile of the Miesbach 1 well and its oil geological interpretation: Erdoel-Erdgas-Zeitschrift, v. 93, p. 115-124.

Kamyar, H. R., 2000, Verteilung der Untergrundstemperaturen an den Beispielen der Bohrlochtemperatur (BHT) – Messungen in den RAG – Konzessionen Oberösterreichs und Salzburgs, (Molasse- und Flyschzone): PhD-thesis, University of Vienna, Austria, 145 p.

Krenmayer, H. G., 1999, The Austrian sector of the North Alpine Molasse: A classic foreland basin: FOREGS (Forum of Euopean Geological Surveys) Dachstein-Hallstatt-Salzkammergut Region, Vienna, p. 22-26.

Kuhlemann, J., and O. Kempf, 2002, Post-Eocene evolution of the North Alpine Foreland Basin and its response to Alpine tectonics, Sedimentary Geology, v. 152, p. 45-78.

Linzer, H.-G., 2001, Cyclic channel systems in the Molasse foreland basin of the Eastern Alps - the effects of Late Oligocene foreland thrusting and Early Miocene lateral escape: AAPG Bulletin, v. 85, p. 118 (abstract).

Linzer, H.-G., 2002, Structural and stratigraphic traps in channel systems and intraslope basins of the deep-water molasse foreland basin of the Alps: AAPG 2002 Annual Convention & Exhibition, Houston, Texas.

Linzer, H.-G., 2009, Gas in Imbricated Channel Systems of the Foreland Basin of the Eastern Alps (Austria): AAPG 2008 Annual Convention & Exhibition, San Antonio, Texas.

Mackenzie, A. S., R. L. Patience, J. R. Maxwell, M. Vandenbroucke, and B. Durand, 1980, Molecular parameters of maturation in the Toarcian shales, Paris basin, France - I: changes in the configurations of acyclic isoprenoid alkanes, steranes and triterpanes: Geochimica et Cosmochimica Acta, v. 44, p. 1709-1721.

Mackenzie, A. S., C. F. Hoffman, and J. R. Maxwell, 1981, Molecular parameters of maturation in the Toarcian shales, Paris basin, France - III: changes in aromatic steroid hydrocarbons: Geochimica et Cosmochimica Acta, v. 45, p. 1345-1355.

Mackenzie, A. S., and D. McKenzie, 1983, Isomerization and aromatization of hydrocarbons in sedimentary basins formed by extension: Geology Magazine, v. 120, p. 417-470.

Majorowicz, J., and S. Wybraniec, 2011, New terrestrial heat flow map of Europe after regional paleoclimatic correction application: International Journal of Earth Sciences 100, p. 881-887.

Malzer, O., F. Roegl, P. Seifert, L. Wagner, G. Wessely, and F. Brix, 1993, Die Molassezone und deren Untergrund, in: F Brix, and O. Schultz, eds., Erdöl und Erdgas in Österreich. Naturhistorisches Museum Wien und F. Berger, p. 281–358.

Nachtmann, W., 1995, Fault-bounded structures as hydrocarbon traps in the Upper Austrian Molasse Basin, Austria: Geologisch palaeontologische Mitteilungen Innsbruck, v. 20, p. 221-230.

Peters, K. E., C. C. Walters, and J. M. Moldowan, 2005, The biomarker guide, 2nd ed., Cambridge University Press, Cambridge, United Kingdom, 1155 p.

Radke, M., and D. H. Welte, 1983, The methylphenanthrene index (MPI). A maturity parameter based on aromatic hydrocarbon, in: M. Bjoroy, C. Albrecht, and C. Cornford, eds., Advances in Organic Geochemistry, John Wiley and Sons, New York, p. 504-512.

Radke, M., D. Leythaeuser, and M. Teichmüller, 1984, Relationship between rank and composition of aromatic hydrocarbons for coal of different origins: Organic Geochemistry, v. 6, p. 423-430.

Reischenbacher, D., and R. F. Sachsenhofer, 2011, Entstehung von Erdgas in der oberösterreichischen Molassezone: Daten und offene Fragen: Berg- und huettenmaennische Monatshefte, v. 156 (11), p. 463-468.

Roeder, D., and G. Bachmann, 1996, Evolution, structure and petroleum geology of the German Molasse Basin, in: P. Ziegler, and F. Horvath, eds., Peri-Tethys Memoir 2, Structure and Prospects of Alpine Basins and Forelands, Mèmoire du Museum National d'Histoire naturelle, v. 170, p. 263-284.

Roegl, F., 1998, Palaeogeographic Considerations for Mediterranean and Paratethys Seaways (Oligocene to Miocene): Annalen des Naturhistorischen Museums in Wien, 99A, p. 279–310.

Rullkötter, J., and R. Marzi, 1989, New aspects of the application of sterane isomerization and steroid aromatization to petroleum exploration and the reconstruction of geothermal histories of sedimentary basins: Reprint Division of Petroleum Geochemistry, American Chemical Society, v. 34, p. 126-131.

Rybach, L., 1984, The paleogeothermal conditions of the Swiss Molasse Basin: Implications for hydrocarbon potential, Rev. Institut Francais Du Petrole, 39, p. 143-146.

Sachsenhofer, R. F., 2001, Syn- and post-collisional heat flow in the Cenozoic Eastern Alps: International Journal of Earth Sciences, v. 90, p. 579-592.

Sachsenhofer, R. F., and H.-M. Schulz, 2006, Architecture of Lower Oligocene source rocks in the Alpine Foreland Basin: a model for syn- and post-depositional source - rock features in the Paratethyan realm: Petroleum Geoscience, v. 12, p. 363-377.

Sachsenhofer, R. F., B. Leitner, H.-G. Linzer, A. Bechtel, S. Coric, R. Gratzer, D. Reischenbacher, and A. Soliman, 2010, Deposition, Erosion and Hydrocarbon Source Potential of the Oligocene Eggerding Formation (Molasse Basin, Austria): Austrian Journal of Earth Sciences, v. 103, no. 1, p. 76-99.

Sachsenhofer, R. F, H.-G. Linzer, A. Bechtel, I. Dunkl, R. Gratzer, J. Gusterhuber, R. Hinsch, and H. Sperl, 2011, Influence of Alpine Tectonics on Source Rock Distribution, Hydrocarbon Generation and Migration in the Austrian Part of the Molasse Basin: AAPG 2011 International Conference and Exhibition, Milan, Italy.

Schegg, R., 1994, The coalification profile of the well Weggis (Sub-alpine Molasse, Central Switzerland): Implications for erosion estimates and the paleogeothermal regime in the external part of the Alps: Bulletin Swiss Assoc. of Petroleum Geol. and Engineers, v. 61, p. 57-67.

Schegg, R., and W. Leu, 1996, Clay mineral diagenesis and thermal history of the Thonex well, western Swiss Molasse Basin: Clays and Clay Minerals, v. 44, no. 5, p. 693-705.

Schegg, R., W. Leu, C. Cornford, and P. A. Allen, 1997, New coalification profiles in the Molasse Basin of Western Switzerland: Implications for the thermal and geodynamic evolution of the Alpine Foreland: Eclogae geol. Helv., v. 90, p. 79-96.

Schmidt, F., and L. T. Erdogan, 1993, Basin modelling in an overthrust area of Austria, in: A. G. Doré, E. Holter, J. H. Augustson, W. Fjeldskaar, S. Hanslien, Ch. Hermanrud, B. Nyland, D. J. Stewart, and O. Sylta, eds., Basin Modelling: Advances and Applications, NPF Special Publications, v. 3, p. 573-581.

Schulz, H.-M., R. F Sachsenhofer, A. Bechtel, H. Polesny, and L. Wagner, 2002, Origin of hydrocarbon source rocks in the Austrian Molasse Basin (Eocene-Oligocene transition): Marine and Petroleum Geology, v. 19, no. 6, p. 683-709.

Schulz, H.-M., A. Bechtel, T. Rainer, R. F. Sachsenhofer, and U. Struck, 2004, Paleocenaography of the western Central Paratethys during nannoplankton zone NP 23: The Dynow Marlstone in the Austrian Molasse Basin: Geologica Carpathica, v. 55, p. 311-323.

Schulz, H.-M., and W. van Berk, 2009. Bacterial methane in the Atzbach-Schwanenstadt gas field (Upper Austrian Molasse Basin), Part II: Retracing gas generation and filling history by mass balancing of organic carbon conversion applying hydrogeochemical modelling: Marine and Petroleum Geology, v. 26, no. 7, p. 1180-1189.

Schulz, H.-M., W. van Berk, A. Bechtel, U. Struck, and E. Faber, 2009, Bacterial methane in the Atzbach-Schwanenstadt gas field (Upper Austrian Molasse Basin), Part I: Geology: Marine and Petroleum Geology, v. 26, no. 7, p. 1163-1179.

Sissingh, W., 1997, Tectonostratigraphy of the North Alpine Foreland Basin: correlation of Tertiary depositional cycles and orogenic phases: Tectonophysics, v. 282, p. 223-256.

Steininger, F. F., G. Wessely, F. Roegl, and L. Wagner, 1986, Tertiary sedimentary history and tectonic evolution of the Eastern Alpine foredeep. Giorn Geol. Bologna Ser. 3, v. 48, p. 285–297.

Sweeney, J. J., and A. K. Burnham, 1990, Evaluation of a simple model of vitrinite reflectance based on chemical kinetics: AAPG Bulletin, v. 74, no. 10, p. 1559-1570.

Taylor, G. H., M. Teichmueller, A. Davis, C. F. K. Diessel, R. Littke, and P. Robert, 1998, Organic petrology, Gebr. Borntraeger, Berlin, 704 p.

Teichmueller, R., and M. Teichmueller, 1986, Relations between coalification and paleogeothermics in variscan and alpidic foredeeps of western Europe: Lecture Notes in Earth Sciences, v. 5, p. 53-80.

Tissot, B. P., and D. H. Welte, 1984, Petroleum Formation and Occurrence, 2nd ed., Springer-Verlag, Berlin, 699 p.

Véron, J, 2005, The Alpine Molasse Basin – Review of petroleum geology and remaining potential: Bulletin angewandte Geologie, v. 10, p. 75-86.

van Husen, D., 1987, Die Ostalpen in den Eiszeiten: Populaerwissenschaftliche Veröffentlichungen der Geologischen Bundesanstalt, Vienna, Map, scale 1:500,000, 1.

Wagner, L. R., K. Kuckelkorn, and W. Hiltmann, 1986, New results on the Alpine Orogeny in Upper Austria based on the Oberhofen 1 Well – Stratigraphy, Facies, Maturity and Tectonics: Erdöl, Erdgas, Kohle, v. 102, no. 1, p. 12-19.

Wagner, L. R., 1996, Stratigraphy and hydrocarbons in the Upper Austrian Molasse Foredeep (active margin), in: G. Wessely, and W Liebl, eds., Oil and Gas in Alpidic Thrustbelts and Basins of Central and Eastern Europe: EAGE Special Publications, 5, p. 217-235.

Wagner, L. R, 1998, Tectono-stratigraphy and hydrocarbons in the Molasse foredeep of Salzburg, Upper and Lower Austria, in: A. Mascle, C. Puigdefàbregas, H.P. Luterbacher, and M. Fernandez, eds., Cenozoic Foreland Basins of Western Europe: Geological Society, Special Publications 134, p. 339-369.

Welte, D. H., and M. A. Yukler, 1981, Petroleum origin and accumulation in basin evolution - A quantitative model: AAPG Bulletin, v. 65, p. 1387-1396.

Welte, D. H., and M.N. Yalcin, 1988, Basin modelling - A new comprehensive method in petroleum geology: Organic Geochemistry, v. 13, p. 141-151.

Wessely, G., 1983, Zur Geologie und Hydrodynamik im südlichen Wiener Becken und seiner Randzone, Mitteilungen der österreichischen Geologischen Gesellschaft, v. 76, p. 27-68.

Wygrala, B., 1988, Integrated computer-aided basin modeling applied to analysis of hydrocarbon generation history in a Northern Italian oil field: Organic Geochemistry, v. 13, p. 187-197.

Wygrala, B., 1989, Integrated study of an oil field in the southern Po Basin, northern Italy: PhD thesis, University of Cologne, 226p.

Xu, J., 1991, Inkohlungsuntersuchungen im oberösterreichischen Molassebecken und seinem praetertiaeren Untergrund: Master thesis, Montan University of Leoben, Austria, 97 p.

Zou, Y.-R., and P. an Peng, 2001, Overpressure retardation of organic matter maturation: a kinetic model and its application: Marine and Petroleum Geology, v. 18, p. 707-71.

Vitae of the authors

Juergen Gusterhuber is a geologist. He holds a M.Sc. in Applied Geosciences from the Montanuniversitaet Leoben, Austria. He has been working for four years as a research fellow at the chair of petroleum geology. Currently he is working at SANTOS. His scientific interests lie in basin analysis, petroleum systems and regional geology. Juergen is member of AAPG and EAGE.

Ralph Hinsch studied geology in Hamburg, Germany and obtained his Ph.D. from the Free University of Berlin in 2001 via a project at GFZ Potsdam. Then he did postdoctoral research and teaching at the University of Vienna. In 2004 he joint RAG as exploration geoscientist. Recently, Ralph changed to OMV E&P as senior structural geologist.

Reinhard F. Sachsenhofer is head of Petroleum Geology at the Montanuniversitaet Leoben, Austria. Previously, he was Visiting Professor at the Donetsk National Technical University, Ukraine. He is also an Honorary Guest Professor at the Jilin University, China. His main research interests are in basin analysis, hydrocarbon systems, coal, and organic petrology. He is on the editorial board of several journals.

Hydrocarbon generation and migration from sub-thrust source rocks to foreland reservoirs: The Austrian Molasse Basin.

Manuscript in review, Austrian Journal of Earth Sciences, 2013/2014

Juergen Gusterhuber[1, 2], Ralph Hinsch[3, 4], Hans-Gert Linzer[3], Reinhard F. Sachsenhofer[1]

[1]Montanuniversitaet Leoben, Department Applied Geosciences and Geophysics, Chair of Petroleum Geology, Peter-Tunner-Strasse 5, A-8700 Leoben, Austria, reinhard.sachsenhofer@unileoben.ac.at
[2]Present address: SANTOS Ltd., 60 Flinders Street, Adelaide SA 5000, Australia, juergen. gusterhuber@santos.com (correspondence author).
[3]RAG Rohöl-Aufsuchungs Aktiengesellschaft, Schwarzenbergplatz 16, A-1015 Vienna, Austria,
hans-gert.linzer@rag-austria.at
[4]Present address: OMV Exploration & Production GmbH, Trabrennstrasse 6-8, 1020 Vienna,
ralph.hinsch@omv.com

Abstract

The Molasse Basin represents the foreland basin at the northern edge of the Alps and extends from Geneva (Switzerland) to Vienna (Austria). Hydrocarbon exploration has been done successfully for decades. Although most petroleum reservoirs were found in the foreland region, the oil kitchen is limited to the area under the Alpine thrust system. However, geological evolution of the southern basin margin and also timing of hydrocarbon generation and migration are still poorly understood. The present

study shows structural and petroleum systems models investigating the hydrocarbon potential of the central part of the Austrian Molasse Basin.

The structural model is a kinematic model with pseudo-geodynamic background. It reflects the structural evolution of the frontal and adjacent orogenic system and serves as input for the basin and petroleum systems models. Total tectonic shortening in the forward modeled section is 48.5 km, corresponding to 69% of shortening.

The reconstructed paleo heat flow based on maturity data is low (32 - 26 mW/m²) and decreases southwards. Formation temperatures suggest that present-day heat flows decrease in the same direction from 52 to 37 mW/m². Most probably heat flow is increased during Pliocene and Pleistocene times.

A combination of ‘paleo’ and ‘present day’ heat flow scenarios was used for the calculation of hydrocarbon generation along a N-S trending section crossing the Sierning Imbricates. According to these models, hydrocarbon generation commenced during the Early Miocene at about 18 Ma BP due to deep burial beneath Alpine nappes and was terminated during the Late Miocene (~ 8 Ma BP) due to cooling caused by uplift and erosion. About 40 % of the total source potential was realized beneath the Northern Calcareous Alps in the Mo1 area.

Hydrocarbon migration commenced contemporaneously with hydrocarbon generation, but continues until present day. Despite of model simplifications, the 2D migration model reflects important processes, which have been suspected previously based on independent information. Amongst these are: (1) Oil migration across faults from the Oligocene source rocks into stratigraphically deeper carrier/reservoir beds; (2) Long-distance (>50 km) lateral migration of oil (and gas); (3) Migration of gas along fault zones into the Sierning Imbricates; (4) Vertical migration of gas into the Puchkirchen and Hall formations, probably as a result of uplift and pressure reduction.

Results of a ‘pseudo 3D‘ flow path model show that absence of commercial accumulation in the western part of the study area is not a result of missing structures, but of the absence of hydrocarbon charge. The mismatch between observations and model results also highlights the important role of fault zones as migration pathways.

‘Palaeopasteurization’ of shallow reservoirs may explain that biodegradation in the Austrian part of the Alpine Foreland Basin is limited to the depth interval down to 800-1000 m sub-sea.

Kurzfassung

Das Molasse Becken (Alpines Vorlandbecken) erstreckt sich von Genf (Schweiz) bis Wien (Oesterreich). Kohlenwasserstoffexploration im Becken wurde ueber Jahrzehnte erfolgreich betrieben. Der groesste Teil der Kohlenwasserstofflagerlagerstaetten wurde im Bereich des Vorlands gefunden, waehrend das Oelfensters jedoch auf den Bereich unterhalb der alpinen Decken begrenzt ist. Wichtige Punkte wie der Zusammenhang zwischen der geolgischen Entwicklung des Beckens und dem Zeitpunkt der Kohlenwasserstoffgeneration sowie der Migration waren bis jetzt weitgehend unbekannt. Die vorliegende Arbeit zeigt Struktur- und Kohlenwasserstoffsystem-Modelle, welche das Potential des zentralen Teils des oesterreichischen Molassebeckens erforschen.

Das strukturgeologische Modell schliesst die Entwicklung des erweiterten noerdlichen Randes des alpinen Orogens mit ein und dient gleichzeitig als Grundlage fuer das Beckenmodell. Die tektonische Verkuerzung im Modell wurde mit 48.5 km angenommen, was 69 % Gesamtverkuerzung entspricht.

Der rekonstruierte Palaeowaermefluss, basierend auf Reifedaten, ist relativ niedrig und nimmt von Norden nach Sueden ab (32 – 26 mW/m²). Der errechnete heutige Waermefluss welcher auf gemessenen Formationstemperaturen basiert, nimmt ebenfalls von Norden nach Sueden ab, wenn auch auf hoeherem Niveau (52 – 37 mW/m²).

Eine Kombination aus diesen beiden Waermeflussszenarien diente als Grundlage fuer die Modellierung der Kohlenwasserstoffgeneration entlang eines 2D Profiles in der Sierninger Schuppenzone. Die Modelle zeigen, dass die ersten Kohlenwasserstoffe vor rund 18 Millionen Jahren gebildet wurden und dieser Prozess vor rund 8 Millionen Jahren zu Ende war. Diese Zeitabfolge kann direkt mit der tiefen Versenkung des Deckenstapels unter die Alpen, gefolgt von nachfolgender Hebung und Erosion vor rund 8 Millionen Jahren, in Verbindung gebracht werden. Ungefaehr 40 % des gesamten Muttergesteinspotentials wurde im suedlichen Bereich des Profiles unterhalb der Noerdlichen Kalkalpen im Bereich der Bohrung Mo1 ausgemacht.

Die Migration der Kohlenwasserstoffe setzt gleichzeitig mit der Bildung derselben ein und bleibt bis heute aktiv. Trotz notwendiger Vereinfachungungen im Modell koennen mit dem 2D Migratinonsmodell viele Prozesse, welche in frueheren Studien bereits als moeglich erachtet wurden, visualisiert werden. Diese sind unter anderem: (1) Oelmigration entlang von Stoerungen von oligozaenen Muttergesteinen in

stratigraphisch tiefere Traeger- und Reservoirhorizonte; (2) Ausgedehnte (>50 km) laterale Migration von Oel und Gas; (3) Gasmigration entlang von Stoerungszonen in den Bereich der Sierniger Schuppenzone; (4) Vertikale Migration von Gas in die Puchkirchen und Hall Formation, welche moeglicherweise ein Ergebnis von Hebung und Druckreduktion ist.
Ein auf Strukturkarten basierendes „Pseudo 3D“ Fliessmodell zeigt, dass das tatsaechliche Nichtvorhandensein von kommerziell nutzbaren Petroleumakkumulationen im westlichen Teil des Untersuchungsgebietes auf fehlende Beschickung mit Kohlenwasserstoffen, und nicht auf fehlende Stoerungsstrukturen zurueckzufuehren ist.
Die Diskrepanz zwischen Beobachtungen und Modellierergebnissen zeigt zugleich den grossen Einfluss von Stoerungszonen, welche als Migrationspfade dienen.
‚Palaeopasteurisierung‘ von seichten Gaslagerstaetten ist eine moegliche Erklaerung dafuer, dass Biodegradation im oesterreichischen Teil des alpinen Vorlandbeckens auf ein Tiefe von ungefaehr 800 – 1000 m (unter Meereshoehe) begrenzt ist.

1 Introduction

The Molasse Basin represents the foreland basin at the northern edge of the Alps (Fig. 1). The basin fill consists of Mesozoic and Cenozoic rocks overlying the Crystalline Basement of the Bohemian Massif (Malzer et al., 1993). Petroleum exploration has been successful for decades. Hence the basin is considered to be mature in terms of petroleum exploration (Veron, 2005). Two reasonably well understood petroleum systems can be distinguished in the investigated area of the basin (Wagner, 1996, 1998): (1) a thermogenic oil system related to Lower Oligocene source rocks (Schmidt and Erdogan, 1993; Schulz et al., 2002; Sachsenhofer and Schulz, 2006; Gratzer et al., 2011), and (2) a biogenic dry gas system located in Oligo-/Miocene sediments (Schulz and van Berk, 2009; Schulz et al., 2009; Reischenbacher and Sachsenhofer, 2011). Previous basin modeling approaches (Schmidt and Erdogan, 1993; 1996) showed that oil and thermogenic gas was formed underneath the Alpine nappes and migrated laterally to the north.
The distribution of gas deposits in the Molasse Basin is an outcome of several complex processes. Hence, there are still a lot of pending issues concerning generation, migration and alteration of hydrocarbon gases. For instance gas from Oligo/Miocene reservoirs, interpreted as biogenic in origin, may show geochemical

signatures of thermal gas and locally even contains liquid hydrocarbons. This indicates migration of thermogenic hydrocarbons from deeper to shallower horizons and mixing of both petroleum systems (Reischenbacher and Sachsenhofer, 2011).

The stratigraphic evolution of the tectonically mainly undeformed foreland is relatively well constrained by hundreds of wells drilled and 3D seismic data (e.g. Linzer, 2001; De Ruig and Hubbard, 2006; Hinsch, 2008; Hubbard et al., 2009). In contrast, the folded and imbricated southernmost part is still poorly understood and the hydrocarbon potential is not fully explored. First attempts to a better understanding of the folded and imbricated southernmost part of the basin were made by Linzer (2001; 2002; 2009) and Covault et al. (2009). New wells and continued seismic acquisition improved the knowledge in the kinematic evolution and the understanding of the hydrocarbon generation potential of the latter in recent times (Gusterhuber et al., in press; Hinsch, 2013). Within the Austrian part of the basin, different regions of imbricated zones can be distinguished based on different structure architecture and kinematics. The Sierning Imbricates represent the easternmost piece of these imbricated zones (Fig. 1) (Hinsch and Linzer, 2010). Due to different timing of tectonic processes, the stratigraphic position of the decollement varies between the eastern and the western basin region. While Upper Cretaceous marls act as detachment horizon in the western part of the area (Perwang Imbricates), the decollement is located above Lower Oligocene source rocks in the Sierning Imbricates and in the Regau Overthrust Segment. Therefore, occurrence of source rocks within the thrust sheets is restricted to the Perwang Imbricates. Gusterhuber et al. (in press) showed (based on modeling results and geochemical data) that source rocks at least in deeper parts of the Perwang Imbricates reached the oil window.

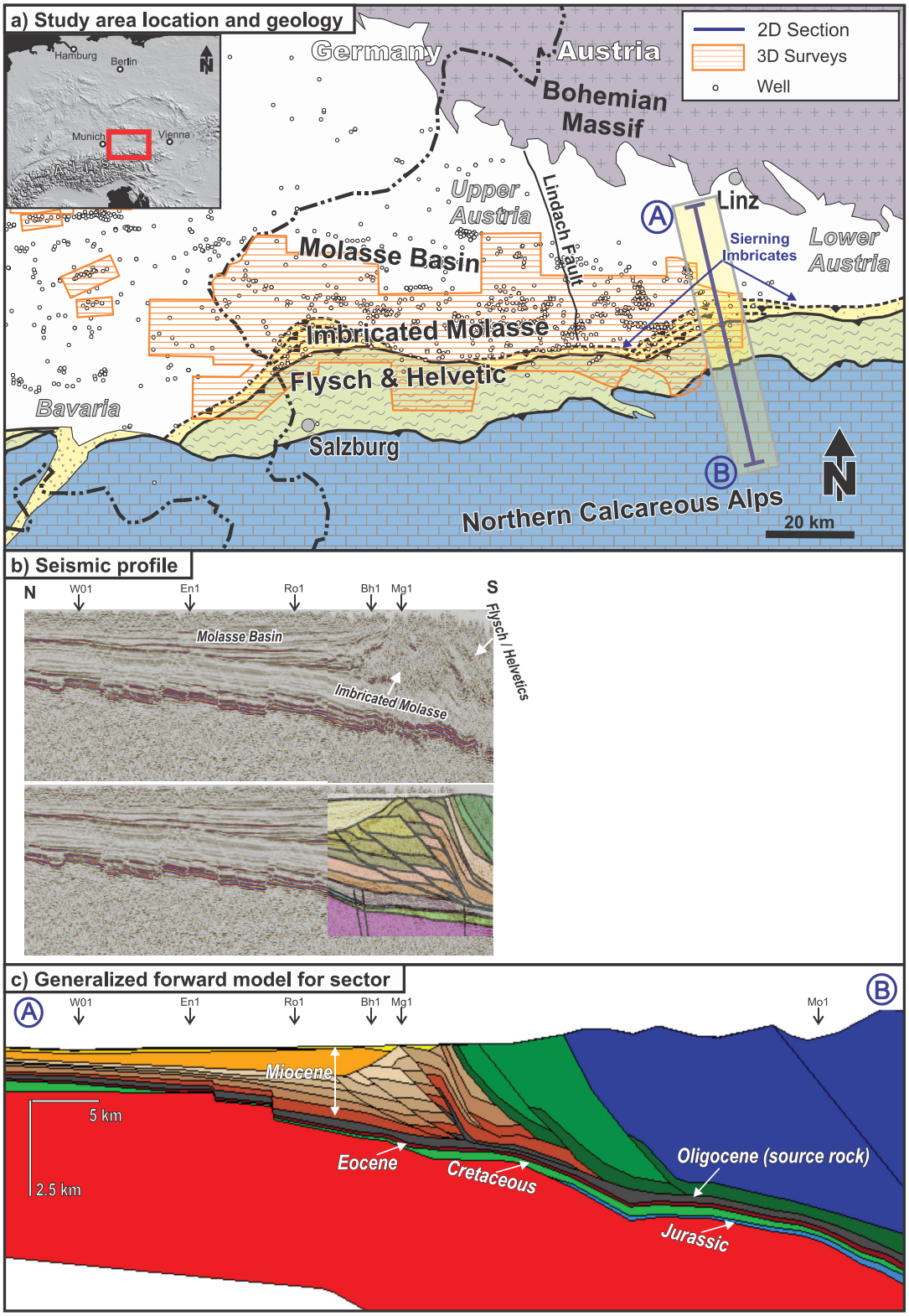

Figure 1: a) Simplified geological map of the study area (outline of the imbricated Molasse from the subsurface); course of the 2D section (A – B) in the Sierning Imbricates as well as the area for which the structural model is considered valid and where the thermal model may have significance to have a similar

thermal history (yellow shading); wells (approx. status 2010); the inset map (top left) shows the position of the study area on a shaded relief in the frame of Central Europe. b) 2D seismic section; interpretation overlay including calibration wells and main geotectonic units c) generalized structural forward model considered to be valid for the specified corridor and important stratigraphic units (e.g. Eocene reservoir rocks: orange; source rocks: dark grey)

The aims of this study are to investigate hydrocarbon generation in the Alpine sub-thrust and hydrocarbon migration into the undeformed foreland. In addition the study addresses biodegradation and mixing processes of gas. To achieve these goals, a two-dimensional basin and petroleum systems model was established crossing the Sierning Imbricates in the eastern part of the study area. Structure maps of the main reservoir horizons have been used to show possible hydrocarbon migration pathways in map view.

The geometry of the thermal basin model is based on a structural forward model. Application of forward modeling was essential to consider the complex evolution of the thrust sheets. Also, the Molasse Basin was subjected to recent erosion and uplift events which represent an additional challenge in terms of basin modeling. This effect was considered in the thermal basin model using data from Gusterhuber et al. (2012).

2 Geological Evolution

The Austrian Foreland Basin of Austria and Bavaria was formed due to collision of the Alps with the southern margin of the European platform during the middle Paleogene (Roeder and Bachmann, 1996; Sissingh, 1997) and represents a typical asymmetric foreland basin in terms of an increasing basin depth toward the Alpine thrust front in the south. The basement of the Molasse through is formed by crystalline rocks of the Bohemian Massif as part of the European shelf. Mesozoic evolution started with the deposition of Jurassic sandstones and platform carbonates as well as Upper Cretaceous sandstones and marls (Fig. 2). Following on a major uplift and erosion event during the latest Cretaceous and earliest Paleogene, the Paratethys Sea transgressed progressively on a peneplain during the latest Eocene. The onset of Molasse sedimentation is characterized by Upper Eocene fluvial to shallow marine sandstones and Lithothamnian limestones. Basically, the Cenozoic succession can be subdivided into autochthonous and allochthonous Molasse units (Steininger et al., 1986). Relatively undisturbed autochthonous units overly either crystalline basement or Mesozoic rocks. Allochthonous units comprise the Molasse

imbricates and are composed of rocks which were incorporated in the Alpine thrusts during tectonic movements.

During the earliest Oligocene the area subsided rapidly to deep water conditions (approx. 800 m; Dohmann, 1991) with the deposition of often organic rich fine grained sediments. Flexural bending of the European plate due to the collision with the Alpine wedge led to reactivation of pre-Cenozoic NNW-SSE trending faults and to the development of E-W (south and north dipping) normal faults being mainly active in early Oligocene times (Wagner, 1996, 1998; Nachtmann, 1995).

During the Late Oligocene and earliest Miocene the continued northward movement of the Alps caused the formation of the Molasse imbricates and increased sediment discharge from the south (Kuhlemann and Kempf, 2002). Fully marine conditions prevailed in the basin up to the Early Miocene and deep water channels developed from W to E along the basin axis, filling the Puchkirchen trough (Linzer, 2002; De Ruig and Hubbard, 2006). This channel belt represents a mixed depositional system consisting of debris flows and turbidity currents (Bernhardt et al., 2012). Towards the northern border of the basin, deep marine sediments graded into brackish sands, clays and minor coal bearing successions (Krenmayer, 1999). At the same time terrestrial coarse grained sediments have been deposited on top of the Alpine wedge. Today these sediments referred to as Augenstein Formation are only preserved in small remnants on plateaus and karst cavities in the Northern Calcareous Alps (NCA) region (Frisch et al., 2001). The lower part of the Hall Formation (Fig. 2) was still dominated by deep-water deposits. Later, prograding deltas indicated the transition to shallow marine conditions and filled the accommodation space of the basal Hall trough (Hubbard et al., 2009; Grunert et al., 2013). Upper Burdigalian sediments of the overlying Innviertel Group are represented by tide dominated silts and brackish-fluvial sands (Roegl, 1998; Grunert et al., 2012).

Subsequently, a several hundred meters thick succession composed of coal-bearing clays, sands and fluvial gravels (Upper Freshwater Molasse) was deposited following on a hiatus. Today these Middle/Upper Miocene sediments are largely eroded due to post-depositional uplift over the last 9 million years (Gusterhuber et al., 2012).

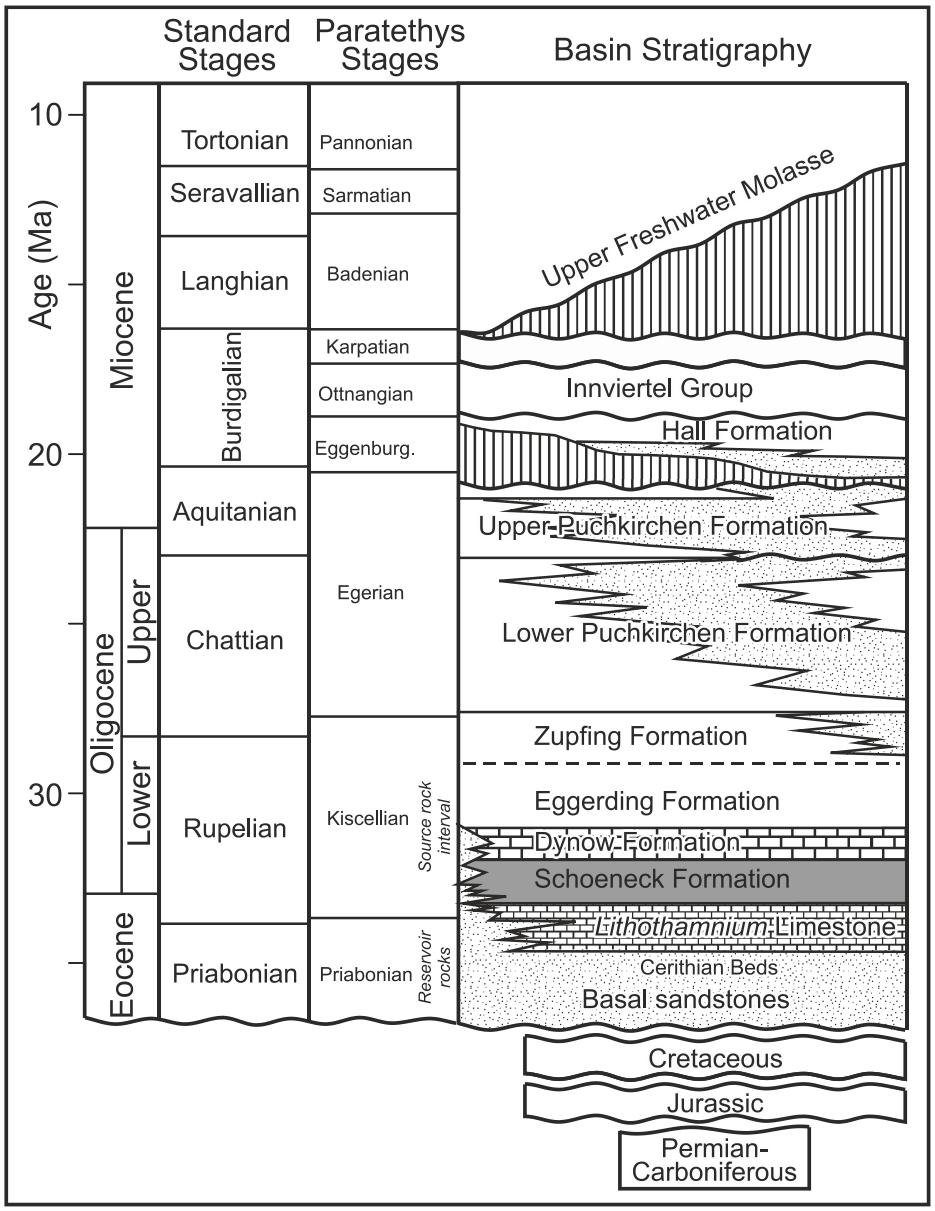

Figure 2: Stratigraphy of the Austrian part of the Molasse Basin (modified after Wagner, 1998).

3 Petroleum Systems

Traditionally two different petroleum systems are distinguished in the Austrian part of the Molasse Basin: (1) a Lower Oligocene to Mesozoic thermally generated oil and gas system and (2) an Oligocene-Miocene biogenic gas system (Wagner, 1996, 1998).

(1) The most important reservoir for oil and minor thermal gas are Upper Eocene basal sandstones (Fig. 2). Additional hydrocarbons are trapped in Upper Eocene Lithothamnium limestones as well as in Upper Cretaceous glauconite sandstones and Lower Oligocene horizons (Malzer et al., 1993). Most thermal oil and gas prospects in the Molasse Basin are bound to fault systems featuring several hundred meters of vertical throw (Nachtmann, 1995). Some shallow Molasse oils from northern reservoirs are classified as heavily biodegraded (Gratzer et al., 2011). Reischenbacher and Sachsenhofer (2011) assume that gas in shallow Eocene reservoirs south of Linz have been formed by anaerobic biodegradation of pre-existing oil accumulations.

Potential source rocks are restricted to the Lower Oligocene succession and comprise (from bottom to top): Schoeneck Formation, Dynow Formation and Eggerding Formation (Tab. 1; Schulz et al., 2002; Sachsenhofer et al., 2010). The deeper-water organic rich shales and marls of the Schoeneck Fm. have the highest source potential. The overlying Dynow Fm. is composed of three sedimentary cycles, each starting with marlstones and grading into organic shales (Schulz et al., 2004). The Eggerding Formation is composed of grey laminated pelites with thin white-colored layers of nannoplankton (Sachsenhofer et al., 2010). The Eggerding Formation is overlain by the Zupfing Formation consisting of clay marl. Only the lower part of the latter 150 m thick succession is rich in organic matter. Present-day distribution of Lower Oligocene rocks is controlled by submarine erosion which affected the northern passive slope of the foreland basin west of the Lindach Fault (Fig. 1) where sediments were removed gravitationally from the northern slope and re-deposited in deeper basin areas. Later, these re-deposited organic rich rocks (termed Oberhofen facies) were overridden by the Alpine nappes (Sachsenhofer et al., 2010). In contrast, lower Oligocene units with a normal source rock facies in autochthonous successions have been encountered in wells east of the Lindach Fault (Sachsenhofer and Schulz, 2006; Sachsenhofer et al., 2011).

(2) Isotopically light gas was probably generated by bacterial activity in Oligocene and Miocene shales (Malzer et al., 1993; Schulz and van Berk, 2009). Based on gas wetness and isotope data, Reischenbacher and Sachsenhofer (2011) described mixing of biogenic and thermogenic hydrocarbons including condensate.

The bacterial gas is associated with thermally immature potential source rocks which contain more than 0.5 % TOC. The reservoirs and source rocks are intimately connected (Schulz et al., 2009). Productive reservoirs are found in different subfacies of the Puchkirchen and Hall channel systems (De Ruig and Hubbard, 2006; Hubbard et al., 2009).

Formation		Av. Thickness [m]	TOC [%]	HI [mgHC/gTOC]
Eggerding Formation	Merged SR interval	35 - 50	1.5 - 6.0	250 - 400
Dynow Formation		5 - 15	0.5 - 3.0	500 - 600
Schoeneck Formation		10 - 20	2.0 - 12.0	400 - 600
Merged source rock interval			2	450
‚Oberhofen facies'		~50	~1.3	400

Table 1: Characteristics of Lower Oligocene source rocks (Schulz et al., 2002; Sachsenhofer and Schulz, 2006; Sachsenhofer et al., 2010). TOC: total organic carbon; HI: hydrogen index.

4 Methodology

4.1 Cross Section Forward Modeling

Hinsch (2013) analyzed the kinematic evolution of the imbricated Molasse based on 3-D seismic and well data interpretation as well as section balancing. For the Sierning Imbricates, a retro-deformed section was presented. For the present study a forward model of Alpine wedge advance and Molasse imbrication is established of which 10 time steps are used. The forward modeling approach allows to include eroded sediments and early evolutionary stages that otherwise would not be represented by an individually balanced and restored section. The same methodology was already successfully used for a section through the Perwang Imbricates approx. 80 km further to the west of the Sierning section (Gusterhuber et al., in press).

The software package LithoTect (Landmark-Halliburton) is used for forward modeling, utilizing standard integrated fault-slip algorithms. The time span considered in the forward model is lower Oligocene to present. Individual model steps are generated after each deformation increment and manual editing to include subsidence, erosion and syntectonic sedimentation. The resulting time steps are later merged into the Tec-Link basin model of PetroMod (Schlumberger).

In LithoTect the forward modeling was done only on a kinematical basis. However, in order to reflect a more realistic, pseudo-dynamic evolution, the section was manually modified to comply with geodynamically plausible geometries. Subsidence, erosion and syntectonic deposition are added after each deformation increment in order to match the known or plausible paleo-geographic conditions like facies distribution and water depth.

The presented model thus can be termed kinematic model with geodynamic background and compares to the approach used in Gusterhuber et al. (in press). Fully geodynamic modeling is far beyond the scope of this study. In addition, too many parameters for a full dynamic simulation are unknown or uncertain, and thus, results would not be more accurate.

4.2 Thermal Basin Modeling

Basin modeling integrates geological, geophysical and geochemical properties (Welte et al., 1997). Based on these properties, temperature and pressure evolution as well as generation and migration of hydrocarbons can be calculated (Welte and Yukler, 1981). The study was performed using the PetroMod TecLink v11 (SP4) software developed by the Schlumberger PetroMod Group. Complex tectonic environments like thrust belts need to be restored structurally and kinematically in order to take mass movements into account. In the present study several balanced paleo-sections were used to forward-model the temperature and maturity history of the section. With the block concept, the TecLink finite element simulator is able to handle multiple z-values on one vertical grid line. Hence each paleo-section is split into several blocks specified by its boundaries and a characteristic layer stack.

4.2.1 Model Input

The conversion of a coherent geological concept into numerical form is the precondition for basin modeling (Welte and Yalcin, 1988). To process the evolution of the basin by the simulator it has to be subdivided into uninterrupted and discrete sequences, named events (Wygrala, 1988) or paleo-sections. An event is a time span during which a geological process (deposition, erosion, hiatus) occurs. The array of the software allows the discrimination of different geological processes in various parts of the basin at the same time. Physically existing sedimentary units at a certain time are called layers. Each layer is deposited during a single event and may be partly or completely eroded during a later erosional event (Wygrala, 1988). The model in this study comprises numerous original layers. Based on core analysis, facies was assigned to each layer, carrying different properties like porosity and thermal conductivity (Tab. 2). Calculations of physical properties are based on Hantschel and Kauerauf (2009). As thermal conductivity values for the rock matrix are shown in Table 2, it is important to note that porosity affects thermal conductivity to an important degree because pore fluids have lower thermal conductivities than rock matrix. A decompaction routine is integrated by default in PetroMod in order to reconstruct the initial thickness of each layer from present day data. As this function

is software-related not applicable for the TecLink tool, compaction of autochthonous sediments was first computed in a preliminary model where thrusting was simulated by increasing thickness of the nappes through time (using Schlumberger PetroMod's Salt movement tool). The achieved information on compaction rates was later integrated in the thermal basin model built with the TecLink tool.

Lithostratigraphic unit	Litho mixture ratio	Thermal conductivity (matrix)	
	[%]	[W/(mK)] at 20 °C	[W/(mK)] at 100 °C
Basin fill			
Innviertel Group	40 Sandst./40 Shale/20 Marl	2.48	2.07
Hall Fm.	60 Siltst./20 Sandst./20 Marl	2.37	2.03
Up. Puchkirchen Fm.	40 Siltst./40 Marl/20 Shale	1.97	1.89
Low. Puchkirchen Fm.	40 Shale/40 Marl/20 Siltst.	1.86	1.85
Source rock interval	75 Shale/25 Marl	1.91	1.86
Eocene Sandst. (reservoir rock)	80 Sandst./10 Limest./10 Marl	3.75	2.52
Mesozoic			
Cretaceous	90 Marl/10 Sandst.	2.17	1.96
Jurassic	40 Limest./40 Dolom./20 Sandst.	3.79	2.54
Thrust			
Flysch	80 Shale/10 Sandst./10 Marl	1.83	1.83
North. Calc. Alps	50 Limest./50 Dolom.	3.71	2.51

Table 2: Assigned thermal conductivities of rock matrix (at 20 °C and 100 °C) for various facies in the model. Calculated thermal properties are based on literature published in Hantschel and Kauerauf (2009).

The Oligocene Schoeneck, Dynow and Eggerding Formations as well as the lower part of the Zupfing Formation are considered to be the source rocks (Schulz et al., 2002; Sachsenhofer et al., 2010). Because of scaling problems caused by limited thicknesses of these layers, the three formations are merged to one source rock interval in the model. The entire interval has a net thickness of approximately 70 to 100 m and is featured with an initial TOC of 2 % and a Hydrogen Index (HI) of 450 mg HC/g TOC (Schulz et al., 2002; Sachsenhofer et al., 2010). Conversion of kerogen to hydrocarbons is driven by temperature and time dependent kinetic reaction processes (Tissot and Welte, 1984). Thermal history in PetroMod is calculated as a steady temperature record in a source rock through time with the purpose to assess the yield of hydrocarbons. Hydrocarbon generation reactions are described in the software by a set of activation energies and an initial potential which is described by the HI. Bulk kinetic parameters comprising activation energy distribution and single frequency factor of 5 immature lower Oligocene source rocks samples from the Molasse Basin were determined at GeoForschungsZentrum Potsdam (GeoS4 GmbH) using non-isothermal open-system pyrolysis at four different laboratory heating rates

(0.7, 2.0, 5.0 and 15°C/min) and a Source Rock Analyzer©. The kinetic parameters of these samples differ only slightly (Fig. 3). An appropriate kinetic data set (named Molasse kinetic) was assigned to the source rock unit. In addition a standard kerogen Type II kinetic model was applied to test the impact of different kinetic data on the model results (Burnham, 1989).

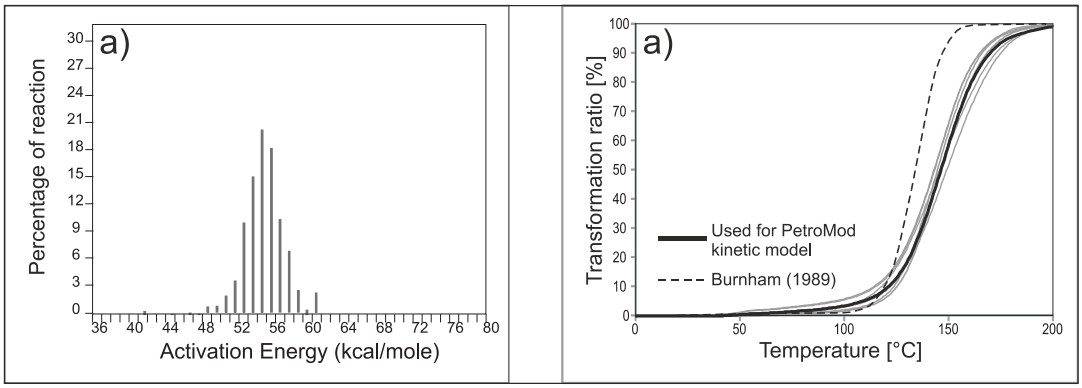

Figure 3: a) Kinetic parameters which were used to model petroleum generation; b) Predictions of transformation ratio for five different Lower Oligocene source rock samples based on kinetic parameters and a heating rate of 3.3 °C/million years. The prediction for the sample selected for modeling is shown by a thick black line. The dashed line represents predictions for a Type II kerogen (Burnham, 1989), which was used for sensitivity analysis.

4.2.2 Boundary conditions

The sediment-water-interface (SWI) temperature represents the upper boundary condition for heat transfer in the basin. Mean surface temperature values over the time are considered in PetroMod based on paleo-temperature distribution maps after Wygrala (1989). Paleo-water depth was selected according to the general understanding of the Molasse Basin evolution (Wagner, 1996). As hydrocarbon generation shows a strong dependence on temperature and time, the heat flow evolution is a very important constraint for modeling (Tissot and Welte, 1984). Paleo heat flow values can be assessed under consideration of tectonic processes in the past. The heat flow evolution at the base of the modeled section represents the lower thermal boundary condition.

4.2.3 Calibration Data

Different temperature-sensitive parameters, such as vitrinite reflectance Ro (reflectance under oil), formation temperature as well as sterane (20S / (20S + 20 R)) and hopane (22S / (22S + 22R)) isomerization ratios (Mackenzie et al., 1980, 1981;

Mackenzie and McKenzie, 1983) were used to calibrate the thermal evolution of the basin.

Vitrinite reflectance is measured on rocks containing remnants of landplants. Only reliable data (mainly from coals) have been used for calibration in the present study. The calculation of vitrinite reflectance is based on the kinetic EASY%Ro-algorithm (Sweeney and Burnham, 1990).

Calculations of sterane and hopane isomerization ratios are based on kinetics of Rullkoetter and Marzi (1989).

The RockEval pyrolysis parameter Tmax (Espitalie et al., 1977) was used to support the validity of the measured vitrinite reflectance data. The empirical formula

Ro (calculated) = 0.0180 x Tmax – 7.16

allows to convert Tmax to reflectance (Peters et al., 2005) and can be applied for low sulfur Type II and III kerogen.

Sterane and hopane isomerization ratios and Tmax were taken from Schulz et al. (2002), Sachsenhofer et al. (2010) and Gratzer et al. (2011).

Two different data sets were used to calibrate the present-day heat flow distribution: (1) temperature data from borehole formation tests and (2) Horner corrected bottom-hole temperatures (BHT) ("Horner-plot"; Horner, 1951). This standard approach considers the time span since circulation of the drilling fluid stopped. Uncorrected temperature data for the Horner-calculation was taken from Kamyar (2000).

All available calibration data for wells En1, Ro1, Bh1, Mg1 and Mo1 are plotted versus depth in Figure 4 (for position of wells see Figure. 1).

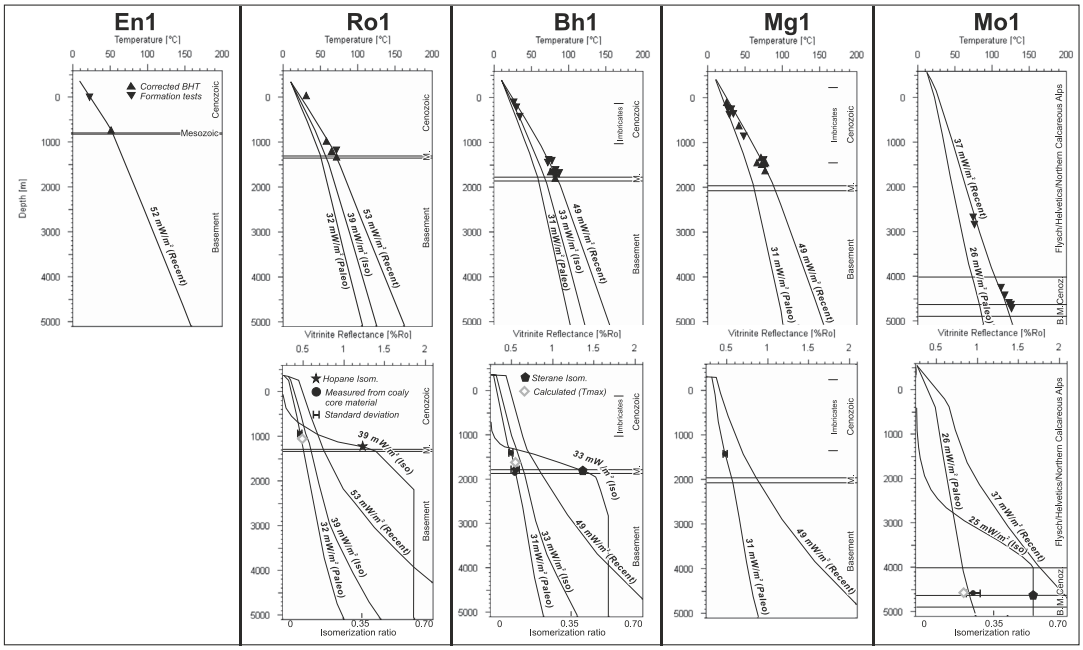

Figure 4: Temperature and maturity (vitrinite reflectance, steranes isomerization, hopanes isomerization) plots versus depth. En1 is the northernmost well, Mo 1 the southernmost well. Calculated trends of different heat flow scenarios are shown by different lines.

4.3 Migration Models

The 2D migration modeling package of PetroMod includes different migration modeling techniques (e.g. Darcy flow, Flow path, Hybrid; Hantschel and Kauerauf, 2009).

Different chemical and physical parameters like critical fluid saturations or relative permeabilities which are expressed by the mobility factor (mobility factor = permeability/viscosity) are used to describe transport processes through porous media. Flow path migration is a completely buoyancy driven migration method which allows fast, high-resolution modeling. However this method requires an arbitrary definition of seal/carrier and therefore represents an incomplete physical method. Darcy flow integrates all relevant physical parameters such as pvT (pressure, volume, Temperature) and requires long computer procession times (Baur, 2010).

The Hybrid migration method was applied in the present study. It combines Darcy and flow path migration methods (Hantschel et al., 2000) and was introduced to allow proper accumulation tracking through time including timing and retention issues. This technique applies the flow path method to all lithologies which have more than 100 millidarcy permeability and a higher porosity than 30 % during the evolution of the

actual layer. Beyond that it applies full Darcy calculations (i.e. hydrocarbon retention) to all layers having less permeable lithologies.
Map based migration modeling was done using PetroCharge Express (another application of PetroMod). This software tool is based on a petroleum systems approach for rapid initial assessment of petroleum charge. The software basically uses the structure of a depth map to calculate drainage areas, potential migration paths and possible locations of hydrocarbon accumulations. The buoyancy driven approach considers features which are filled to its spill point.

5 Results and Discussion

To model the petroleum system in the Sierning Imbricates, a kinematic forward model was performed first, based on seismic interpretation (Fig. 1). Several wells along the profile provided data for calibration of the thermal history and the kinematic model. Obtained results are considered valid for the entire main part of the Sierning Imbricates.

5.1 Cross Section Forward Modeling

In order to model the petroleum system in the Sierning Imbricates we use the results from retro-deformation (Hinsch, 2013) and further elaborate them in a regional kinematic, pseudo-dynamic forward model (Fig. 5).
10 time / deformation increments reflect the kinematic evolution of the Sierning Imbricates since Middle Oligocene times (~30 Ma). Thus, the forward modeled section covers a longer time span and consequently accommodates more shortening than the balanced section of Hinsch (2013).
Total tectonic shortening in the forward modeled section is 48.5 km [L_0-L] (L= deformed length, L_0= undeformed length), corresponding to 69% of shortening (measured from the assumed Hinterland end of the Penninic-Flysch and Helvetic Wedge, excluding some shortening in the Northern Calcareous Alps). Note, that Fig. 5 does not show the whole deformation length as it focuses on the area of interest for the subsequent basin model. It needs to be considered that this shortening value is not a minimum shortening. Lateral orogenic movements (Linzer et al., 2002) are not considered in this study.

a) The forward model includes some overthrusting of the orogenic wedge that is not documented in preserved frontal accreted imbricates. In addition, other imbricates are eroded.
b) In the forward model some out-of-sequence thrusting in the Penninic-Flysch and Helvetic Wedge is accommodated. The timing and amount of deformation in this unit inside the considered period is relatively poorly constrained.
c) The position of the footwall cut-off of Oligocene sediments in Fig. 5e is loosely constrained by the presence of Oligocene sediments in Well Molln 1. In the forward model the ramp was positioned approx. 20 km south of the well.

Despite these uncertainties, it is considered, that the presented forward model sufficiently reflects the evolution of the Alpine orogenic front in the study area. This is supported by the fit of the forward model with the seismic interpretation (Fig. 1) and the balanced section of Hinsch (2013). In addition, the calculated shortening velocity for the section of 4 mm/yr (48.5 km shortening in 12 million years) fits well to velocities calculated by balancing. The shortening velocities calculated for the balanced profile through the Sierning Imbricates are 4 mm/yr and in other sections in the imbricated Molasse 4.5-8 mm/yr (Hinsch, 2013). Beidinger and Decker (submitted) assume deformation velocities of approximately 4.6-5.2 mm/yr for a comparable area for the Egerian to Karpatian period.
Thus, to conclude, the present forward model is considered to reflect the structural evolution of the frontal orogenic system in an adequate way for subsequent basin modeling.

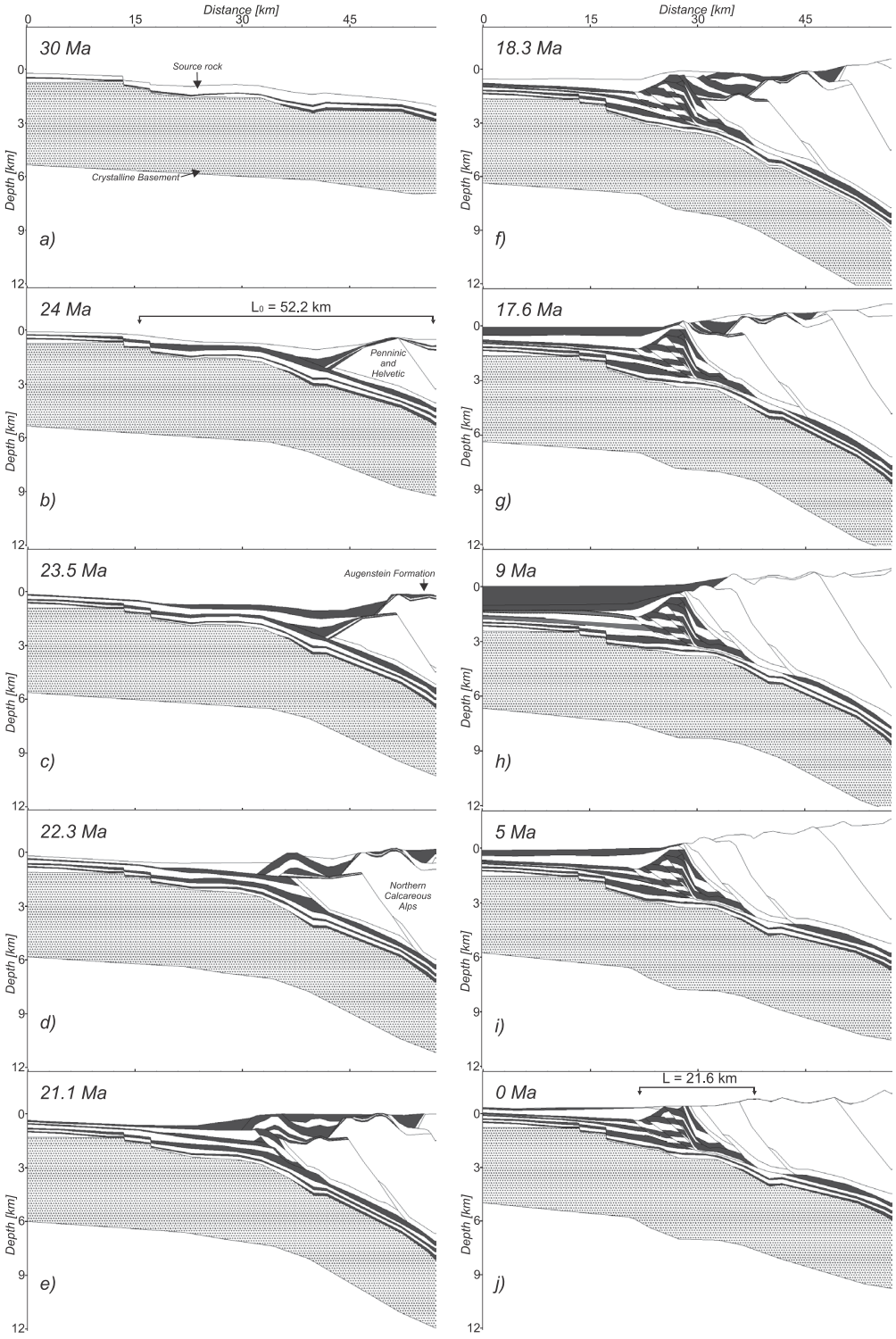

Figure 5: 2D basin evolution shown on a N-S section in the Sierning Imbricates area (see Fig. 1). The length between reference points for calculation of tectonic shortening is displayed on Fig. 5b as well as on the present day section (Fig. 5j; black arrows).

5.2 Thermal Modeling

5.2.1 Heat flow scenarios

Different heat flow scenarios were applied in the calibration process to model the thermal history along the section (Fig. 6).

In a first scenario (Fig. 6; Base case 'paleo'), a time constant heat flow decreases from north to south from 32 mW/m² to 26 mW/m². This scenario results in a fit with measured vitrinite reflectance data, but underestimates present-day temperatures.

In the second scenario (Base case 'recent'), heat flow decreases from north to south from 52 to 37 mW/m². This scenario results in a good fit with corrected bottom hole and formation test temperatures, but overestimates vitrinite reflectance data. Vitrinite reflectance calculated from Tmax was available for wells Ro1, Bh1 (middle part of the section) and Mo1 (southernmost well) and fits to case 'paleo'. Isomerization data was available for the same wells. However, because steranes isomerization in Mo1 reached the equilibrium value (0.50), only data from wells Ro1 and Bh1 in the middle part of the section can be used for heat flow calibration. The attempt to integrate these results in the actual scenarios shows that the heat flow scenario 'isomerization data fit' represents only slightly higher values than the base case 'paleo'.

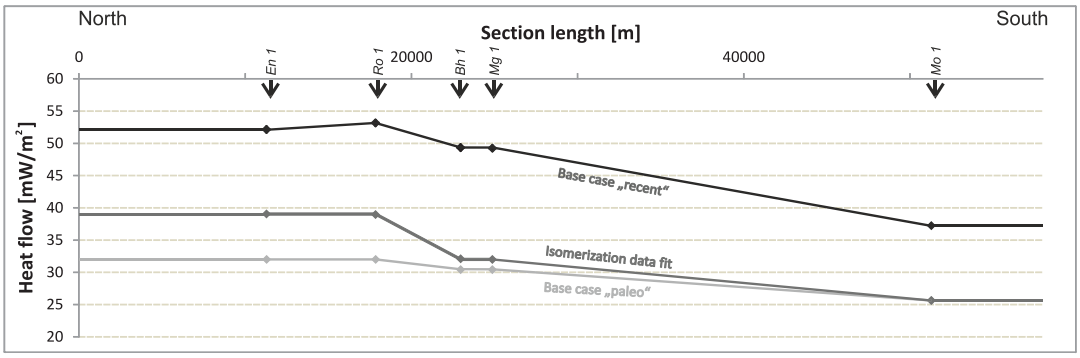

Figure 6: Assigned heat flow scenarios along the section. The scenario applied for petroleum systems modeling is a combination of the base cases 'paleo' and 'recent' (see text for discussion.).

Given the gap between the cases 'paleo' and 'recent', a fit for both maturity and present-day temperature data was gained by accepting the 'paleo' case heat flows until the time of maximum burial (9 million years) in order to meet the maturity data and by using the increased 'recent' heat flow for the last 4 million years.

5.2.2 Sensitivity analysis

Although a sub-recent increase in heat flow in the Molasse Basin has been described previously (e.g. Sachsenhofer, 2001; Gusterhuber et al., in press), it is difficult to decide whether it is a fact or artificial. Therefore, different aspects which may bias heat flow reconstructions are considered within the frame of sensitivity analysis.

- Calibration data quality

  Paleo-heat-flow is calibrated with measured and calculated vitrinite reflectance data applying the EASY%Ro algorithm. Recent heat flow is calibrated using measured formation temperature values. This means that apart from geological reasons, discrepancies between paleo- and present-day heat flows may occur due to biased vitrinite and temperature data or due to inaccuracies of the applied algorithm. In order to exclude the probability that the low paleo-heat flow is due to biased vitrinite data (e.g. Carr, 2000), several samples were re-measured. These samples yielded identical results and did not show indications of suppression. In addition, measured vitrinite data are supported by vitrinite reflectance calculated using Tmax values.

  Temperature data derived from formation test measurements are considered highly reliable and are available from all wells. Measured BHT temperatures have been corrected using the approach of Horner (1951). The corrected BHT temperatures fit reasonably well with formation test measurements, but in some cases slightly underestimate formation test temperatures. This agrees with the observation of Hermanrud et al. (1990) that the Horner plot method generally underestimates formation temperatures, if the time since circulation stopped is limited. In any case, the higher present-day heat flows are obviously not due to biased temperature data.

- Effect of erosion estimates on reconstructed thermal histories

  Significant uplift and erosion affected the NCA (Frisch et al., 2001) and the Alpine Foreland Basin during the Neogene (Gusterhuber et al., 2012). The adopted thickness of eroded rocks influences paleo-heat flow estimates and, consequently, the amount of the sub-recent heat flow increase. In order to test the possibility to eliminate the heat flow increase, absolute minimum amounts of eroded thickness have been adopted in the sensitivity analysis for wells Bh1 (located within the Molasse imbricates) and Mo1 (located ~30 km south of the Alpine front in the NCA; see Fig. 1c for position). In case of Mo1 also the effect of a maximum estimate was tested.

Bh-1: Based on Gusterhuber et al. (2012), erosion of sediments, 1200 m thick (800 m Freshwater Molasse + 400 m Innviertel Gr.), has been adopted in the conceptual model (Fig. 7). Considering this assumption, a good fit with calibration data is obtained using a sub-recent heat flow increase of 18 mW/m² (Fig. 7a). In a sensitivity run, erosion was set to a minimum value of only 400 m. Even in this scenario time-constant heat flows cannot yield good fits with both, present-day temperatures and maturity. Figure 7b shows this for a time-constant heat flow of 42 mW/m², which tends to underestimate present-day temperatures, but overestimates maturity.

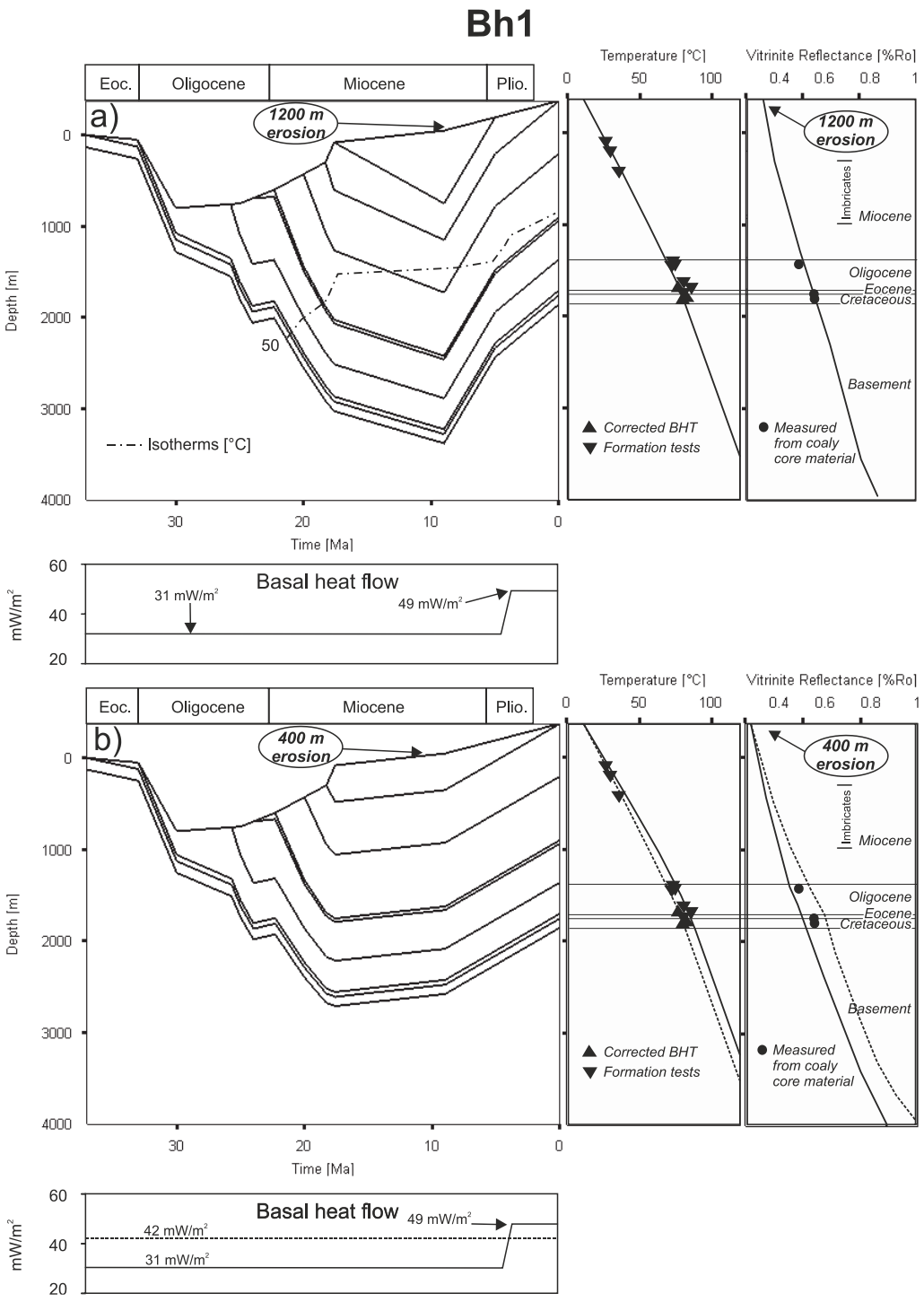

Figure 7: (a) Burial history of borehole Bh1 (see Fig. 1 for position) based on the input parameters from the 2D conceptual model including erosion of rocks, 1200 m thick. A combination of heat flow base cases 'paleo' and 'recent' (Fig. 6) results in a good fit between measured and calculated calibration data. (b) Burial history plot considering erosion of rocks, 400 m thick. Calibration data show that a time-constant heat flow of 42 mW/m² overestimates maturity. This result indicates that even if an unrealistic low thickness of eroded rocks is applied, a time-constant heat flow does not result in a successful fit.

Mo1: According to Frisch et al. (2001), thermochronological data suggest a maximum thickness of the Augenstein Fm. in the Dachstein area (~ 50 km further west of the study area) of more than 1300 m (or even more than 2000 m). However, the thickness near the present eastern margin of the NCA was probably much lower. The current altitude in the Mo1 area is ~590 m, adjacent mountain summits reach heights between 1200 m (Reichraminger Hintergebirge) and 2200 m (Haller Mauern). Considering these facts, erosion of 2000 m (NCA + Augenstein Fm.) has been adopted in the conceptual model resulting in a sub-recent heat flow increase of 11 mW/m² (Fig. 8a). Similar to Bh1, even in scenarios with a thickness of eroded rocks considered as a minimum estimate (1200 m NCA + Augenstein Fm.) heat flow has to be increased by 7 mW/m² (Fig. 8b). In an additional scenario the eroded section was 2500 m thick (maximum estimate) resulting in a sub-recent heat flow increase of 14 mW/m² (Fig. 8b).

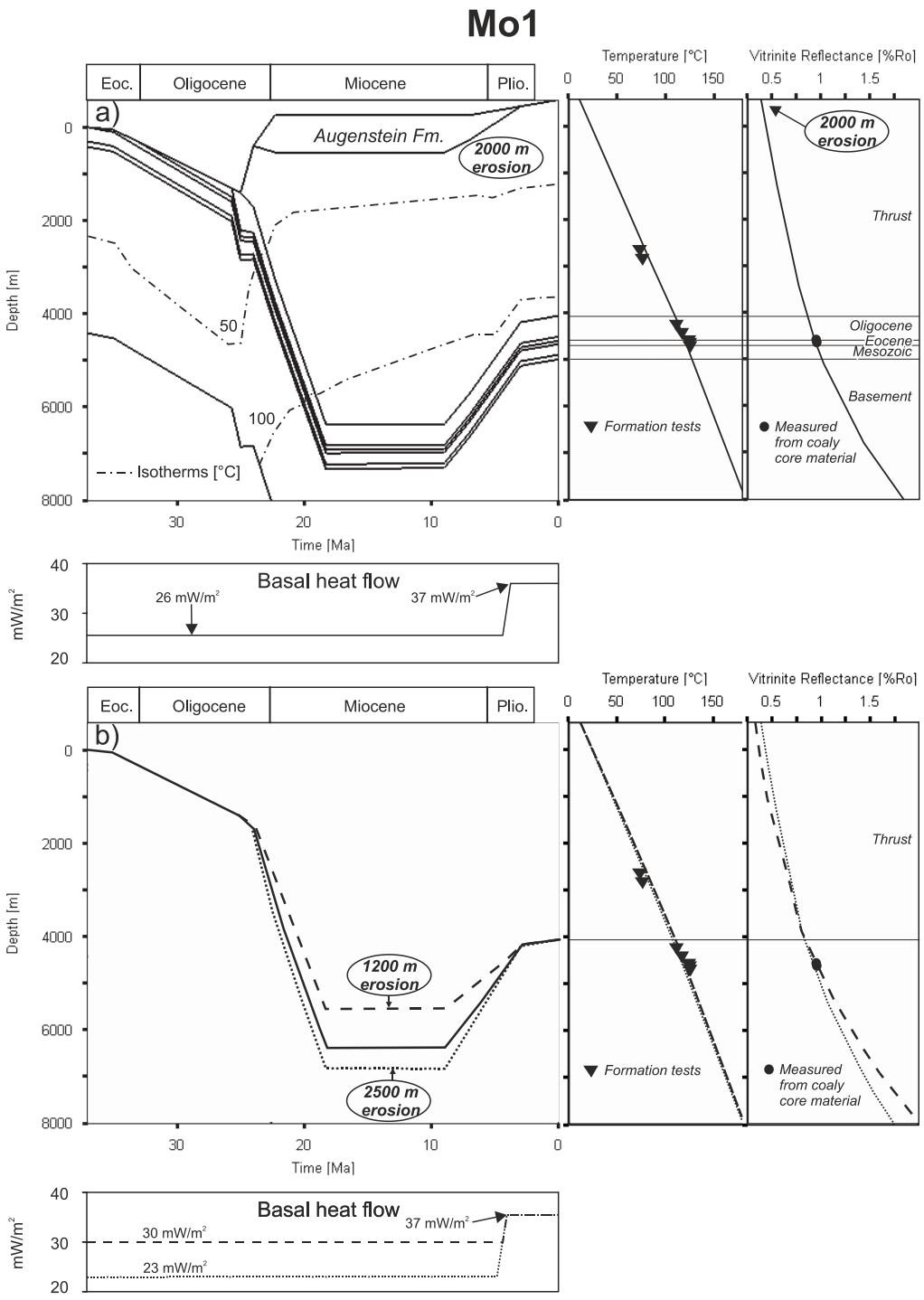

Figure 8: (a) Burial history of borehole Mo1 (see Fig. 1 for position) based on the input parameters from the 2D conceptual model including erosion of rocks, 2000 m thick. A combination of heat flow base cases 'paleo' and 'recent' (Fig. 6) results in a good fit between measured and calculated calibration data. (b) Burial history plots considering extremely low (1200 m) and high (2500 m) thicknesses of eroded rocks. Calibration data show that even in the scenario with minor erosion, a heat flow increase during Pliocene time has to be assumed.

5.2.3 Discussion of Heat Flow History

(1) Present-day heat flow

According to our models, present-day heat flow varies between 37 and 52 mW/m². This range is lower than that indicated in a heat flow map of Europe (Majorowicz and Wybraniec, 2011) for the same area (50-70 mW/m²). Majorowicz and Wybraniec (2011) have shown that glaciation may have led to a substantial reduction in temperature at shallow depth (mainly <1 km) resulting in an underestimation of present-day heat flow. However, not even the southernmost (Alpine) parts of the study area were affected by Pleistocene glaciation (Van Husen, 1987). Moreover, the lowest present-day heat flows (37 mW/m²) are based on highly reliable formation test data from more than 3 km depth in the Mo1 well. Thus, glaciation probably has no significant effect on the reconstructed present-day heat flow. Moreover, the application of paleoclimatic corrections would enlarge the difference between Neogene and present-day heat flow. In contrast, the difference between model-based present-day heat flow and the heat flow in the Majorowicz and Wybraniec (2011) map may be caused by different assessments of thermal conductivities. Predefined conductivities provided by the software have been used in this study in case of lack of measured data.

(2) Oligocene and Miocene heat flow

Reconstructed Oligocene and Miocene heat flows are rather low (26-32 mW/m²) resulting in low average paleo-geothermal gradients of approximately 23 °C/km. Similar conditions have been observed in wells in the Swiss (Rybach, 1984; Schegg, 1994; Schegg and Leu, 1996; Schegg et al., 1997), German (Jacob and Kuckelkorn, 1977; Teichmueller and Teichmueller, 1986) and Austrian Molasse Basin and its fold-and-thrust belt (Sachsenhofer, 2001; Gusterhuber et al., in press).

(3) Pliocene and Pleistocene increase in heat flow

Sensitivity analyses suggest that the increase in heat flow is not an artifact. However geological reasons are still poorly understood and include (see also Gusterhuber et al., in press).

- changes in hydrodynamics caused by a Pleistocene change in the stress field (Schmidt and Erdogan, 1993, 1996; Horvath and Cloetingh, 1996),
- topography-induced perturbation of the isotherms e.g. due to high exhumation rates in the Eastern Alps. However, present-day exhumation rates are clearly below values which are considered to affect the shape of isotherms (450 m/mio. year; Glotzbach et al., 2009) and

- a large scale increase in mantle heat flow, which should have affected major parts of the Alps. Without more and better heat flow data from the central Eastern Alps, the latter possibility remains pure speculation.

(4) Southward decrease in heat flow

- Both, reconstructed paleo-heat flow and present-day heat flow decrease towards the south. Similar heat flow patterns have also been observed by Rybach (1984) in the Swiss, Teichmueller and Teichmueller (1986) in the Bavarian as well as Sachsenhofer (2001) and Gusterhuber et al. (in press) in the Austrian part of the Molasse Basin, respectively. The southward decrease in heat flow may have different causes: (I) thermal disequilibrium due to down-bending and thickening of the earth crust (Teichmueller and Teichmueller, 1986); (II) a thermal blanketing effect driven by the fast approach of the already compacted nappe system; (III) deep infiltration of cold surface water in the karstified rocks of the Northern Calcareous Alps (Wessely, 1983); (IV) elevated heat flows in the northern part of the Molasse Basin due to heat transfer by northward migrating fluids from beneath the Alpine nappes (Schmidt and Erdogan, 1993, 1996) which influenced the temperature field in the upper few kilometers of the crust (Rybach, 1984); (V) or any combination of the above.

5.3 Petroleum Systems Modeling

Bulk kinetic data determined for immature source rocks in the Austrian part of the Alpine Foreland Basin (´Molasse kinetic´; Fig. 3) and the most likely heat flow scenario (combination of heat flow base cases ‘paleo’ and ‘recent’ involving an increase in heat flow for the last 4 million years BP; Fig. 6) have been used to model hydrocarbon generation and migration.

5.3.1 Hydrocarbon Generation

As this study focuses on location and timing of hydrocarbon generation, Fig. 9 shows enlargements of the specific area of interest. In this figure, generation zones based on calculated vitrinite reflectance (early oil generation: 0.55-0.70 % Ro; main oil generation: 0.70-1.00 %Rr) are shown for three different time stages (22.3 Ma, 18.3 Ma, present-day). Although vitrinite reflectance isolines (red lines) cross all rock units, color codes are shown exclusively for source rock units. In addition, temperature, maturity and hydrocarbon generation histories are shown in Figure 9 for the source rock unit at three different sites: X (beneath present day imbricates); Y (beneath present day Flysch wedge), Z (present day location of Mo1).

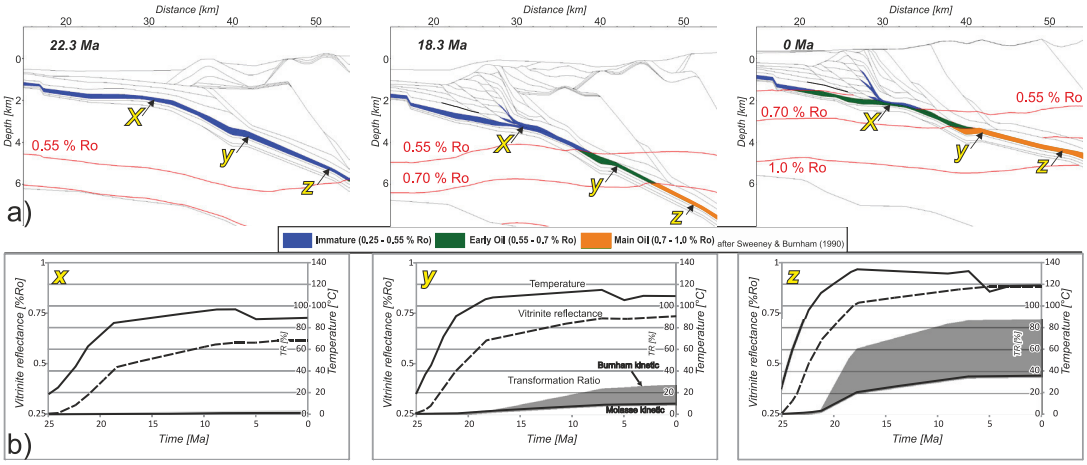

Figure 9: Petroleum generation beneath the Alpine nappes.
(a) Generation zones at different time-slices. Red lines indicate the boundaries between different maturity stages.
(b) Time plots showing the evolution of temperature, vitrinite reflectance and the transformation ratio (TR) over time for three different sites (X, Y, Z) under the thrust belt. Grey shaded areas mark the difference in TR between the 'Molasse kinetic' and the kinetic data set for Type II kerogen of Burnham (1989).

Figure 9 shows that 22.3 million years BP the studied section was still immature. Between 22.3 and 18.3 million years BP deep burial due to (ongoing) overthrusting resulted in a strong increase in temperature at all studied sites (X: 95°C; Y: 115°C; Z: 135°C). Consequently the early and main oil windows are reached at sites Y and Z, respectively. Nevertheless, the calculated transformation ratio suggests that minor hydrocarbons (<20 % of the total potential) have been generated at site Z. Till 7 million years BP site Y reached the main oil window and additional hydrocarbons have been generated at sites Y and Z. Later uplift and erosion resulted in cooling and terminated hydrocarbon generation.

The calculated transformation ratio at site Z is 38 %. This value fits well with the observed average HI of the source rock unit in well Mo1, which is about 285 mgHC/gTOC (Gratzer et al., 2011) and thus 30 to 52 % lower than that of immature equivalents (400-600 mgHC/gTOC; Table 1).

5.3.2 Sensitivity analysis

Correlations of geophysical well logs suggest that in the area east of the Lindach Fault the source rock facies north of the Alpine nappes and in the sub-thrust subthrust is identical (Sachsenhofer and Schulz, 2006). Thus it is useful to apply the ´Molasse kinetic´ data set. However, to study the sensitivity of the study results to different kinetic data sets, an alternative kinetic data set (Type II kerogen of Burnham, 1989;

Fig. 3) was considered for sensitivity analysis. The comparison between the calculated transformation ratios shows that the timing of hydrocarbon generation is similar. However, more generated hydrocarbons (higher transformations ratios) are predicted using the Burnham (1989) kinetics (e.g. 82 vs. 32 % for site Z).

5.3.3 Hydrocarbon Charge

2D Migration Model

In Figure 10, four representative time steps (18.3, 9.0, 5.0 Ma and present day) of the modeled 2D section were chosen to illustrate hydrocarbon migration from the oil kitchen below the Alpine nappes towards the foreland.

The time step of 18.3 Ma (Fig. 10) was selected because it represents a time of major hydrocarbon generation beneath the Alpine wedge (see site X in Fig. 9). At 18.3 Ma years, the migrating liquid hydrocarbons (green arrows) reached a position between Ro1 and En1. The model shows that oil migrated along the source rock interval until it reached a fault juxtaposing the Lower Oligocene source rock interval against Cenomanian and Eocene reservoir units (see also migration models in Malzer et al., 1993). The presence of oil fields proves that relevant faults have acted as migration pathways at least at certain times. Since exact times are unknown, an intermediate time-constant shale gouge ratio of 50 % was set for the faults in the model to allow at least part-time migration. This fault type is expressed by a shale ratio with regard to the offset lithologies. Typical values are 35 % (low shale content) for relatively permeable faults or 70 % (high shale content) for relatively impermeable faults. Typical Early stage liquid hydrocarbon accumulations apparently occurred at this time in the fault bounded block between Bh1 and Mg1. Minor gas was generated at 18.3 Ma. According to the model, gas migrated at a relatively higher stratigraphic position and partly diffuses into overlying low-permeability layers (Zupfing Fm.; red arrows).

The time step of 9 Ma is close to the supposed time of maximum burial and shortly before the termination of hydrocarbon generation (Fig. 9). Liquid and gaseous hydrocarbons continued to migrate northward. A small oil accumulation is predicted near the northern well WO1.

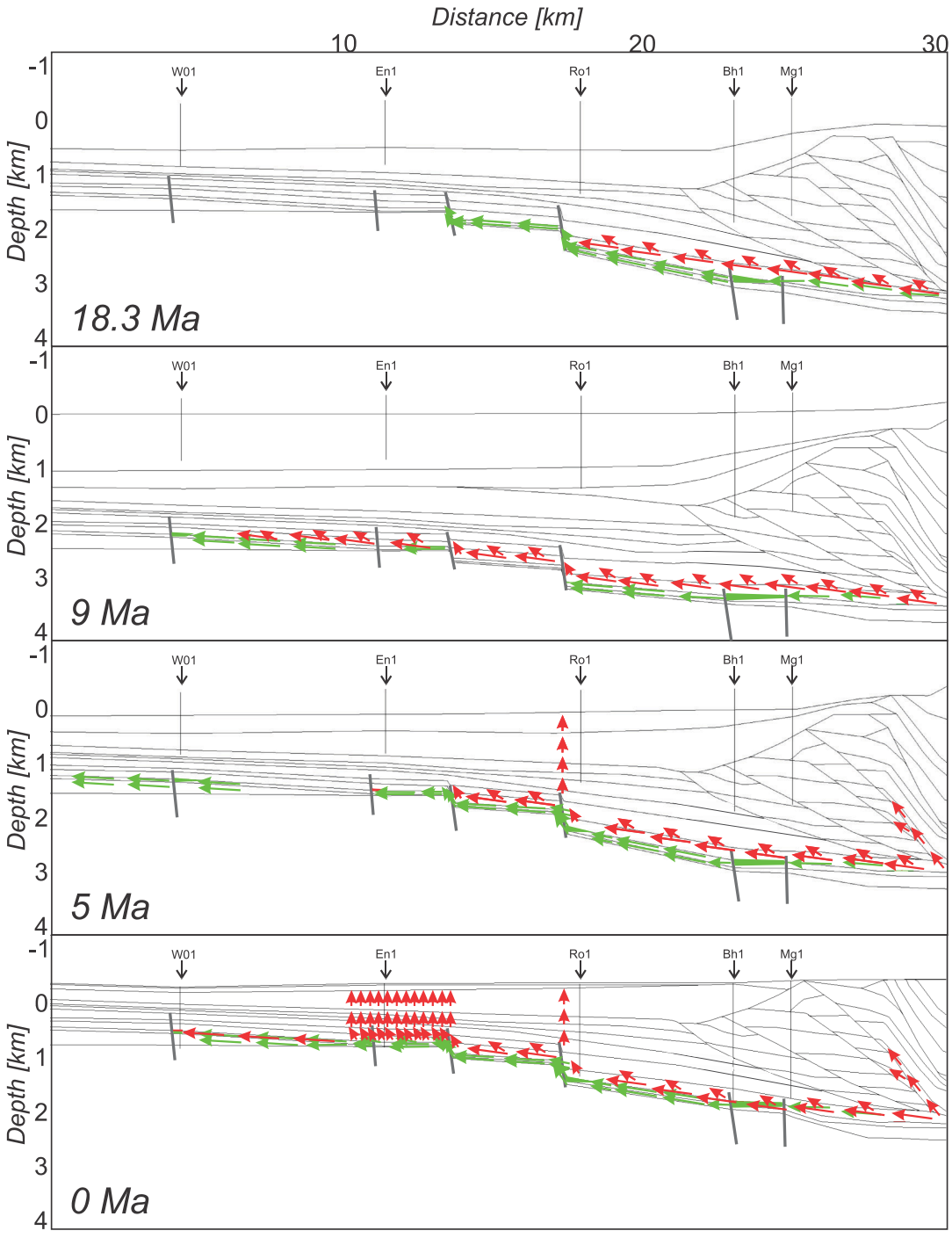

Figure 10: 2D migration model (see Fig. 1 for location). Green (for liquids) and red (for gas) arrows indicate migration pathways based on calculated hydrocarbon saturations at certain time steps. Little patches having the same color coding indicate possible petroleum accumulations.

Because of considerable uplift between 9 Ma and present day (Gusterhuber et al., 2012), almost no hydrocarbons were generated during the late stage evolution of the

sub-thrust (Fig. 9). However, significant re-migration occurred along the section. Important model results include:

(1) Long-distance northward migration of liquid hydrocarbons. Long-distance migration is also supported by oil seeps near the northern basin margin west of Linz (Gratzer et al., 2012) proving tens of kilometers of lateral migration.

(2) Migration of (thermogenic) gas along fault zones into Molasse imbricates. This may be a consequence of uplift and erosion causing a significant pressure drop in the subsurface. Actually minor thermogenic gas has been found in biogenic gas accumulations in the Sierning Imbricates (Pytlak, pers. comm., 2013).

(3) Apparent vertical migration indicated by saturations of thermogenic gas into the Puchkirchen and Hall formations. Vertical diffusive migration of thermogenic gas (and condensate) and mixing with biogenic gas accumulations in the Puchkirchen and Hall formations have been described by Reischenbacher and Sachsenhofer (2011).

'Pseudo 3D' Migration Model

Fig. 11 shows structure maps of the main reservoir horizons: Cenomanian and Eocene (base Oligocene in areas where Eocene sediments are missing). The maps were compiled using the 3D seismic volume (see outline in Fig. 1) and were extended to the south and north considering 2D seismic and well data in order to include the oil kitchen and hydrocarbon accumulations located north of the 3D seismic volume. The northern boundary of the oil kitchen is defined by the 0.6 % Ro reflectivity isoline (Linzer and Sachsenhofer, 2010).

A very rough estimate of the total hydrocarbon volume migrating from the sub-thrust area to the foreland can be derived from the source potential index (SPI) of the Lower Oligocene succession (~1 ton hydrocarbon/m² surface; Sachsenhofer et al., 2010), the kitchen area (~100 x 20 km), the average density of Molasse oil (850 kg/m³ corresponding to an API grade of 35; Gratzer et al., 2011) and losses during primary migration in the order of 25 %. This assessment gives a volume in the order of 11 billion barrels of oil (BBO).

To be conservative, a total volume of 7 BBO was injected close to the northern boundary of the oil kitchen (0.6 % Ro) into Cenomanian (3.5 BBO) and Eocene horizons (3.5 BBO) in order to visualize migration pathways in the foreland (Fig. 11).

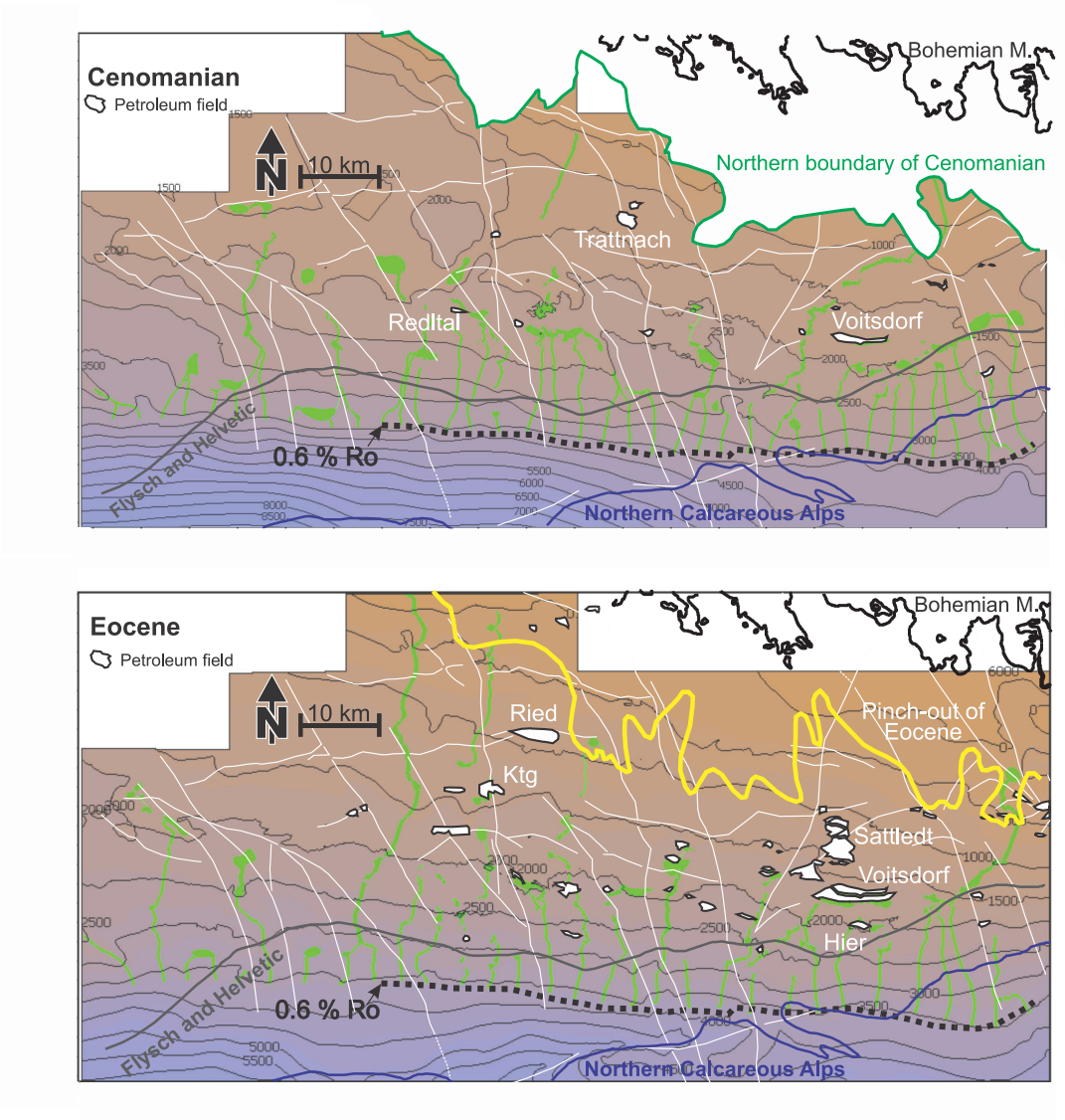

Figure 11: Depth structure maps representing Upper Cretaceous and Eocene carrier/reservoir horizons. The (dotted) 0.6 % Ro iso-reflectivity represents a rough assessment of the oil kitchen boundary. Bright green traces and batches show possible simulated oil migration pathways and accumulations, respectively. Petroleum fields and fault patterns (white lines) are shown in each horizon.

As expected, modeled migration pathways are northward trending (Fig. 11). Some oil migrates across the northern model border and may cause oil seeps detected at the basin margin (Gratzer et al., 2012). Several hydrocarbon fields with Cenomanian and/or Eocene reservoir units are predicted by the model. These include the large Voitsdorf Field and a number of smaller fields (e.g. Redltal, Hier, Ktg; Fig. 11). Other major fields with Cenomanian (e.g. Trattnach) and Eocene reservoirs (e.g. Sattledt, Ried) are not clearly predicted by the models. In contrast a number of fields

are predicted in the western part of the study areas, where no commercial oil has been found yet.

Models are useful, both if they make a fit or a misfit with observations. In this case, it is obvious that part of the mismatch is related to low model resolution outside of the 3D cube and the fact that present-day structure maps instead of paleo-structures maps (e.g. 9 Ma, time of main migration pulse; see Fig. 9) have been used. Moreover, facies changes and pressure regimes are not considered in the simple flow path approach. Apart from that, we see two main reasons for the mismatch, which are discussed below:

(1) Sachsenhofer and Schulz (2006) and Gusterhuber et al. (in press) emphasized that source rocks in the western part of the study area have been removed by tectonic erosion and are now found in the Molasse imbricates. This suggests, together with the model results that the absence of petroleum fields in the western sector of the basin is a consequence of missing charge rather than of missing structures.

(2) Migration probably did not only occur within the major carrier beds, but seemingly also along major fault systems

These results look plausible but however some uncertainties have to be considered. Although the best resolution available from the 3D seismic volume was used, parts off the 3D coverage were interpolated and may be too smooth to chase the exact location of reservoirs. Another uncertainty may be caused by the fact that present day but not paleo maps were used. Present day maps are only able to show the actual migration not migration at the time of initiation. In addition, important factors like facies behaviors and pressure regimes are not considered in these migration models. Unfortunately, existing data of the area which includes the oil kitchen is very sparse. 3D seismic data is limited to the foreland and there are only a few wells drilled in this part. However, this preliminary work provides a proper basement for further studies.

5.3.4 Biodegradation Risk

Fig. 12a shows a plot of API gravity of Molasse oils versus depth. The plot indicates that biodegraded oils, characterized by API grades <30, are restricted to shallow levels (<800 m sub-sea) with present-day temperatures ≤50° (see also Gratzer et al., 2011). At first sight the shallow threshold depth for biodegradation in the study area is astonishing, because bacteria responsible for biodegradation are known to occur up to 80°C (e.g. Head et al., 2003).

The lack of biodegraded oil at greater depth may be explained by the ‘palaeopasteurization’ model (Wilhelms et al., 2000), postulating that petroleum reservoirs were pasteurized at 80-90°C, inactivating any hydrocarbon-degrading

microorganisms present, during deep burial before the main oil charge and subsequent uplift of the reservoir to cooler conditions.

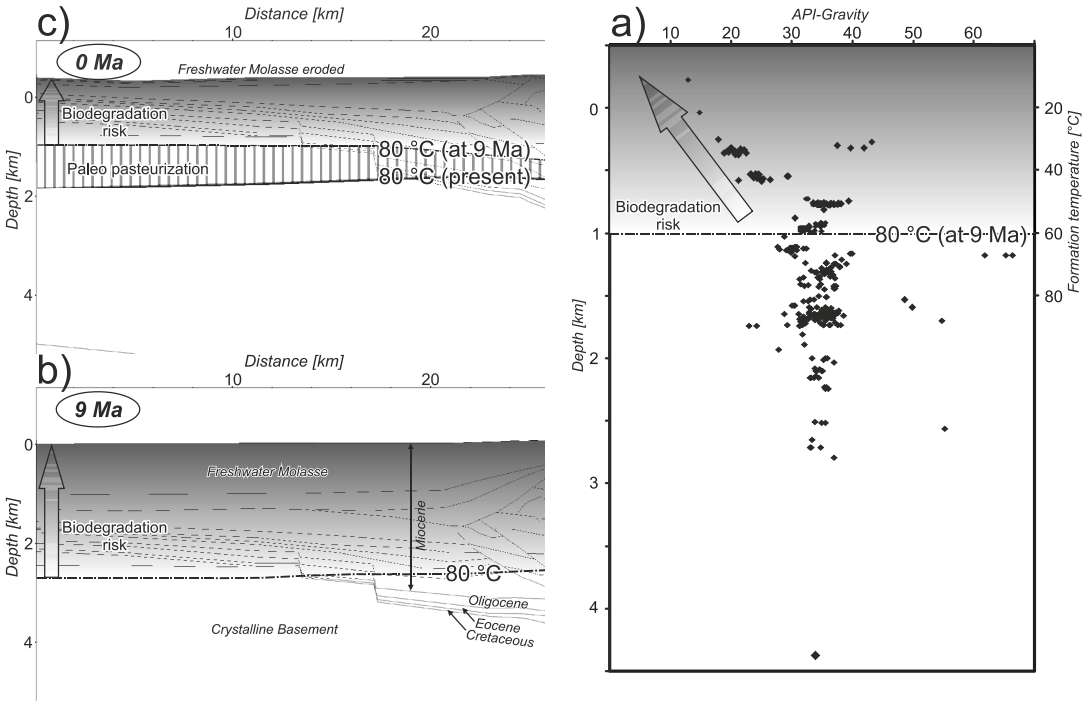

Figure 12: (a) Plot of API gravity of Molasse oils versus depth. Biodegraded oils with low API grades occur at shallow depth (above 800 m sub-sea) corresponding to present formation temperatures of about 50 °C. (b) Modeled 80°C isotherms in the northern part of the 2D section for the time of maximum burial (9 Ma). Grey shading indicates the upward increasing biodegradation risk. (c) Modeled 80°C isotherms in the northern part of the 2D section for present-day (0 Ma). The position of the paleo-80°C isotherm is also shown.

The 2D model is used to test the applicability of the 'palaeopasteurization' model in the Alpine Foreland Basin. In Fig. 12b the position of the 80°C isotherm along the northern sector of the modeled cross-section is shown for the time of maximum burial (9 Ma). Different grey shadings indicate the upward increasing risk for biodegradation. In Fig. 12c the present day situation is shown together with the paleo-80°C isotherm. The depth interval between the paleo- and the present-day 80°C isotherm has been affected by 'palaeopasteurization'. The present-day position of the paleo-80°C isotherm is at about 1 km below sea level fitting reasonable well with the observed depth of biodegradation. Thus 'palaeopasteurization' may have a positive effect on the preservation of hydrocarbons in the Alpine Foreland Basin.

Important to note, that the 'palaeopasteurization' model is only applicable if most hydrocarbons migrated into shallow reservoirs after maximum burial. Although some

oil reached petroleum traps in the northern part of the cross-section (e.g. WO1) already during maximum burial (9 Ma), figure 10 shows that additional oil accumulated during (5 Ma) and after uplift (present-day).

6 Conclusions

- The presented structural model is a kinematic model with geodynamic background and provides an appropriate input for the petroleum systems model. It supposes that total tectonic shortening in the modeled section is at least 48.5 km which corresponds to 69 % of shortening (mainly in the Molasse sediments, including some limited shortening in the Penninic-Flysch and Helvetic Wedge but excluding shortening of the Northern Calcareous Alps).
- Maturity data indicate rather low paleo-heat flows along the modeled section decreasing from north to south from 32 to 26 mW/m² (base case `paleo´). Formation temperatures indicate present-day basal heat flows decreasing in the same direction from 52 to 37 mW/m² (case `recent´). Consequently, a heat flow scenario which involves a sub-recent (~4 Ma BP) increase in heat flow from base case `paleo´ to base case `recent´ is accepted as most likely. This heat flow history is similar to that reconstructed for a parallel cross-section through the Perwang Imbricates (~90 km west of the present cross-section) by Gusterhuber et al. (in press).
- The above heat flow history and bulk kinetic data from Oligocene source rocks have been used for petroleum systems modeling. According to these models, hydrocarbon generation commenced about 18 Ma BP (Early Miocene) due to deep burial beneath Alpine nappes and was terminated about 8 Ma BP (Late Miocene) due to cooling caused by uplift and erosion. Whereas the sub-thrust area beneath the Flysch Wedge remained immature, about 40 % of the total source potential was realized beneath the Northern Calcareous Alps in the Mo1 area.
- Hydrocarbon migration commenced contemporaneously with hydrocarbon generation, but continued until present day. Main model results include: (1) Oil migrated along the source rock interval till it reached faults with sufficient vertical throw to allow hydrocarbon migration into stratigraphically deeper reservoir units; (2) Long-distance (>50 km), lateral, northward migration of oil (and gas); (3) Migration of gas along fault zones into the Sierning Imbricates; (4) Apparent

vertical diffusive migration of gas into the Oligo-/Miocene Puchkirchen and Hall formations.

- Detected and producing hydrocarbon deposits in Cenomanian and Eocene horizons (e.g. Malzer et al., 1993), oil seeps along the northern basin margin (Gratzer et al., 2012), mixtures of biogenic and thermogenic gas in the Sierning Imbricates and the Puchkirchen and Hall formations (Reischenbacher and Sachsenhofer, 2011) show that the model results fit well with observations.
- A flow path approach for modeling migration pathways in the main carrier/reservoir units ('Pseudo 3D Model') produces ambiguous results. Whereas some major petroleum fields are successfully predicted, others are not. Moreover, accumulations are predicted in areas, where no hydrocarbons have been detected yet. Apart from model simplifications, the mismatch reflects the absence of source rocks in the western part of the study area (e.g. Sachsenhofer and Schulz, 2006) as well as the important role of fault zones for hydrocarbon migration.
- The applied 2D model suggests that deep burial (9 Ma) and subsequent uplift to cooler conditions (Gusterhuber et al., 2012) resulted in 'palaeopasteurization' of reservoirs near the northern basin margin. This model may explain that biodegradation in the Austrian part of the Alpine Foreland Basin is limited to the depth interval down to 800-1000 m sub-sea.

Keywords: Austrian Molasse Basin Hydrocarbon Generation Migration

Acknowledgements

The authors thank RAG AG for their kind permission to publish the data. The used software PetroMod was generous granted as academic license by the Schlumberger Technology Center, Aachen, Germany. We would also like to thank Doris Gross, Reinhard Gratzer and Achim Bechtel (Montanuniversitaet Leoben) for providing a wealth of appropriate geochemical data.

References

Baur, F., 2010. Quantification of heat and fluid flow through time by 3D modeling: an example from the Jeanne d'Arc basin, offshore eastern Canada. PhD thesis, RWTH Aaachen, 170 p.

Beidinger, A. and Decker, K., submitted: Quantifying Early Miocene in-sequence and out-sequence thrusting at the Alpine-Carpathian junction. Tectonics.

Bernhardt, A., Stright, L. and Lowe, D.R., 2012. Channellized debris-flow deposits and their impact on turbidity currents: the Puchkirchen axial channel belt in the Austrian Molasse Basin. Sedimentology, DOI: 10.1111/j.1365-3091.2012.01334.x.

Burnham, A.K., 1989. A simple kinetic model of petroleum formation and cracking. Lawrence Livermore National Laboratory Report, UCID-21665, 11 p.

Carr, A.D, 2000. Suppression and retardation of vitrinite reflectance, part 1. Formation and significance for hydrocarbon generation. Journal of Petroleum Geology, 23, 313–343.

Covault, J.A., Hubbard, S.M, Graham, S.A, Hinsch, R. and Linzer, H.-G., 2009. Turbidite-reservoir architecture in complex foredeep-margin and wedge-top depocenters, Tertiary Molasse foreland basin system, Austria. Marine and Petroleum Geology, 26, 379-396.

De Ruig, M.J. and Hubbard, S.M., 2006. Seismic facies and reservoir characteristics of a deep marine channel belt in the Molasse foreland basin. AAPG Bulletin, 90, 735-752.

Dohmann, L., 1991. Die unteroligozaenen Fischschiefer im Molassebecken. Ph.D. thesis, Ludwig Maximilian Universitaet, Munich, 365 pp.

Espitalié, J., LaPorte, J.L., Madec, M., Marquis, F., Leplat, P., Poulet, J. and Boutefeu, A., 1977. Méthode rapide de charactériasation des roches mères de leur potential pétrolier et de leur degré d´evolution. Revue de l´Institut Francais du Pétrole, 32, 23-42.

Frisch, W., Kuhlemann, J. and Dunkl, I., 2001. The Dachstein paleosurface and the Augenstein Formation in the Northern Calcareous Alps – a mosaic stone in the geomorphological evolution of the Eastern Alps. International Journal of Earth Sciences, 90, 500-518.

Glotzbach, C., Spiegel, C. Reinecker, J., Rahn, M. and Frisch, W., 2009. What perturbs isotherms? An assessment using fission-track thermochronology and thermal modelling along the Gotthard transect, Central Alps. Geological Society of London, Special Publications, 324, 111-124.

Gratzer, R., Bechtel, A., Sachsenhofer, R.F., Linzer, H.-G., Reischenbacher, D. and Schulz, H.-M., 2011. Oil-oil and oil-source rock correlations in the Alpine Foreland Basin of Austria: Insights from biomarker and stable carbon isotope studies. Marine and Petroleum Geology, 28, 1171-1186.

Gratzer, R., Schmid, C. and Stanzel, A.I., 2012. Bewertung und Abgrenzung eines natürlichen Ölaustrittes im Eferdinger Becken. Beiträge zur Hydrogeologie, 59, 203-217.

Grunert, P., Soliman, Coric A., S. Roetzel, R. Harzhauser, M. and Piller, W.E., 2012. Facies development along the tide-influenced shelf of the Burdigalian Seaway: An example from the Ottnangian stratotype (Early Miocene, middle Burdigalian). Marine Micropaleontology, 84-85, 14-36.

Grunert, P., Hinsch, R., Sachsenhofer, R.F., Bechtel, A., Coric, S., Harzhauser, M., Piller, W.E. and Sperl, H. 2013. Early Burdigalian infill of the Puchkirchen Trough (North Alpine Foreland Basin, Central Paratethys): facies development and sequence stratigraphy. Marine and Petroleum Geology, doi:http://dx.doi.org/10.1016/j.marpetgeo.2012.08.009.

Gusterhuber, J., Dunkl, I., Hinsch, R. Linzer, H.-G. and Sachsenhofer, R.F., 2012. Neogene uplift and erosion in the Alpine Foreland basin (Upper Austria and Salzburg). Geologica Carpathica, 63, 295-305.

Gusterhuber, J., Hinsch, R. and Sachsenhofer, R.F., in press. Evaluation of hydrocarbon generation and migration in the Molasse fold and thrust belt (Central Eastern Alps, Austria) using structural and thermal basin models. AAPG Bulletin.

Hantschel, T., Kauerauf, A., Wygrala, B., 2000. Finite element analysis and ray tracing modeling of petroleum migration. Marine and Petroleum Geology, 17, 7, 815-820.

Hantschel, T. and Kauerauf, A., 2009. Fundamentals of Basin Modeling. Springer Verlag, 425 p.

Head, I.M., Jones, D.M. and Larter, S.R., 2003. Biological activity in the deep subsurface and the origin of heavy oil. Nature, 426, 344-352.

Hermanrud, C., Cao, S. and Lerche, I., 1990. Estimates of virgin rock temperature derived from BHT measurement: Bias and errors. Geophysics, 55 (7), 924-931.

Hinsch, R., 2008. New Insights into the Oligocene to Miocene Geological Evolution of the Molasse Basin of Austria. Oil & Gas European Magazine, 34 (3), 138-143.

Hinsch, R. and Linzer, H.-G., 2010. Along-strike variations of structural styles in the Imbricated Molasse of Salzburg and Upper Austria: A 3D seismic perspective. European Geosciences Union General Assembly, Geophysical Research Abstracts, 12, EGU2010-4966-3.

Hinsch, R., 2013. Laterally varying structure and kinematics of the Molasse fold and thrust belt of the Central Eastern Alps: implications for exploration. AAPG Bulletin, 97, 10, 1805-1831.

Horner, D.R., 1951. Pressure buildup in wells, in: Brill, E.J. (Ed.), Proceedings of the Third World Petroleum Congress. The Hague Section II, Cologne, 503-521.

Horvath, F. and Cloetingh, S., 1996. Stress-induced late-stage subsidence anomalies in the Pannonian basin. Tectonophysics, 266, 287-300.

Hubbard, S.M., De Ruig, M.J. and Graham, S.A, 2009. Confined channel-levee complex development in an elongate depo-center: Deep-water Tertiary strata of the Austrian Molasse basin. Marine and Petroleum Geology, 26, 85-112.

Jacob, H. and Kuckelkorn, K., 1977. The carbonization profile of the Miesbach 1 well and its oil geological interpretation: Erdoel-Erdgas-Zeitschrift, 93, 115-124.

Kamyar, H. R., 2000. Verteilung der Untergrundstemperaturen an den Beispielen der Bohrlochtemperatur (BHT) – Messungen in den RAG – Konzessionen Oberösterreichs und Salzburgs, (Molasse- und Flyschzone). PhD-thesis, University of Vienna, Austria, 145 pp.

Krenmayer, H. G., 1999. The Austrian sector of the North Alpine Molasse: A classic foreland basin. FOREGS (Forum of Euopean Geological Surveys) Dachstein-Hallstatt-Salzkammergut Region, Vienna, 22-26.

Kuhlemann, J. and Kempf, O., 2002. Post-Eocene evolution of the North Alpine Foreland Basin and its response to Alpine tectonics. Sedimentary Geology, 152, 45-78.

Linzer, H.-G., 2001. Cyclic channel systems in the Molasse foreland basin of the Eastern Alps - the effects of Late Oligocene foreland thrusting and Early Miocene lateral escape. AAPG Bulletin, 85, 118 (abstract).

Linzer, H.-G., 2002. Structural and stratigraphic traps in channel systems and intraslope basins of the deep-water molasse foreland basin of the Alps. AAPG 2002 Annual Convention & Exhibition, Houston, Texas.

Linzer, H.-G., Decker, K., Peresson, H., Dell'Mour, R. and Frisch, W., 2002b. Balancing lateral orogenic float of the Eastern Alps. Tectonophysics, 354, 211 –237.

Linzer, H.-G., 2009. Gas in Imbricated Channel Systems of the Foreland Basin of the Eastern Alps (Austria). AAPG 2008 Annual Convention & Exhibition San Antonio, Texas.

Linzer, H.-G. and Sachsenhofer, R.F., 2010. Submarine Large Scale Mass Movements in the Deepwater Foreland Basin of the Alps - Implications to Hydrocarbon Generation and Distribution of Source and Reservoir Rocks. AAPG 2010 Annual Convention & Exhibition New Orleans.

Mackenzie, A.S., Patience, R.L., Maxwell, J.R., Vandenbroucke, M. and Durand, B, 1980. Molecular parameters of maturation in the Toarcian shales, Paris basin, France - I: changes in the configurations of acyclic isoprenoid alkanes, steranes and triterpanes. Geochimica et Cosmochimica Acta, 44, 1709-1721.

Mackenzie, A.S., Hoffman, C.F. and Maxwell, J.R., 1981. Molecular parameters of maturation in the Toarcian shales, Paris basin, France - III: changes in aromatic steroid hydrocarbons. Geochimica et Cosmochimica Acta, 45, 1345-1355.

Mackenzie, A.S. and McKenzie, D., 1983. Isomerization and aromatization of hydrocarbons in sedimentary basins formed by extension. Geology Magazine, 120, 417-470.

Majorowicz, J. and Wybraniec, S. 2011. New terrestrial heat flow map of Europe after regional paleoclimatic correction application. International Journal of Earth Sciences, 100, 881-887.

Malzer, O., Roegl, F., Seifert, P., Wagner, L., Wessely, G. and Brix, F., 1993. Die Molassezone und deren Untergrund. In: F. Brix and O. Schultz (eds.), Erdöl und Erdgas in Österreich. Naturhistorisches Museum Wien und F. Berger, 281–358.

Nachtmann, W., 1995. Fault-bounded structures as hydrocarbon traps in the upper Austrian Molasse Basin. Geol. Palaeontolog. Mitt. Innsbruck, 20, 221-230.

Peters, K.E., Walters, C.C. and Moldowan, J.M., 2005. The biomarker guide, 2nd ed. Cambridge University Press, 1155 pp.

Reischenbacher, D. and Sachsenhofer, R., 2011. Entstehung von Erdgas in der oberösterreichischen Molassezone: Daten und offene Fragen. BHM, 156 (11), 463-468.

Roeder, D. and Bachmann, G., 1996. Evolution, structure and petroleum geology of the German Molasse Basin, In: P. Ziegler and F. Horvath, (eds.), Peri-Tethys Memoir 2, Structure and Prospects of Alpine Basins and Forelands. Mèmoire du Museum National d'Histoire naturelle, 170, 263-284.

Roegl, F., 1998. Palaeogeographic Considerations for Mediterranean and Paratethys Seaways (Oligocene to Miocene). Annalen des Naturhistorischen Museums in Wien, 99A, 279–310.

Rullkoetter, J. and Marzi, R., 1989. New aspects of the application of sterane isomerization and steroid aromatization to petroleum exploration and the reconstruction of geothermal histories of sedimentary basins. Reprint Division of Petroleum Geochemistry, American Chemical Society, 34, 126-131.

Rybach, L., 1984. The paleogeothermal conditions of the Swiss Molasse Basin: Implications for hydrocarbon potential. Rev. Institut Francais Du Petrole, 39, 143-146

Sachsenhofer, R. F., 2001. Syn- and post-collisional heat flow in the Cenozoic Eastern Alps: International Journal of Earth Sciences, 90, 579-592.

Sachsenhofer, R.F. and Schulz, H.-M., 2006. Architecture of Lower Oligocene source rocks in the Alpine Foreland Basin: a model for syn- and post-depositional source - rock features in the Paratethyan realm. Petroleum Geoscience, 12, 363-377.

Sachsenhofer, R.F., Leitner, B., Linzer, H.-G., Bechtel, A., Coric, S., Gratzer, R. Reischenbacher, D. and Soliman, A., 2010. Deposition, Erosion and Hydrocarbon Source Potential of the Oligocene Eggerding Formation (Molasse Basin, Austria). Austrian Journal of Earth Sciences, 103, 76-99.

Sachsenhofer, R.F, Linzer, H.-G., Bechtel, A., Dunkl, I. Gratzer, R., Gusterhuber, J., Hinsch, R. and Sperl, H., 2011. Influence of Alpine Tectonics on Source Rock Distribution, Hydrocarbon Generation and Migration in the Austrian Part of the Molasse Basin. AAPG 2011 International Conference and Exhibition, Milan, Italy.

Schegg, R., 1994. The coalification profile of the well Weggis (Sub-alpine Molasse, Central Switzerland): Implications for erosion estimates and the paleogeothermal regime in the external part of the Alps. Bulletin Swiss Assoc. of Petroleum Geol. and Engineers, 61, 57-67.

Schegg, R. and Leu, W., 1996. Clay mineral diagenesis and thermal history of the Thonex well, western Swiss Molasse Basin. Clays and Clay Minerals, 44 (5), 693-705.

Schegg, R., Leu, W., Cornford, C. and Allen, P. A., 1997. New coalification profiles in the Molasse Basin of Western Switzerland: Implications for the thermal and geodynamic evolution of the Alpine Foreland. Eclogae geol. Helv., 90, 79-96.

Schmidt, F. and Erdogan, L. T., 1993. Basin modelling in an overthrust area of Austria.In: A.G. Doré, E. Holter, J.H. Augustson, W. Fjeldskaar, S. Hanslien, Ch. Hermanrud, B. Nyland, D. J. Stewart and O. Sylta, (eds.), Basin Modelling: Advances and Applications. NPF Special Publications, 3, 573-581.

Schmidt, F. and Erdogan, L. T., 1996. Paleohydrodynamics in exploration. In: W. Liebl and G. Wessely, (eds.), Petroleum exploration and production in thrust belts, foreland basins and orogenic basins. EAPG Spec.Publ., 5, 255-265.

Schulz, H.-M., Sachsenhofer, R.F., Bechtel, A., Polesny, H. and Wagner L., 2002. Origin of hydrocarbon source rocks in the Austrian Molasse Basin (Eocene-Oligocene transition). Marine and Petroleum Geology, 19, 683-709.

Schulz. H.-M., Bechtel, A., Rainer, T., Sachsenhofer R.F. and Struck, U., 2004. Paleoceanography of the western central paratethys during nannoplankton zone NP 23. The Dynow Marlstone in the Austrian Molasse Basin. Geologica Carpthica, 55, 311-323.

Schulz, H.-M. and van Berk, W., 2009. Bacterial methane in the Atzbach-Schwanenstadt gas field (Upper Austrian Molasse Basin), Part II: Retracing gas generation and filling history by mass balancing of organic carbon conversion applying hydrogeochemical modelling. Marine and Petroleum Geology, 26, 1180-1189.

Schulz, H.-M., van Berk, W., Bechtel, A., Struck, U. and Faber, E., 2009. Bacterial methane in the Atzbach-Schwanenstadt gas field (Upper Austrian Molasse Basin), Part I: Geology: Marine and Petroleum Geology, 26, 1163-1179.

Sissingh, W., 1997. Tectonostratigraphy of the North Alpine Foreland Basin: Correlation of Tertiary depositional cycles and orogenic phases. Tectonophysics, 282, 223-256.

Steininger, F.F., Wessely, G., Roegl, F. and Wagner, L., 1986. Tertiary sedimentary history and tectonic evolution of the Eastern Alpine foredeep: Giornale di Geologia Bologna, 48 (3), 285-297.

Sweeney, J.J. and Burnham, A.K., 1990. Evaluation of a simple model of vitrinite reflectance based on chemical kinetics. AAPG Bulletin, 74, 1559-1570.

Teichmueller, R. and Teichmueller, M., 1986. Relations between coalification and paleogeothermics in variscan and alpidic foredeeps of western Europe. Lecture Notes in Earth Sciences, 5, 53-80.

Tissot, B.P. and Welte, D.H., 1984. Petroleum Formation and Occurrence. 2nd ed., Springer-Verlag, Berlin, 699 pp.

van Husen, D., 1987. Die Ostalpen in den Eiszeiten. Populaerwissenschaftliche Veröffentlichungen der Geologischen Bundesanstalt, Vienna, Map, scale 1:500,000.

Veron, J., 2005. The Alpine Molasse Basin – Review of petroleum geology and remaining potential. Bulletin fuer Angewandte Geologie, 10, 75-86.

Wagner, L.R., 1996. Stratigraphy and hydrocarbons in the Upper Austrian Molasse Foredeep (active margin). In: G. Wessely and W. Liebl (eds.), Oil and Gas in Alpidic Thrustbelts and Basins of Central and Eastern Europe. EAGE Special Publications, 5, 217-235.

Wagner, L.R, 1998. Tectono-stratigraphy and hydrocarbons in the Molasse foredeep of Salzburg, Upper and Lower Austria. In: A. Mascle, C.Puigdefàbregas, H.P.Luterbacher and M.Fernandez (eds.), Cenozoic Foreland Basins of Western Europe. Geological Society, Special Publications, 134, 339-369.

Welte, D. H. and Yukler, M. A., 1981. Petroleum origin and accumulation in basin evolution - A quantitative model. AAPG Bulletin, 65, 1387-1396.

Welte, D. H. and Yalcin, M.N., 1988. Basin modelling - A new comprehensive method in petroleum geology. Organic Geochemistry, 13, 141-151.

Welte, D. H., Horsfield, B. and Baker, D.R., 1997. Petroleum and Basin Evolution. Springer Verlag, 535 p.

Wessely, G., 1983. Zur Geologie und Hydrodynamik im südlichen Wiener Becken und seiner Randzone. Mitteilungen der österreichischen Geologischen Gesellschaft, 76, 27-68.

Wilhelms, A., Larter, S.R., Head, I., Farrimond, P., di-Primio, R. and Zwach, C., 2000. Biodegradation of oil in uplifted basins prevented by deep-burial sterilisation. Nature, 411, 1034-1037.

Wygrala, B., 1988. Integrated computer-aided basin modeling applied to analysis of hydrocarbon generation history in a Northern Italian oil field. Organic Geochemistry, 13, 187-197.

Wygrala, B., 1989. Integrated study of an oil field in the southern Po Basin, northern Italy. PhD thesis, University of Cologne, 226pp.